Laboratory Investigation of the Effects of Temperature and Moisture on Interface Shear Strength of Textured Geomembrane and Geosynthetic Clay Liner

A Thesis

Presented to

the Faculty of California Polytechnic State University,

San Luis Obispo

In Partial Fulfillment

of the Requirements for the Degree

Master of Science in Civil and Environmental Engineering

by

Taki S. Chrysovergis

December 2012

COMMITTEE MEMBERSHIP

TITLE: Laboratory Investigation of the Effects of Temperature and Moisture on Interface Shear Strength of Textured Geomembrane and Geosynthetic Clay Liner

AUTHOR: Taki S. Chrysovergis

DATE SUBMITTED: December 2012

COMMITTEE CHAIR: James Hanson, Professor, Civil and Environmental Engineering, California Polytechnic State University, San Luis Obispo

COMMITTEE MEMBER: Nazli Yesiller, Director, Global Waste Research Institute, California Polytechnic State University, San Luis Obispo

COMMITTEE MEMBER: Gregg Fiegel, Professor, Civil and Environmental Engineering, California Polytechnic State University, San Luis Obispo

ABSTRACT

Laboratory Investigation of the Effects of Temperature and Moisture on Interface Shear Strength of Textured Geomembrane and Geosynthetic Clay Liner

Taki S. Chrysovergis

A laboratory investigation was conducted to determine the effects of temperature and moisture on the shear strength of textured geomembrane (T-GM) and geosynthetic clay liner (GCL) interface. Several landfill slope failures involving geosynthetics have occurred within the past three decades. Interface shear strength of T-GM/GCL is well documented for testing conducted at laboratory temperatures and at moisture contents associated with GCLs in submerged conditions. However, in-service conditions for landfill liner systems include a wide range of temperatures (extending from below 0 °C to above 40 °C) and a wide range of moisture conditions. Large-scale interface direct shear tests were performed at normal stresses of cover liners (10, 20, and 30 kPa) and bottom liners (100, 200, and 300 kPa). Cover liner specimens were subjected to temperatures of 2, 20 and 40 °C; and bottom liner specimens were subjected to temperatures of 20 and 40 °C. Both cover and bottom liner specimens were prepared at moisture contents of as-received (approx. 18-19%), 50%, and 100%.

Cover liner specimens exhibited decreased peak interface shear strength (τ_p) with increasing temperature. Specimens sheared at 2 °C exhibited greater τ_p than those sheared at 20 °C by as much as 27%. Specimens sheared at 20 °C exhibited greater τ_p than those sheared at 40 °C by as much as 16%. Large-displacement interface shear strength (τ_{ld}) generally exhibited a bell-shaped

relationship with increasing temperature with the greatest τ_{ld} at 20 °C. A bell-shaped relationship was exhibited between temperature and peak and large-displacement interface friction angle (δ_p and δ_{ld}). δ_p ranged from 17.4 to 26.3°, 23.8 to 29°, and 20.4 to 22.2° for 2, 20, and 40 °C, respectively. δ_{ld} ranged from 12.7 to 18.2°, 18.2 to 20.6°, and 15.9 to 16.7° for 2, 20, and 40 °C, respectively. Decreased δ at 2 and 40 °C were largely attributed to increased geosynthetic damage. Bottom liner specimens exhibited decreased τ_p and τ_{ld} with increasing temperature by up to 12% and 16%, respectively. Bottom liner specimens exhibited decreased τ_p and τ_{ld} with increasing moisture content by up to 14% and 36%, respectively. For bottom liner specimens, a trend of decreased δ_p with increased temperatures was exhibited. δ_p ranged from 20 to 24.7° and 19.5 to 22.2° for 20 °C and 40 °C, respectively. δ_{ld} ranged from 10.4 to 15.6° and 8.9 to 13.9° for 20 °C and 40 °C, respectively. Decreased δ at 40 °C was largely attributed to increased geosynthetic damage and increased bentonite extrusion. Increased moisture content resulted in decreased δ_p and δ_{ld} by up to 4.7 and 5.1°, respectively. Results of this testing program indicated that T-GM/GCL interface shear strengths are influenced by temperature and moisture content within ranges representative of field conditions. Interpolation factors and reduction factors were developed for use to avoid overestimation of δ when determined at standard laboratory temperatures. For cover liners, reduction factors of 0.8 and 0.85 are recommended for δ_p and δ_{ld}, respectively. For bottom liners, reduction factors of 0.9 and 0.85 are recommended for δ_p and δ_{ld}, respectively.

ACKNOWLEDGEMENTS

I would like to thank Dr. Jim Hanson for devoting his time to provide advice and guidance from literature review to testing to data analysis. I would like to thank Dr. Gregg Fiegel and Dr. Nazli Yesiller for providing their time and serving on the thesis committee. I would like to thank Michael Onnen, Andy Flores, and Christopher Ethier for their assistance with performing laboratory testing. This study was partially supported by the Global Waste Research Institute. I would like to thank CETCO for providing GCL samples and Chris Athanassopoulos for providing technical information. I would like to thank GSE for providing geomembrane samples and Jimmy Youngblood for providing technical information. I would like to thank Amanda Howarth and Pavlo Chrysovergis for their support throughout the entire process. And lastly I would like to thank my parents, Stavros and Helen Chrysovergis, for funding my education and believing in me from beginning to end.

Table of Contents

List of Tables

List of Figures

Chapter 1: Introduction

Municipal solid waste (MSW) landfills are constructed to contain household and commercial wastes. Leachate and gas emissions produced by the waste result in required containment systems to prevent toxic interaction with the environment. Multiple types of geosynthetics that provide various functions are used to line the waste containment facility. Geosynthetic clay liners (GCLs) and geomembranes (GMs) are the geosynthetics used for landfill containment. GCLs typically consist of a thin layer of low permeability sodium bentonite sandwiched between two geotextiles. GMs are very low hydraulic conductivity polymer liners that typically overlay compacted clay liners or GCLs to produce a composite liner. Landfill slopes are designed to maximize waste containment volume (i.e., airspace) while providing geotechnical stability. Geosynthetic interfaces represent potential failure slip surfaces. Several landfill slope failures involving geosynthetics have been reported within the last three decades. A particularly critical geosynthetic interface for slope stability purposes is that between GMs and GCLs. Textured geomembranes (T-GMs) have been developed to maximize the shear strength along interface adjacent to the GM. Even so, concern exists for the interface shear strength of T-GM interfaces.

Moisture and temperature conditions vary widely for GCLs in service. GCLs exhumed from cover liner systems have been measured to have GCL moisture contents between 15 and 100% (Benson et al. 2007, Meer and Benson 2007, Scalia and Benson 2011). Temperatures exceeding 40 °C have been recorded in cover liner and bottom liner systems, and temperatures below 0 °C

have been recorded in bottom liner systems (Hanson et al. 2005, Koerner and Koerner 2006, Yesiller et al. 2008, Hanson et al. 2010). The majority of previous investigation of T-GM/GCL interface shear strength has been performed at 20 °C and under submerged conditions. Investigation on the effects of temperature or variable (i.e., targeted over a wide range) moisture content of GCLs on T-GM/GCL has generally not been reported.

An extensive laboratory testing investigation was conducted to determine the effects of temperature and moisture content on shear strength of T-GM/GCL interface. Large-scale interface direct shear tests were performed at normal stresses representing cover liner and bottom liner normal stresses of 10 to 30 kPa and 100 to 300 kPa, respectively. GCL specimens were prepared at as-received (AR), 50%, and 100% bentonite gravimetric moisture content and tested at cover liner and bottom liner normal stresses. T-GMs and GCLs were sheared at temperatures of 2, 20, and 40 °C at cover liner normal stresses and at temperatures of 20 and 40 °C at bottom liner normal stresses to represent coupled stress-temperature conditions in service.

Background of topical subject matter including MSW landfill liner systems, clay behavior (including temperature and moisture effects), past landfill slope stability failures, interface shear strength, GCL and T-GM interaction, and temperature effects on polymer behavior is presented in Chapter 2. Description of the experimental test program and test materials is presented in Chapter 3. Results and analysis of the interface direct shear test data and bentonite extrusion data are presented in Chapter 4. Engineering significance of the

investigation, including slope stability analyses that were conducted to determine effects of temperature on factor of safety, is presented in Chapter 5. Conclusions from the entire investigation are presented in Chapter 6.

Chapter 2: Literature Review

2.1 Introduction

This chapter provides an overview of information available related to landfill liner systems, clay behavior, landfill slope stability, GCL and geomembrane interaction, temperatures of MSW landfills, and temperature effects on geosynthetics. Up to 250 million metric tons of municipal solid waste (MSW) are generated in the United States per year (EPA 2012a). MSW landfills are engineered to safely store waste generated by homes, schools, hospitals, and businesses, which includes paper, food scraps, yard trimmings, and plastics among others (EPA 2012a). Moisture in the disposed waste and precipitation that interacts with the waste forms a contaminated liquid termed leachate. Decomposition of the waste creates high levels of methane, carbon dioxide, and other gases, which must be processed prior to release into the environment (Koerner 2005). The Resource Conservation and Recovery Act (RCRA) in 1967 required the environmentally harmful gases and leachate to be properly collected and disposed of, resulting in strict guidelines for MSW landfill design and operation (EPA 2012b). With more than 1,900 MSW landfills in the United States, knowledge of the design of these large facilities is critical (EPA 2012a). In order to minimize the exposure of leachate and harmful gases produced by the waste in landfills to the environment, polymer products termed geosynthetics are placed above and below the waste.

2.2 Landfill Liner System

2.2.1 Containment Systems

Geosynthetics perform a wide variety of functions: separation, reinforcement, filtration, drainage, and containment (Koerner 2005). In landfill liner applications, four of these five functions (as listed with the exception of reinforcement) are typically used in conjunction to prevent gas and leachate pollution. Separation and filtration are used to separate the gases and leachate from the waste (Yesiller and Shackelford 2010), drainage is used to remove the collected gases and leachate, and containment is used to prevent the gases and leachate from escaping into the environment (Koerner 2005). Containment (liner) systems are placed above and below the waste and consist of either single or double liners. Single liners consist of one layer of barrier system and are used for MSW, while double liners are used for hazardous waste containment and consist of two layers of barrier system with a leak detection system in between (Qian et al. 2002). Individual liners consist of either compacted clay or a geomembrane to line the waste, while composite liners utilize a geomembrane (GM) overlaying a compacted clay liner (CCL) or geosynthetic clay liner (GCL) to contain the waste (Figure 2.1) (Qian et al. 2002). Originally, containment systems were composed of single liner systems with individual liners; however, more modern containment systems use composite liners. The single liner system with a composite liner is used in both cover liner and bottom liner applications and is more effective than a single liner system with an individual liner (Yesiller and Shackelford 2010).

The engineered containment system below the waste is termed the bottom liner system, which is constructed prior to the placement of waste. A typical modern bottom liner system, from top to bottom, consists of a protective soil layer, a drainage layer (to remove leachate) and a composite liner system (for containment) (Yesiller and Shackelford 2010).

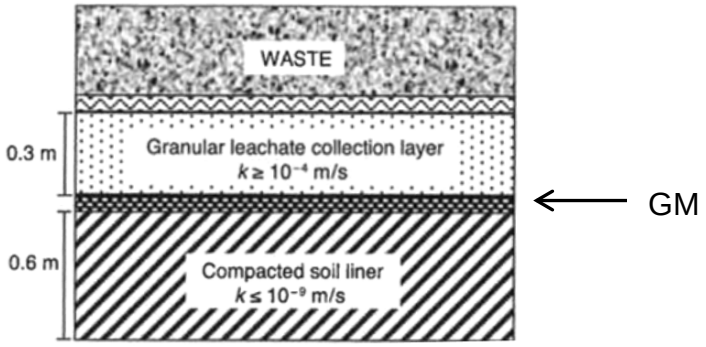

Figure 2.1. Composite Liner System with GM and CCL
(Yesiller and Shackelford 2010)

The engineered containment system above the waste is termed the cover liner system. Cover liner systems are constructed after the placement of waste and consist of from top to bottom an erosion layer (sometimes covered in vegetation to minimize erosion) in contact with the environment with a drainage layer below to remove any precipitation. Underlying the drainage layer is the liner system, which is typically a composite liner system, designed to prevent the gases produced in the waste from being released into the environment (EPA 2012a). Below the liner system is a protective soil layer and waste. A cross section of a typical cover liner system is displayed in Figure 2.2.

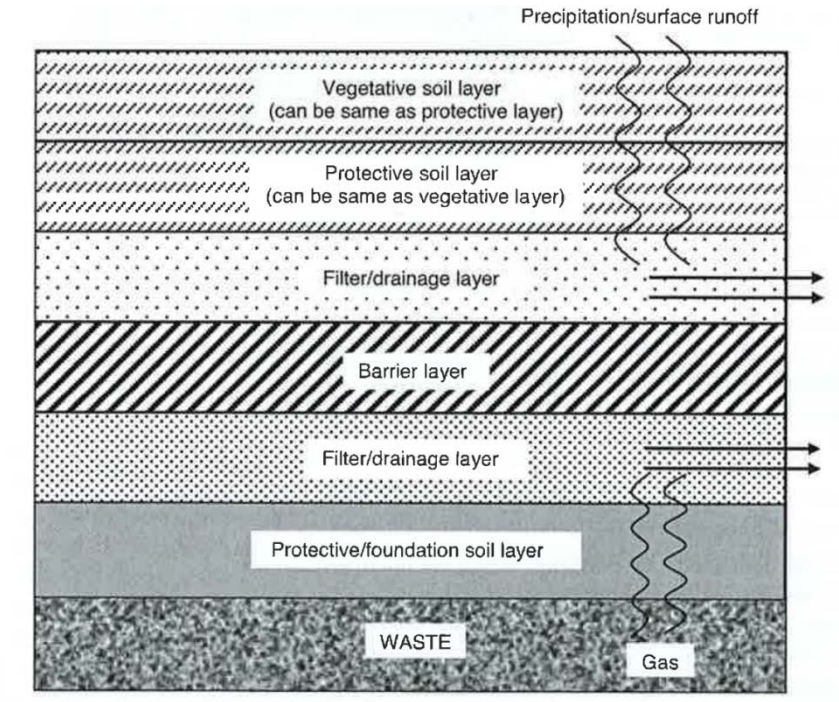

Figure 2.2. Typical MSW Cover Liner System (Yesiller and Shackelford 2010)

2.2.2 Geomembranes

Geomembranes (GMs) are thin sheets of flexible thermoplastic polymeric material. Hydraulic conductivity of GM ranges from $1x10^{-13}$ to $1x10^{-16}$ m/s and almost all applications of geomembranes are some form of hydraulic barrier (Qian et al. 2002). The three most commonly used geomembranes in the industry are high density polyethylene (HDPE), linear low density polyethylene (LLDPE), and polyvinyl chloride (PVC) (IFAI 2012). Due to its high chemical resistance and strength, HDPE is the most common geomembrane type in the United States, accounting for about 40% of total geomembrane sales (Koerner 2005). Landfill application is the primary use of HDPE geomembranes, as over 80% of HDPE geomembranes are sold for landfill use in the United States (Koerner 2005).

Geomembranes are manufactured by mixing pelletized polymer resin with antioxidants, plasticizers, fillers, and carbon black. The mixture is passed through an extruder and emerges as a molten material. The molten material is then passed through a die, resulting in a smooth sheet of controlled thickness ranging from 0.75 to 3.0 mm and a density of approximately 0.95 g/cm^3 (Frost et al. 2002). When a high friction surface is desired, textured geomembranes (T-GMs) can be used instead of smooth geomembranes. The primary texturing processes in North America are coextrusion and structuring, though coextrusion is far more common (Hebeler et al. 2005, Koerner 2005). The process of coextrusion generates a random, broad size range of textures on the freshly extruded smooth geomembrane (Figure 2.3). As the smooth geomembrane is extruded to create the textures, secondary extruders deliver molten resin with a blowing agent, forming bubbles. Textures are formed when the blowing agent cools and the bubbles break from the shearing action of the extruder. These random textures vary in size, shape, and placement. Macrotextures greater than 0.125 mm and microtextures less than 0.05 mm provide additional frictional resistance not present with smooth geomembranes (Hebeler et al. 2005). In comparison, structured geomembranes are manufactured by passing the smooth GM through a patterned mold, forming the structured pattern.

Figure 2.3. Cross Section View of Coextruded Textured Geomembrane (Hebeler et al. 2005, 10 mm wide)

2.2.3 Geosynthetic Clay Liners

A composite liner system is designed to minimize leachate or gas migration. The EPA requires a compacted clay liner of at least 600 mm thickness or a hydraulically equivalent structure below a geomembrane in a landfill composite liner system (Rowe and Brachman 2004). An acceptable replacement to a compacted clay liner is a geosynthetic clay liner (GCL) (EPA 2012c). GCL is a thin layer of compacted sodium granular bentonite typically sandwiched between two geotextiles.

The entire GCL product is approximately 6 mm thick (IFAI 2012). The geotextiles prevent loss of bentonite by mechanically binding the GCL through needle-punching, stitching, or chemical adhesives (EPA 2012c). Needle punching is a common type of binding due to strengthening of the GCL along the plane of the bentonite layer (Figure 2.4). GCLs are an acceptable replacement to CCLs because the sodium bentonite present in a GCL has a low hydraulic conductivity, typically less than 3.0×10^{-11} m/s (Yesiller and Shackelford 2010).

GCLs have multiple benefits over CCLs in landfill applications. The volume saved for waste placement by using a GCL instead of a CCL can amount to large cost savings. Installation of GCLs is much more simple and cost effective than installation of CCLs. CCLs may need to be imported from an offsite location and using a specified roller, compacted to a narrow range of specifications including moisture content and density (Yesiller and Shackelford 2010). GCLs, however, are delivered as a roll and installed by placing the GCLs over the desired area. CCLs have some benefits over GCLs in landfill containment applications, including greater resistance to puncture, a greater certainty for long term performance including resistance to diffusive flow (Rowe and Brachman 2004), and no potential problems with integrity of panel seams (Koerner 2005).

Figure 2.4. Cross Section of Needle Punched GCL (Koerner 2005)

2.2.4 Geotextiles

Geotextiles (GT) are defined by ASTM D4439-09 as “a permeable geosynthetic comprised solely of textiles.” Generally, two types of geotextiles are used in production of GCLs: woven and nonwoven. Woven geotextiles (W) are comprised of high tensile strength polymeric fibers which are woven, resulting in a thin sheet. Nonwoven geotextiles (NW) are comprised of similar polymeric

fibers that are introduced as a fibrous web to hundreds of specially designed barbed needles (Koerner 2005). The fibers reorient and tangle as the needles punch through the web, tightening it to a thin sheet (Koerner 2005). Geotextile mass is typically characterized in units of mass per unit area (g/m^2), which generally ranges from 150-800 g/m^2 and 90-300 g/m^2 for GTs in GCLs (IFAI 2012).

2.3 Clay Behavior

2.3.1 Clay Mineralogy

As rocks experience mechanical and chemical weathering, the mean particle size reduces. When certain minerals are chemically weathered, clay minerals can form (Holtz et al. 2011). Generally, clay minerals form in planar sheets of repeating lattices, which are comprised of densely packed oxygen anions and silicon or aluminum ions. Net negative charges on the mineral surfaces occur due to a process termed isomorphous substitution and presence of broken edges. Isomorphous substitution occurs when the ideal cation (e.g., Al^{3+} for montmorillonite) is replaced by a lower valence element (Mg^{2+}). In the case of montmorillonite, one Mg^{2+} is replaced for every sixth Al^{3+} (Mitchell 1993). To balance the negative charge deficiency caused by isomorphous substitution, cations are attracted to the surface and edges of the particles and exchanged depending on environmental conditions. The ease of cation exchange for a particular mineral is termed the cation exchange capacity (CEC). CEC is typically reported in milliequivalents of exchangeable cation per 100 g of dry soil and can vary from 0 to 150 or greater (Mitchell 1993, Yesiller and Shackelford

2010). The large net negative charge caused by isomorphous substitution results in a high CEC, and provides a large attraction to the mineral surface to available positively charged particles, including water (Mitchell 1993).

When available, the bipolar water particles or another liquid are attracted and squeeze between the negatively charged lattice sheets, causing the sheets to push apart resulting in swelling on a macroscopic level. The layer formed around the clay particles is called the diffuse double layer (DDL) (Mitchell 1993, Holtz et al. 2011). Due to the high level of electrochemical attraction between the liquid and clay particles, the liquid contained within the DDL becomes nearly immobile (Figure 2.5).

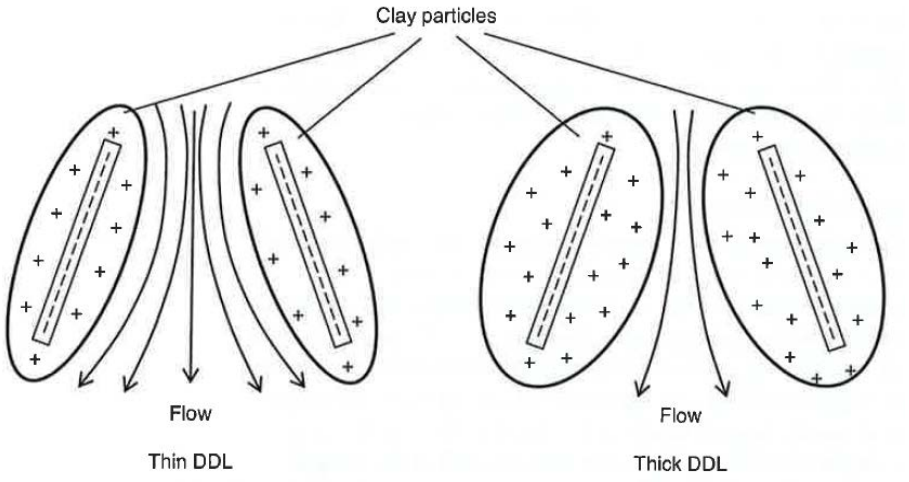

Figure 2.5. Effect of DDL Thickness on Flow (Yesiller and Shackelford 2010)

The three most common clay minerals are: kaolinite, illite, and montmorillonite (Yesiller and Shackelford 2010). The order from lowest to highest CEC possessed by each clay mineral is: kaolinite, illite, and montmorillonite. The clay contained in GCLs is sodium bentonite, which is primarily composed of montmorillonite. The large CEC can cause an increase in

the DDL thickness when in contact with a liquid and restrict flow between sodium bentonite particles. The flow restriction causes a decrease in hydraulic conductivity, which is the main contribution sodium bentonite provides to GCLs (Qian et al. 2002, Rowe and Brachman 2004).

2.3.2 Effect of Moisture on Clay Shear Strength

The shear strength of clay soil is dependent on the forces between adjacent clay particles. Water, especially in saturated soils, has a large effect on the interparticle forces with its dissolved electrolytes and by governing the distance between clay particles (Scott 1963). Unlike cohesionless soils, the behavior of cohesive soils (especially clays) is affected by the presence of water. An inverse relationship between shear strength and water content for cohesive soils has been suggested by Scott (1963) and Mitchell (1993) among others. Daniel et al. (1998) and Seo et al. (2007) indicated the shear strength of bentonite decreased significantly from 0 to 50% moisture content, but the shear strength at a water content of 50% was approximately the same as that of fully hydrated bentonite.

2.3.3 Consolidation of Clay Soil

Soil settlement occurs when soil is loaded or stressed and responds with deformation. Some soils deform instantaneously, while others require a relatively long time for deformation to occur. The rate of consolidation settlement of saturated clay soils is controlled by the rate water is able to squeeze out of the pores, which is governed by the hydraulic conductivity of a soil. As a saturated clay layer is loaded, the pore water pressure is increased beyond its static pore

water pressure. As water squeezes out of the pores, the pore water pressure decreases until eventually reaching a static level (Holtz et al. 2011).

In addition to hydraulic conductivity of the soil, drainage distance has an influence on the rate of consolidation. Drainage distance is defined as the distance the pressurized pore water must travel to be relieved. A 6-mm-thick saturated GCL subjected to loads causing excess pore pressure will have a drainage distance of only 3 mm assuming proper drainage is available on either side of the GCL. Proper drainage of either surface of the GCL should occur due to transmissivity of geotextiles (i.e., in-plane flow).

2.3.4 Effect of Temperature on Clay Soil

The behavior of clay can also be influenced by temperature. When clay is subjected to a change in temperature, changes in pore pressures and/or void ratio are possible. Thus, a coupled effect caused by a change in temperature can result in an increase or decrease in clay shear strength depending on the circumstances (Mitchell 1993). Sherif and Burrous (1969) performed a study in which the unconfined shear strength of kaolinite clay was measured at multiple temperatures above room temperature (24, 38, 52, and 66 ^{o}C). A trend of decreasing compressive strength of the clay with increasing temperature developed (Figure 2.6). The decreased compressive strength was attributed to decreased viscosity of the water in the DDL, increasing the pore water pressure and decreasing the effective stresses and shear strength of the soil (Sherif and Burrous 1969).

Similarly, Perkins and Sjursen (2009) conducted oedometer and triaxial tests on Troll Clay from the North Sea at 0 and 20 °C. The clay tested at 0 °C was measured to have an undrained shear strength between 8 and 21% larger than that of the clay tested at room temperature, confirming the trend of a higher temperature resulting in a lower shear strength.

Temperature can also affect consolidation of clay soil. Plum and Esrig (1969) performed consolidation tests on illite clay at 24 and 50 °C. The results indicated the higher temperature clay was more compressible when subjected to vertical stresses less than 210 kPa. The clay experienced similar compressibility under both temperatures when subjected to vertical stresses larger than 210 kPa.

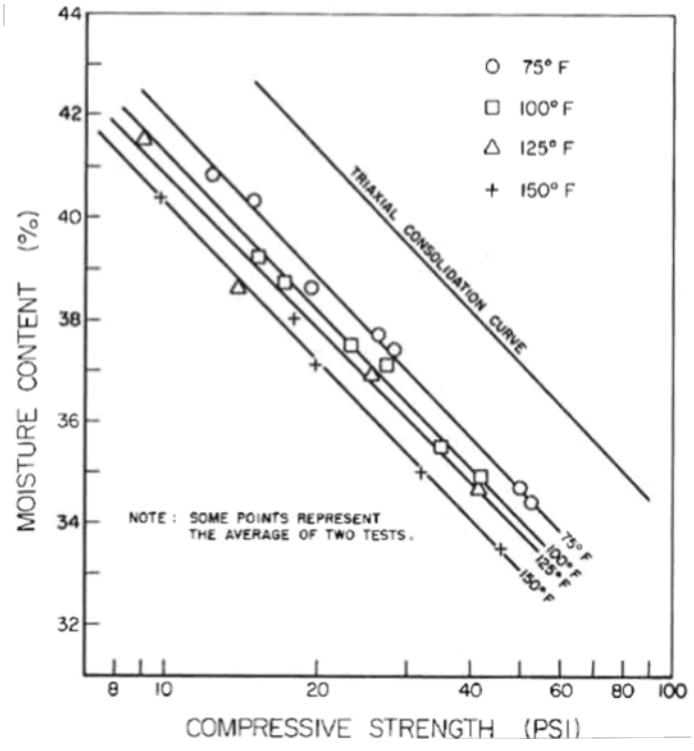

Figure 2.6. Effect of Temperature on Clay Compressive Strength (Sherif and Burrous 1969)

2.4 Landfill Slope Stability

Landfill geometry is designed to maximize the volume available for waste placement over a given area while maintaining geotechnical stability. Designing side slopes as steep as possible is one method to maximize waste volume in a landfill; however, an overly steep slope can result in slope stability issues, as geosynthetics can provide planes of weakness (Boutwell 2002, Qian et al. 2002).

Any failure involving the landfill liner can result in large remediation costs, especially if waste had been placed prior to failure (Qian et al. 2002). If a bottom liner fails, the waste must be removed and placed in a lined location, which may be very difficult to find nearby. Thus, an important aspect of landfill design consists of slope stability analysis. A summary of eight landfill slope failures involving geosynthetics within the last 25 years was collected from literature (Table 2.1). The eight summarized landfill failures is lower than the suspected number, as most landfill failures are not reported for political reasons (Jones and Dixon 1998). Of the eight reported slope failures, six failures were reported to be triggered by liquid. Thus, geosynthetics interface shear testing under varying moisture conditions is warranted.

Table 2.1: Summary of Geosynthetic Related Landfill Slope Failures

Reference	Failed Interfaces	Failure Year	Triggering Mechanism
Daniel et al. (1998)	T-GM/GCL	1994, 1995	Hydrated Bentonite
Koerner and Soong (2000)	Smooth GM/CCL	1988	Wetted GM/CCL
Koerner and Soong (2000)	Smooth GM/CCL	1994	Wetted GM/CCL
Koerner and Soong (2000)	Internal GCL (Unreinforced)	1996	Hydrated Bentonite
Koerner and Soong (2000)	Smooth GM/GT	1988	Static Failure
Blight (2004)	Smooth GM/GT	1997	Increased Pore Pressures
Amaya et al. (2005)	Smooth PVC GM/CCL	1997	Possibly Traffic Induced Shear Stresses
Blight (2007)	Unknown Cover Layer Other Than Smooth GM	1997	Increased Pore Pressures

2.5 GCL and Geomembrane Interaction

Failure in geotechnical engineering applications occurs when stress is applied beyond the maximum stress the material can sustain. With respect to landfill slope failures involving geosynthetics (specifically between two geosynthetics), the definition of failure can vary. Peak shear strength is the maximum shear stress that can be resisted along a geosynthetic interface. Large-displacement shear strength is a constant minimum shear stress after the peak shear strength has occurred (Thiel 2001).

Much attention (Triplett and Fox 2001, Fox and Stark 2004, McCartney et al. 2009a) has been given to the interface shear strength of GCLs and geomembranes due to their common use and low shear strength of hydrated sodium bentonite (which can result in a potential failure surface. Investigation of

internal shear strength of GCLs is not as critical, as the use of needle punched (NP) reinforced GCLs has resulted in internal shear strengths to be greater than interface shear strengths under the majority of investigated normal stresses (McCartney et al. 2002, Fox and Stark 2004, Zornberg and McCartney 2009, McCartney et al. 2009a). Many researchers have investigated the shear resistance along geosynthetic interfaces, specifically between GCLs and geomembranes (e.g., Hewitt et al. 1997, Triplett and Fox 2001, Fox and Stark 2004, Seo et al. 2007, Vukelic et al. 2008, McCartney et al. 2009a, Zornberg and McCartney 2009, and Chen et al. 2010). The majority of GCL interface shear research reported uses a large scale direct shear device to determine the interface shear strengths between GCLs and geomembranes (Hewitt et al. 1997, Triplett and Fox 2001, Fox and Stark 2004, McCartney et al. 2009a).

2.5.1 Direct Shear Testing

The testing methodology described in ASTM standard D 6243-09 "Standard Test Method for Determining the Internal and Interface Shear Resistance of Geosynthetic Clay Liner by the Direct Shear Method" was adopted by Triplett and Fox (2001), McCartney et al. (2002), Fox and Stark (2004), McCartney et al. (2004), and McCartney et al. (2009a). ASTM D 6243-09 describes the apparatus as "a rigid device to hold the specimen securely and in such a manner that a shear force without torque can be applied to the tested interface". A schematic of a typical large scale direct shear apparatus is presented in Figure 2.7. The top box is locked in place while the bottom box displaces at a predetermined constant rate. The resulting shear stress is

measured and recorded to determine the peak and large-displacement shear strengths.

A 300 mm by 300 mm or larger specimen size has been commonly used with interface shear testing (Fox and Stark 2004, Seo et al. 2007, Chen et al. 2010). Generally, the dimensions of one specimen are larger than the other so as one specimen displaces, the shearing area can remain equal throughout the test.

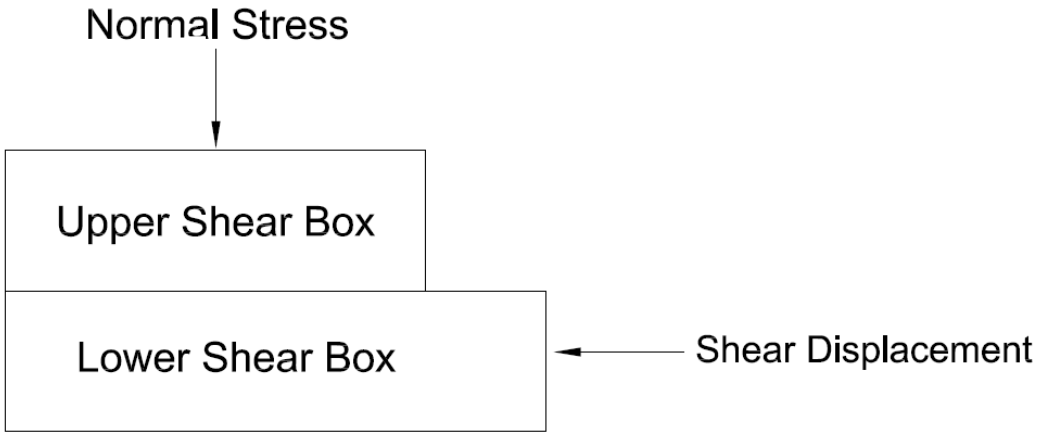

Figure 2.7. Graphic of Typical Direct Shear Device

2.5.2 Interface Shear Strength

At least three shear tests under different normal stresses must be performed to obtain frictional and adhesive properties between two interfaces (ASTM 2012d). The three graphs with shear stress as a function of displacement should be plotted, as in Figure 2.8.

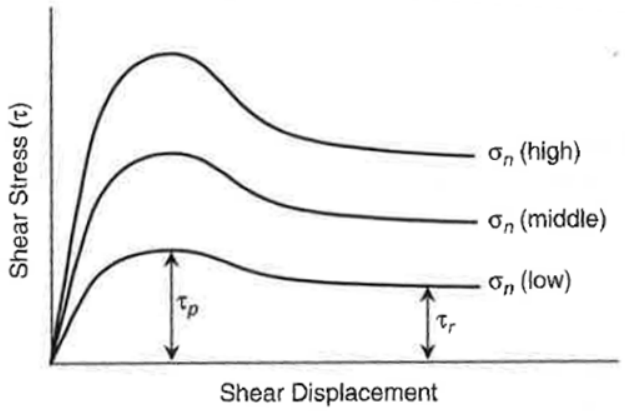

Figure 2.8. Shear Stress versus Displacement under Three Normal Stresses (Koerner 2005)

The peak or large-displacement stresses for all three curves should be plotted against their respective normal stresses. The three points are connected with a best fit line to construct a Mohr Coulomb failure envelope.

$$\tau = \sigma_n \times \tan(\delta) + a \quad (1)$$

Where:

τ = interface shear strength (kPa)

σ_n = normal stress (kPa)

δ = interface friction angle (degrees)

a = adhesion (kPa)

The slope of the line is equal to tan(δ) and the τ intercept (y-axis) is defined as the adhesion between the two interfaces. The interface shear strength envelope is described by Equation 1.

Similar to soils, failure envelopes for geosynthetic interfaces are often non-linear. The failure mode of a geosynthetic test specimen can change as a function of normal stress, possibly resulting in a curvilinear failure envelope

(Figure 2.9). Therefore, extrapolation of the failure envelope beyond the tested stress range is not recommended (Fox and Stark 2004).

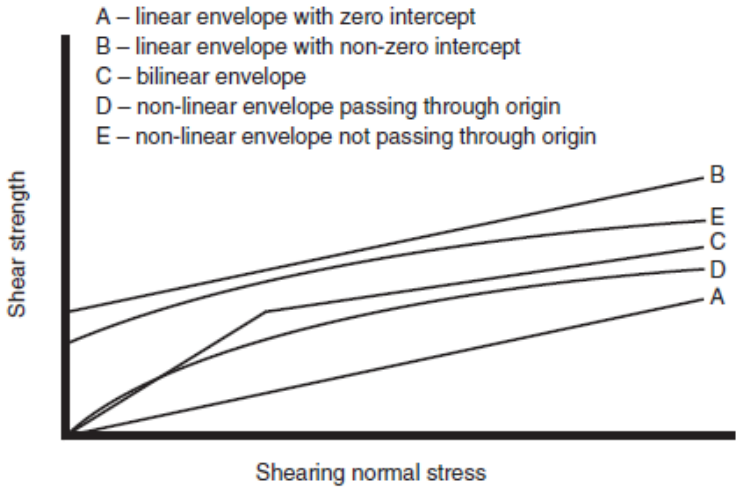

Figure 2.9. Typical GCL Failure Envelopes (Fox and Stark 2004)

2.5.3 Hook and Loop Interaction

The effectiveness of replacing smooth GMs with textured GMs for increased shear resistance along a nonwoven geotextile has been well documented (Stark et al. 1996, Fox and Stark 2004, McCartney et al. 2009a). Stark et al. (1996) reported a 300% increase in peak shear strength and 200% increase in large-displacement shear strength when shearing textured GMs compared to smooth GMs against nonwoven geotextiles. Most of the increase in shear strength is contributed by a mechanism termed “hook and loop” interaction.

The mechanism of hook and loop interaction is analogous to that of Velcro (Hebeler et al. 2005), where the asperities (i.e., textures) on the GM act as the hooks, and the nonwoven filaments (i.e., fibers) act as the loops. Normal stress can affect the extent of hook and loop interaction because of the wide distribution

of macrotextures and microtextures available to interact with nonwoven geotextile filaments (Figure 2.10).

Bacas et al. (2011) determined that the following factors caused an increase in shear resistance along a textured GM and a nonwoven geotextile: greater asperity height (texture height) of the GM, and increased normal stress. When the interface is subjected to low normal stress, the GM textures and geotextile filaments interact on a surficial level (Hebeler 2005). However, when the interface is subjected to high normal stress, the GM textures become increasingly embedded in the geotextile filaments, increasing the shear resistance (Hebeler 2005, Bacas et al. 2011).

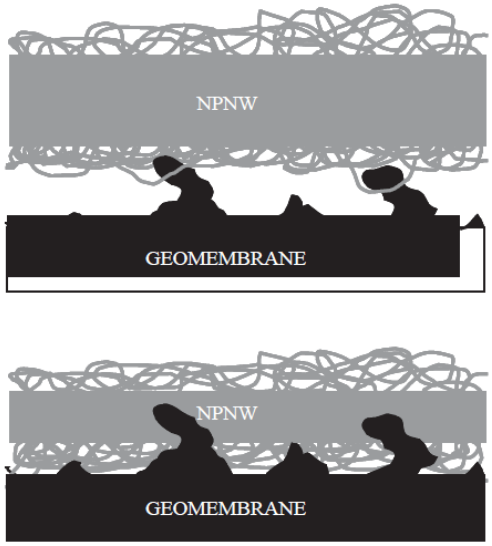

Figure 2.10. Sketch of Interaction of T-GM/NW GT Interface under Low and High Normal Stress (Hebeler 2005)

2.5.4 Post-peak Shear Interaction

Post-peak strength loss of up to 60% has been observed in T-GM/NW GT interfaces (Stark et al. 1996, Triplett and Fox 2001). Damage to the shearing material surfaces was considered the primary cause. Stark et al. (1996) and Seo

et al. (2007) observed significant changes in NW GTs and T-GMs after shearing. Observation of scanning electron microscope images provided visual evidence of random orientation of fibers prior to shearing and “combing” and tearing of the fibers in an oriented manner to the shearing direction after shearing (Figure 2.11). Polishing of T-GM asperities (decrease in asperity height), especially under higher normal stresses, also contributed to post-peak strength loss (Stark et al. 1996, Seo et al. 2007). Limited data is available regarding investigation of the effects of temperature on structure of the shearing surfaces.

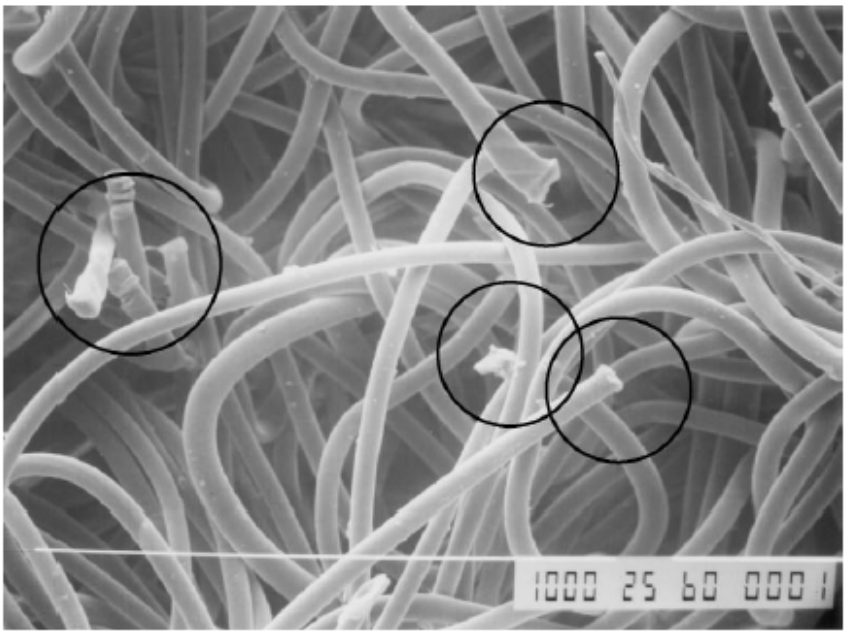

Figure 2.11. Breakage of GT Fibers Imaged after Shearing of T-GM/GT Interface (Seo et al. 2007)

2.5.5 Exhumed GCL Moisture Content

GCLs in the cover liner system can be exposed to moisture from above by any leaking of precipitation, or from below, where vaporization of moisture from the waste mass can occur. GCLs in the bottom liner system can be exposed to

moisture from above by any leaking of leachate through the overlying GM, or from below, where GCLs can absorb moisture from underlying soil. Koerner (2005) reported bentonite water contents in a GCL can reach 50% when exposed to overlying sand with a water content of 1% and can reach over 175% when exposed to overlying sand with a water content of 17%. Olsen (2012) conducted field simulation tests to determine GCL moisture content as a function of subgrade moisture content. GCL specimens were placed in a sealed container over subgrade, which was clay or sand, at a specific moisture contents. Sand with a moisture content of 2% resulted in GCL moisture contents between 47% and 78%. Sand with a moisture content of 8% resulted in GCL moisture contents between 75% and 150%. Dry of optimum clay compacted with a moisture content of 8% resulted in GCL moisture contents between 20% and 25%. Clay compacted wet of optimum with a moisture content of 16% resulted in GCL moisture contents between 78% and 125%.

Benson et al. (2007), Meer and Benson (2007), and Scalia and Benson (2011) conducted field sampling of GCLs by exhuming GCLs from existing cover liner systems. A total of 75 GCL samples were exhumed from cover liner systems with and without vegetative cover liner and GCL moisture contents were determined.

Benson et al. (2007) exhumed 11 GCLs from the final cover liner of a coal ash landfill to investigate elevated percolation rates. Six GCLs were exhumed without a vegetative cover liner and were determined to have a moisture content ranging from 59 to 69% with a mean of 63%. Five GCLs exhumed with a

vegetative cover liner were determined to have a moisture content ranging from 18 to 26% with a mean of 21%.

Meer and Benson (2007) exhumed 28 GCLs from four sites with cover liner systems (one with a GM/GCL composite liner and three with only GCLs) after being in service from 4.6 to 11.1 years. The GCLs were exhumed to determine the effects of ion exchange on hydraulic conductivity tests. The moisture contents ranged from 32.5 to 204.2% with a mean of 78.6%.

Scalia and Benson (2011) exhumed 36 GCLs from four composite liner cover liner systems after being in service from 4.7 to 6.7 years to conduct hydraulic conductivity tests. All four cover liner systems contained vegetation above and soil above and below the composite liner. The water contents of the exhumed GCLs ranged from 18 to 70% with an average moisture content of 47.5%. Moisture contents of the underlying soils ranged from 2.3 to 16%.

Daniel et al. (1993) indicated that GCLs were typically expected to reach full hydration in the field unless encapsulated by two geomembranes. The investigation of GCL shear strength using direct shear in saturated condition typically results in GCL moisture content above 100% (Fox and Stark 2004). However, data produced by Benson et al. (2007), Meer and Benson (2007), and Scalia and Benson (2011) indicates the moisture content of GCLs in cover liner systems typically reside between 15 to 105%, which are mostly unsaturated. A summary of the frequency of exhumed GCL moisture contents is displayed in Figure 2.12. Limited data is available related to the effects of moisture content

on GCL interface shear strength over a representative range of moisture contents to field conditions.

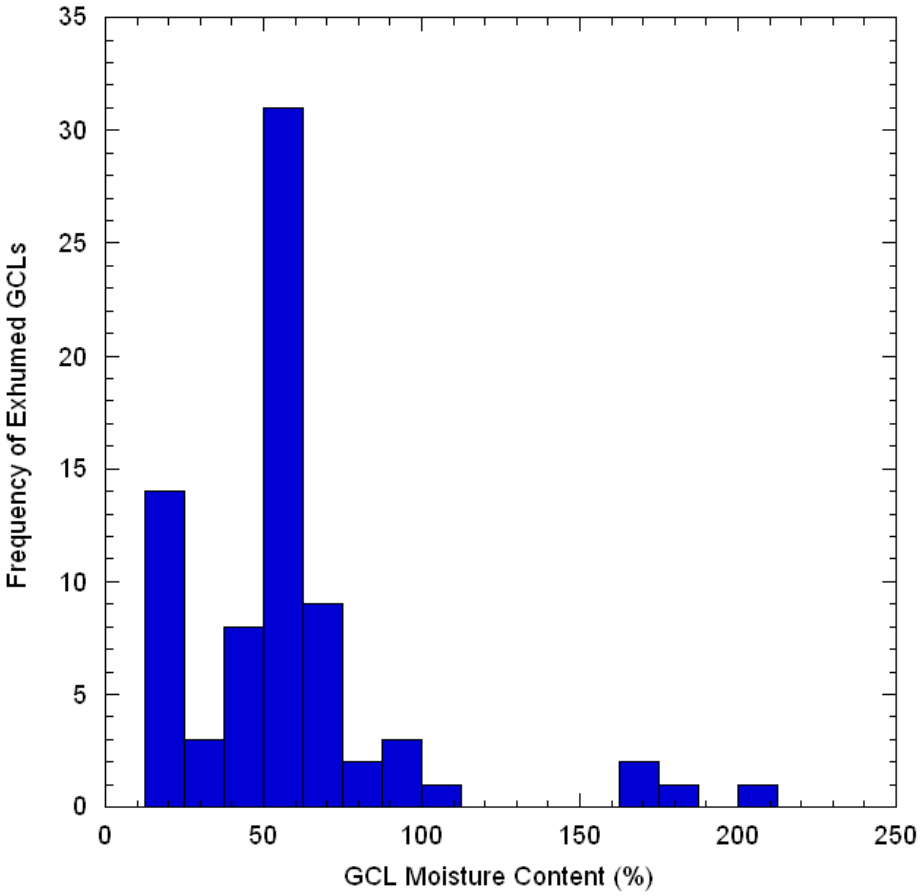

Figure 2.12. Frequency of Compiled Exhumed GCLs by Moisture Content (Graphic Assembled Using Data from Benson et al. 2007, Meer and Benson 2007, Scalia and Benson 2011)

2.5.6 Bentonite Extrusion

When a GCL is sheared along another surface under an appreciable normal stress, hydrated bentonite can squeeze through the nonwoven fibers, resulting in bentonite being deposited on the interface. This mechanism is called bentonite extrusion. Between a textured GM and a GCL, the bentonite can act as a lubricant, decreasing the interface friction angle (Seo et al. 2007). As the

moisture content increases, the bentonite becomes less viscous, increasing the amount of extrusion (Seo et al. 2007, Vukelic et al. 2008, Chen et al. 2010). Vukelic et al. (2008) reported that bentonite primarily extrudes through woven geotextiles and through thin nonwoven geotextiles (having mass per unit area less than 220 g/m^2). The amount of bentonite extruded generally increases as the geotextile becomes thinner, the bentonite is wetted, and more water flows to the interface during consolidation (Fox and Stark 2004). This trend also demonstrates the need to investigate interface shear strength as a function of moisture content.

2.5.7 GCL Shear Testing and Hydration

A GCL specimen should be allowed to fully hydrate prior to testing to measure conservative shear strengths. Hydration for up to 3 weeks may be necessary; however, many production laboratories hydrate GCLs for 1 to 2 days (Fox and Stark 2004). Incomplete hydration may result in unconservative interface shear strengths. Thus, using proper accelerated hydration procedure is critical to complete testing at relatively low costs while providing accurate measurement of GCL shear strength (Fox and Stark 2004).

Fox et al. (1998) proposed a 4-day 2-stage accelerated hydration method for GCL shear testing, which has since been used directly by Triplett and Fox (2001), Fox and Stark (2004), and Fox et al. (2004); and as a basis for methodology by McCartney et al. (2004), Seo et al. (2007), Vukelic et al. (2008), McCartney et al. (2009b), and Chen et al. (2010).

Stage 1 involves placing the GCL specimen in a shallow pan with sufficient tap water to allow the GCL to reach the final desired moisture content before shearing (which is generally above 100%, Fox and Stark 2004). Fox and Stark (2004) indicated that tap water is commonly used as the hydration liquid due to convenience and its comparable chemistry to pore water of most soils. Using tap water as the hydration liquid provides a conservative shear strength relative to mild leachate, harsh leachate, and diesel fuel (Koerner 2005). The GCL is then covered to prevent change in moisture and is allowed to hydrate for 2 days with 1 kPa normal stress to prevent free swelling.

Stage 2 involves the GCL being placed in the shearing device with free access to tap water and allowed to consolidate for two days under the desired shearing normal stress. The accelerated hydration procedure proposed by Fox et al. (1998) maximizes the number of GCL shear tests that can be conducted in a given period, as a GCL specimen is occupy the shearing device for only two days. After completion of stage 2, the GCL specimen is sheared.

2.5.8 Effects of Moisture Content on Interface Shear Strength

Limited data is available regarding investigation of the effects of moisture on T-GM/GCL shear strength by targeting GCL or bentonite moisture contents. McCartney et al. (2004) and McCartney et al. (2009a) reported that unhydrated GCL specimens had a higher peak and large-displacement interface shear strength than hydrated specimens. Seo et al. (2007) investigated the effects of wet condition on interface shear strength, where T-GMs were sheared against a GT and a GCL under both wet and dry conditions. The GCLs were hydrated in

both constrained (CH, low hydration normal stress) and free swelling (FS, no hydration normal stress) conditions. Seo et al. (2007) reported the T-GM/GT interface had a lower δ at dry than wet condition and T-GM/GCL had a lower δ at wet than dry condition (Figure 2.13). Seo et al. (2007) determined that the water may have worked as an adhesive, or absorbed in the geotextile fibers to cause the fibers to become more pliable and more able to grip the GM textures. The opposite relationship of interface friction angle with moisture content between these two interfaces is likely due to the presence of bentonite.

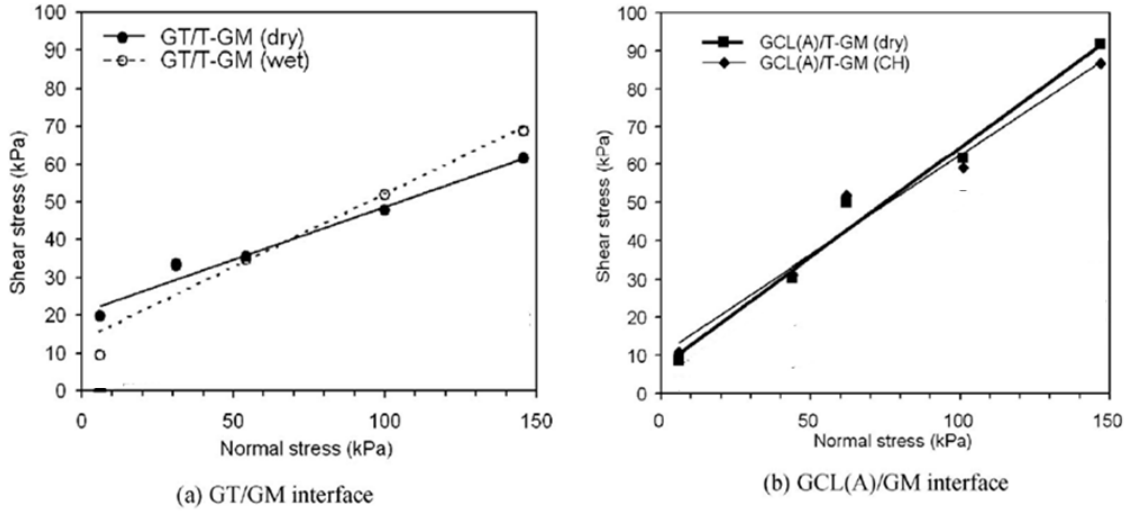

Figure 2.13. Interface Shear Strengths of (a) T-GM/GT and (b) T-GM/GCL under Wet and Dry Conditions (Seo et al. 2007)

2.5.9 Effect of Hydration Normal Stress on Shear Strength

One of the factors controlling the moisture content of bentonite in a GCL is the hydration stress. Lower normal stress during hydration of the GCL allows the bentonite to absorb additional moisture and swell. Thus, applying a hydration normal stress representative of GCL field conditions prior to shearing is critical to obtaining representative results (Fox and Stark 2004). For bottom liner systems

where GCLs are placed in contact with damp soil, GCLs are generally hydrated before waste placement, so the hydration normal stress is minimal (Fox and Stark 2004). For cover liner systems, relatively small normal stresses (overburden of vegetation, soil, and geosynthetics) are applied on the GM and GCL.

McCartney et al. (2004) reported relationships of decreasing interface shear strength with both decreasing hydration stress and with increasing hydration time. In both cases, the decrease in interface shear strength was caused by increased bentonite moisture content resulting in increased bentonite extrusion (McCartney et al. 2009b). McCartney et al. (2009a) reported GCL hydration beyond 24 hours had little effect on shear strength for T-GM/NW GCL interfaces.

2.5.10 Effect of Consolidation on Shear Strength

If the hydration normal stress is less than the shearing normal stress, consolidation of the GCL specimen after hydration is generally necessary (McCartney et al. 2009a). Once consolidation of the GCL specimen is completed, shearing can occur (Fox and Stark 2004). Fox et al. (1998) allowed 48 hours to complete consolidation in the original 2-stage 4-day procedure. Triplett and Fox (2001) recorded vertical displacement and interface pore pressure between interfaces of GCLs and textured GMs at normal stresses between 6.9 and 486 kPa. All specimens reached equilibrium within the 48 hour consolidation period (Figure 2.14). One exception was a specimen loaded under

a normal stress of 6.9 kPa, which experienced a change in vertical displacement after 48 hours, likely due to swelling (Triplett and Fox 2001).

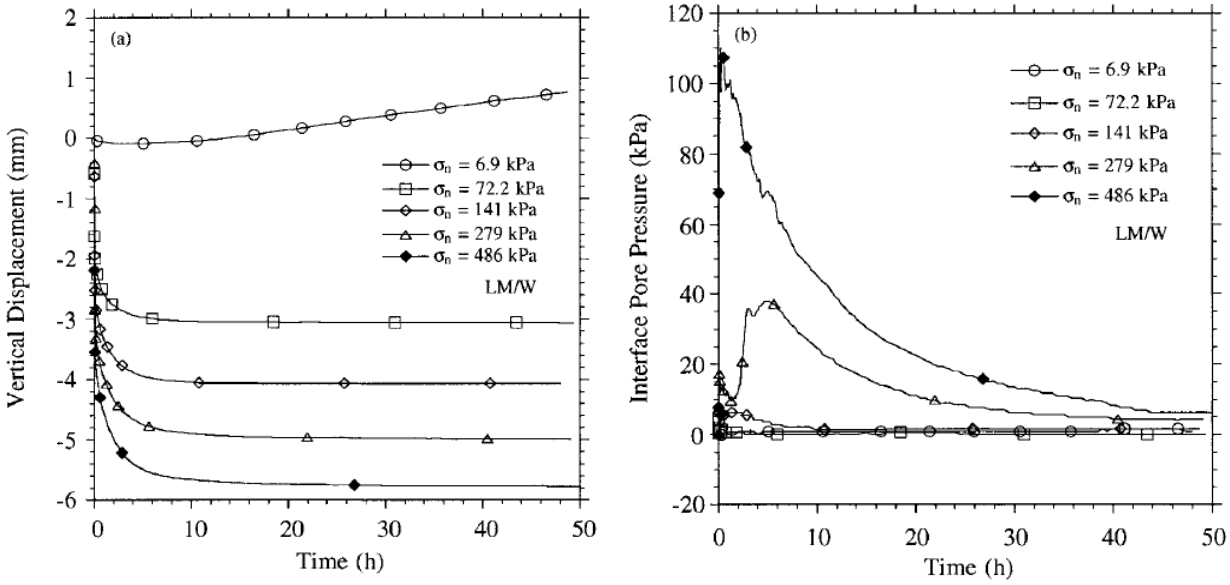

Figure 2.14. GCL (a) Vertical Displacement and (b) Interface Pore Pressure Measurement with Time (Triplett and Fox 2001)

2.5.11 Effect of Consolidation Load Application Rate on Shear Strength

Multiple authors have discussed the importance applying of the consolidation normal stress in small increments over many hours rather than rapidly applying the shearing normal stress in one step (Triplett and Fox 2001, McCartney et al. 2009a, Chen et al. 2010). Large excess pore pressures can develop and increased bentonite extrusion can occur in response to rapid loading potentially, affecting the shear strength results. Multiple methods for applying consolidation normal stress have been recommended. Fox and Stark (2004) recommended using continuous loading (consolidation loads increased

continuously over a period of time) or incremental-loading consolidation procedures (consolidation loads applied using daily or half daily increments). Although continuous loading can be the most effective consolidation method (i.e., minimizing detrimental effects of rapid development of excess pore pressure), many laboratories do not have the available equipment for such load application. In addition, Fox and Stark (2004) indicated that no accelerated procedure currently exists to rapidly consolidate hydrated GCLs besides simultaneously consolidating multiple GCL specimens outside the shear box.

2.5.12 Specimen Gripping

Gripping of GCL and T-GM specimens is essential for representative measurement of interface shear strength (Fox and Kim 2008). Gripping surfaces transfer the shear stress to the test specimen rather than allow the specimens to experience progressive failure. Progressive failure results in shear displacement along surfaces other than the desired shearing interface. The most representative recorded shear strength occurs when the intended failure surface has the lowest shear resistance of any possible sliding surface.

Various gripping methods for GCLs and GMs have been used by investigators. GCL gripping surfaces must allow drainage, as excess pore pressures often develop during consolidation and shearing of GCLs. Triplett and Fox (2001) used modified metal truss plates (with sharpened teeth 1-2 mm long) to grip the GCL and glued the GM specimen to the pullout plate. Fox and Stark (2004) used a rough gripping surface for both GCL and GM specimens in addition to clamping the geosynthetics. McCartney et al. (2009a) clamped the

GM to the bottom shear box and wrapped the GCL around a rigid porous substrate with steel gripping teeth to allow transfer of shear stress to the GCL. Fox and Kim (2008) investigated the effects of progressive failure on the shear strength of a T-GM/GCL interface in which the T-GM and GCL were gripped using multiple methods. Four interface shear tests were conducted with glued T-GM and four were run with clamped T-GM. The peak shear stresses of the tests using clamped GMs were lower, and displacements were larger compared to the glued GMs (Figure 2.15).

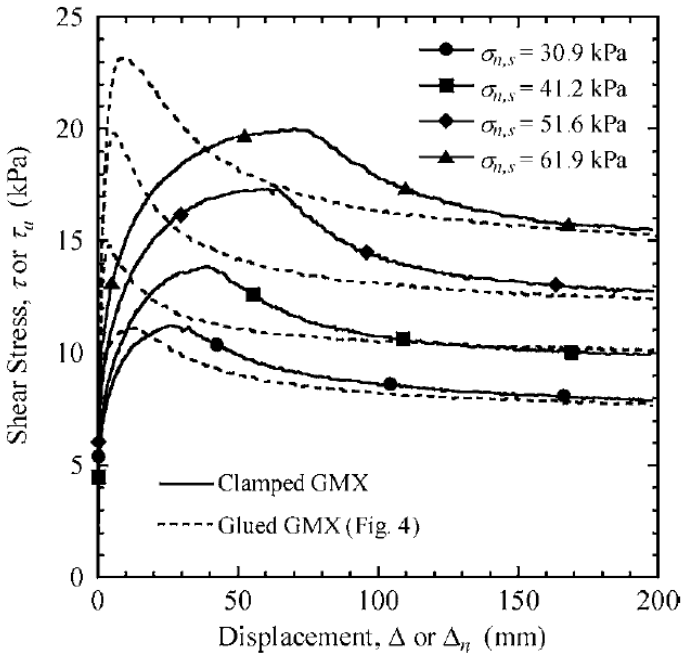

Figure 2.15. Stress-Displacement Relationships for Glued and Clamped T-GM/GCL Interface Shear Tests (Fox and Kim 2008)

2.5.13 Shear Displacement Rate

Shear displacement rate (SDR) is an important aspect of direct shear testing mainly due to development of excess pore pressures caused by shearing,

which can affect the shear strength results. The maximum allowable SDR is generally selected due to time and cost considerations (Fox and Stark 2004). Investigations by Triplett and Fox (2001), Fox and Stark (2004), and McCartney et al. (2009a) indicated that a displacement rate of 1 mm/min is acceptable for textured GM and GCL interfaces because SDR less than 1 mm/min had little effect on interface shear strength. Fox and Stark (2004) reported that SDR generally affected internal shear GCL testing more than interface shear testing due to the higher reliance on bentonite component.

2.5.14 Shear Displacement

Interface shear tests can only reach correct peak and large-displacement shear stresses if specimens are properly gripped. Triplett and Fox (2001) concluded that T-GM/GCL interfaces reached their peak shear stress at approximately 7 to 21 mm of horizontal displacement. Fox and Stark (2004) determined a specimen should be sheared to a minimum displacement of 50 mm to properly determine the large displacement shear stress for a T-GM/GCL interface.

2.5.15 GCL Specimen Preparation

ASTM D5993-99 indicates that “GCL test specimens should be trimmed from the GCL roll using a sharp utility knife or scissors”. Bentonite lost from exposed edges of the specimen can have a significant impact on accuracy of results (ASTM 2012c). A reported method to reduce bentonite loss is to wet the edge of the specimen prior to cutting (Fox and Stark 2004).

2.6 Temperatures in MSW Landfills

Decomposition of organic components in MSW waste results in generation of heat. Factors such as depth of waste, rate of filling, waste properties, and particularly waste moisture content were determined to affect waste temperature (e.g., Rowe 1998, Yesiller et al. 2005, and Hanson et al. 2010). Maximum temperatures occur at middle depths of the landfill and have been reported to occur approximately between 1 and 10 years and may potentially be longer. Shallow depths yield temperatures similar to seasonal air temperatures and depths near the base yield elevated temperatures intermediate to temperatures of shallow and middle depths (Yesiller et al. 2005).

Koerner and Koerner (2006) reported bottom liner temperatures between 18 and 46 °C. Cover liner system temperatures have been reported by Yesiller et al. (2008) and Koerner and Koerner (2006). Yesiller et al. (2008) reported cover liner system temperatures from landfills in four sites: Michigan, New Mexico, Alaska, and British Columbia (4 distinct climatic conditions). Sensor arrays were placed parallel and perpendicular to the cover liner systems. Cover liner temperatures approximately up to 34 °C and as low as 2 °C were reported. Hanson et al. (2005) reported GCL temperatures as low as -1 °C in a bottom liner system prior to the placement of waste. Koerner and Koerner (2006) reported cover liner system temperatures from landfills at two sites where thermocouples were placed along the cover liner and bottom liners. The cover liner temperatures ranged from approximately 0 to 36 °C. Bottom liner temperatures of up to 46 °C

were recorded. Thus, temperatures can be expected to reach approximately 0 to 40 °C for cover liner systems and 20 to 40 °C for filled bottom liner systems.

2.7 Temperature Effects on Geosynthetics

As discussed in previous sections, the interface shear strength of GCLs and GMs has been well documented as a function of hydration conditions (e.g., hydration normal stress) and consolidation of GCLs, normal stress, and other parameters. However, almost all interface shear testing has been performed at approximately 20 °C, even though landfill liners are commonly exposed to temperatures both significantly warmer and colder than standard laboratory conditions. Therefore, investigation into temperature effects on interface shear strength is important in order to accurately design landfill slopes. Investigation of the effects of temperature on the interface shear strength of geosynthetics is highly limited.

2.7.1 Previous Investigations into Temperature Effects on Geosynthetics

Akpinar and Benson (2005) investigated the effects of four temperatures (0, 10, 21 and 33 °C) on the shear strength of HDPE GM (smooth and textured) and NW-GT interfaces at normal stresses ranging from 7.5 to 49.5 kPa. The T-GM/GT interface friction angle increased 2.3° when subjected to an increase from 0 to 33 °C (Figure 2.16). Karademir and Frost (2011) investigated the effects of three temperatures (21, 35, and 50 °C) on the shear strength of HDPE T-GM and NW-GT at three normal stresses (100, 200, and 400 kPa). A relationship of increasing shear strength with increased temperature was established at all three normal stresses (Karademir and Frost 2011).

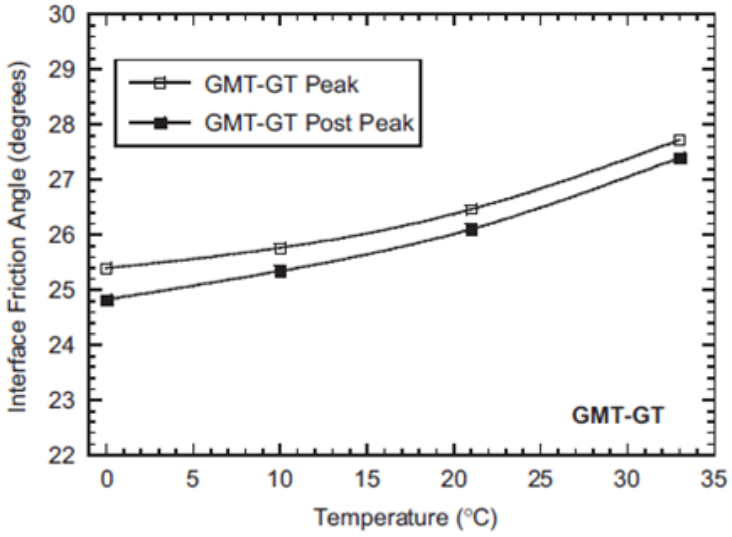

Figure 2.16. Interface Friction Angles of T-GM/GT as a Function of Temperature (Akpinar and Benson 2005)

2.7.2 Polymer Structure

HDPE geomembranes and nonwoven geotextiles are primarily composed of polyethylene and polypropylene, respectively. Both polymers are thermoplastic materials, meaning the material can soften and flow under heat and pressure (Ebewele 1996).

Polyethylene is comprised of repeating units of a carbon (C) atom bonded to two hydrogen (H) atoms (Figure 2.17) (Koerner 2005). The repeating units form long chains, resulting in a tough plastic solid (Sperling 2006). Polypropylene is comprised of repeating units of two hydrogen (H) atoms bonded to a carbon (C) atom, which is bonded to a CH_3 molecule and an H atom (Figure 2.18) (Koerner 2005).

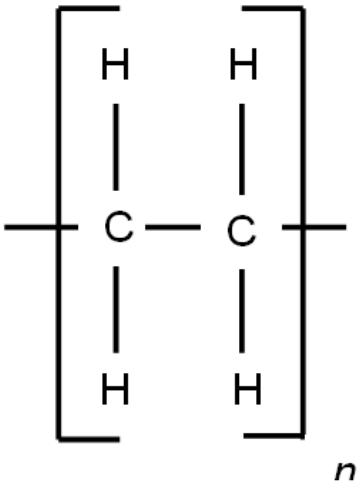

Figure 2.17 Polyethylene Repeating Unit in Chain (adapted from Koerner 2005)

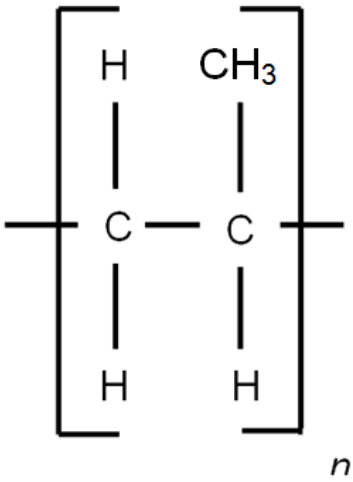

Figure 2.18. Polypropylene Repeating Unit in Chain (adapted from Koerner 2005)

Polymers can be cooled into two molecular arrangements: amorphous and crystalline. An amorphous arrangement is caused by randomly coiled and entangled polymer chains, resulting in a soft and pliable material. A crystalline arrangement is caused by individual chains folded and packed in a regular order,

resulting in a tough and hard material. Polymers may be both amorphous and crystalline.

2.7.3 Thermal Transitions in Polymers

Unlike water molecules where phase changes occur over a minimal temperature change, thermoplastic polymers change phases gradually over a larger temperature range (Ebewele 1996). Two main transition temperatures of polymers exist, displayed in Figure 2.19: glass transition (T_g, (2)) and melting temperature (T_m, (4)). Temperatures below T_g yield a material with a high modulus (solid, (1)), while temperatures above T_m yield a material with a low modulus (liquid, (5)). The intermediate temperatures result in a material with rubbery properties (3) (Sperling 2006).

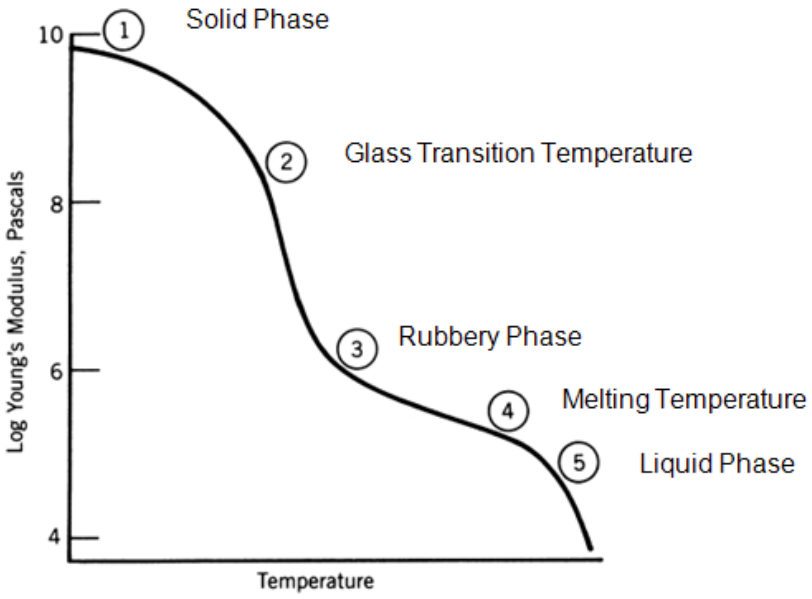

Figure 2.19. Polymer Phases with Temperature (Sperling 2006)

Thermoplastic polymers experience a decrease in modulus with increasing temperature because the linear and branched molecules, which are not chemically tied together, allow the chains to slide past each other under increasing temperatures (Ebewele 1996). The glass transition temperature of polyethylene and polypropylene was determined to be approximately -120 ˚C and -10 ˚C, respectively. Polyethylene has a melting temperature of 135 ˚C, while polypropylene has a melting temperature of 176 ˚C (Ebewele 1996). Thus, the behavior of both polymeric materials resides in the intermediate rubbery phase in most landfill applications.

Despite extensive investigation of T-GM/GCL interface shear strength, the effects of temperature and field representative moisture contents have been largely neglected. Interface shear testing of T-GM/GCLs is almost exclusively performed at laboratory temperatures and with GCLs in submerged or as-received condition. Therefore, an investigation of temperature and moisture on T-GM/GCL interface shear strength is warranted.

Chapter 3: Testing Program

3.1 Introduction

An interface shear testing program was conducted to determine the effects of temperature, moisture content, and normal stress on interface shear strength between textured geomembranes (T-GM) and geosynthetic clay liners (GCLs). Interface shear strengths were measured using large-scale interface direct shear tests under representative field conditions. Targeted temperatures and moisture contents were tested, unlike the majority of previous investigations of T-GM/GCL interface shear strength (Hewitt et al. 1997, Triplett and Fox 2001, Fox and Stark 2004, McCartney et al. 2004, Seo et al. 2007, Vukelic et al. 2008, McCartney et al. 2009a, Zornberg and McCartney 2009, and Chen et al. 2010).

A supplemental investigation was conducted to determine the effects of temperature, moisture content, and normal stress on bentonite extrusion from GCLs. Bentonite extrusion was measured by applying normal stress on a GCL specimen using a 1-D consolidometer. Targeted temperatures and moisture contents were tested and level of bentonite extrusion was quantified.

3.2 Interface Shear Testing Program

3.2.1 Test Materials

One type of GCL and one type of T-GM were selected for the testing program. The geosynthetics tested are among the most commonly used products in MSW landfill bottom and cover liner systems.

3.2.1.1 GCL

The GCL selected for the investigation was Bentomat DN, which is manufactured by CETCO Lining Technologies. The GCL was selected because of its common use in landfill slope applications (CETCO 2011). Bentomat DN properties are presented in Table 3.1.

Table 3.1. Bentomat DN Reported and Measured Properties

Bentomat DN Properties	Value	Reference
Reported Bentonite Mass Per Unit Area (g/m^2)	3660	IFAI 2012
Reported Total Dry GCL Mass Per Unit Area (g/m^2)	4060	IFAI 2012
Reported GT Mass Per Unit Area (g/m^2)	200	IFAI 2012
Measured Bentonite Mass Per Unit Area (g/m^2)	4350	ASTM D5993-99
Measured Total Dry GCL Mass Per Unit Area (g/m^2)	4750	ASTM D5993-99
Reported Needle-Punched Peel Strength (N/m)	610	IFAI 2012
Reported Swell Index (mL/2g)	24	IFAI 2012
Reported 80% by Mass of Particle Diameter (mm)	0.075 to 2	IFAI 2012

The GCL contained VOLCLAY CG-50 bentonite, which is a granular sodium bentonite. The GCL is secured by needle-punching. The GCL has two nonwoven geotextiles, each of a different color; one side is gray and the other side is white. The white side is manufactured to face upwards when unrolled on a landfill site to minimize radiation heating if exposed to the sun prior to

installation of the GM (CETCO 2011). Therefore, in field applications, the white side of the GCL is oriented toward the overlying T-GM.

3.2.1.2 Textured Geomembrane

The T-GM used for the testing program was GSE HD Textured Geomembrane, which was a 1.5 mm (60 mil) thick coextruded double-sided textured HDPE membrane. The reported thickness of 1.5 mm is the minimum per roll with a lowest individual reported thickness of 1.35 mm (IFAI 2012). The T-GM is black with a reported asperity height of 0.45 mm. The tensile strength at break and yield are 16 and 22 N/mm, respectively. The puncture resistance and tear resistance are 400 and 187 N, respectively (GSE 2012).

3.2.2 Large Scale Direct Shear Device

The large scale direct shear device used for interface shear testing was model LG-117 manufactured by Durham Geo Slope Indicator. The upper shear box is 305 x 305 mm with a depth of 102 mm, while the lower shear box is 305 x 406 mm with a depth of 102 mm. The apparatus allows for shearing at rates between 0.00256 and 5.13 mm/min. The GCL was placed in the upper shear box and the T-GM was placed in the lower shear box. The GCL was placed in the smaller dimension upper shear box to prevent exposure of a portion of the GCL to air and potential drying. Care was taken so both GM and GCL specimens were oriented in the same direction for each test. Previous research has indicated that orientation of T-GM/GCL interface affects interface shear strength results (Triplett and Fox 2001). Normal stress was applied to the interface using an air bladder controlled by a pressure regulator. Interface shear

response was measured by moving the lower shear box. Spacers were placed in the upper and lower shear boxes to transfer normal stresses from the air bladder to the geosynthetics.

3.2.2.1 Spacers

Separate spacers were used for the upper and lower shear box due to different shear box sizes and spacer functions. The upper shear box spacers, from top to bottom, consisted of: a 6 mm thick 305 x 305 mm aluminum plate, two 305-mm-long square steel tubes (89 x 89 mm x 4.5 mm wall thickness), and the GCL gripping system which is described in Section 3.3.3. The aluminum plate functioned to transfer the normal stress from the air bladder to the spacers below. The steel square tubing was selected to have sufficient rigidity to transfer the normal stress downwards to the gripping plate over the distance while being lightweight to place and remove between each test. A schematic of the upper shear box spacers is presented in Figure 3.1.

The lower shear box spacers, from top to bottom, consisted of: 305 x 406 mm by 9.5 mm thick steel plate and three sections of square steel 89 x 89 mm by 4.5 mm thick square tubing. The steel plate provided a planar surface for the geomembrane, and the square tubes provided stiffness to prevent movement of the steel plate when applied with normal stress. A schematic of the lower shear box spacers is presented in Figure 3.2. A tolerance was provided between the upper and lower shear boxes to ensure shearing occurred at the desired interface.

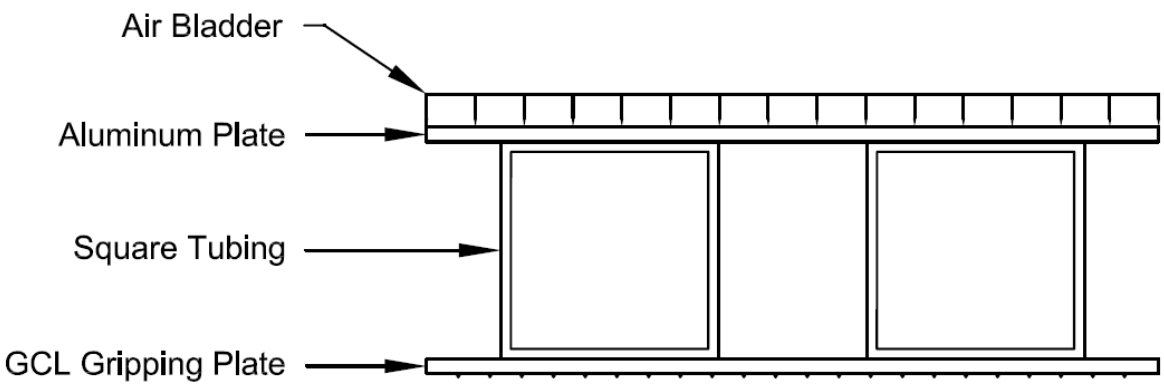

Figure 3.1. Schematic of Upper Shear Box Spacers

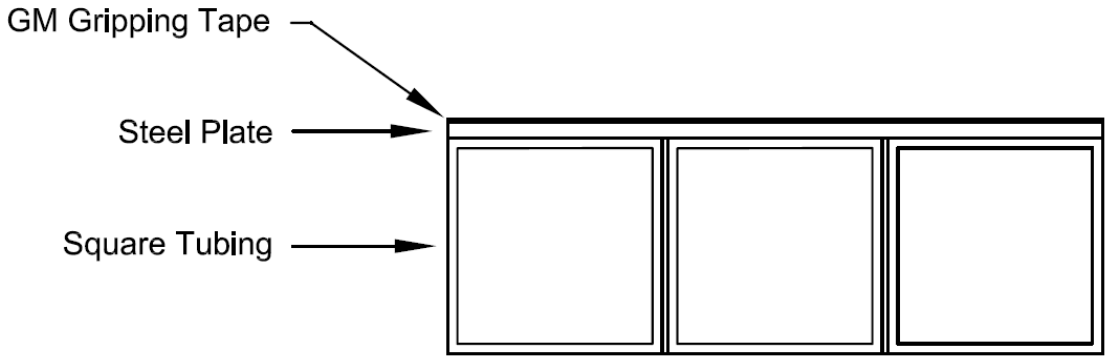

Figure 3.2. Schematic of Lower Shear Box Spacers

3.2.2.2 Specimen Gripping

Three gripping systems were used to ensure proper transfer of stress to the desired interface and to prevent progressive failure: the GCL gripping system, the frictional GM gripping system, and the clamping GM gripping system.

The GCL gripping system consisted of a bed of 529 wood screws, which evenly transferred shear stress to the GCL by embedding the screw tips into the GCL by approximately 1.5 mm. GCL specimens were inspected subsequent to

shearing to ensure that no slippage occurred. The screws were drilled through a 6-mm-thick 300 mm x 300 mm PVC plate, while a second PVC plate with equal dimensions with holes was placed over the first plate aligning with the screw heads to provide a flat top surface. In addition, each PVC plate contained 484 1.6 mm diameter holes spaced every 13 mm, which provided drainage of the GCL during consolidation. A nonwoven GT was placed over the screws to provide drainage for any free water from consolidation of bentonite. A photograph of the GCL gripping system is presented in Figure 3.3. A schematic of the GCL gripping system is presented in Figure 3.4. Thermocouples were placed through two screw holes into the GT to measure temperature of the GCL.

Figure 3.3. Photograph of Screw Tip Side of GCL Gripping Plate

One of the GM gripping systems was a distributed frictional gripping mechanism, where adhesive emery cloth (i.e., ladder tread tape) was adhered to

the 9.5-mm-thick 305 mm x 406 mm steel plate located in the lower shear box. The adhesive emery cloth was placed below the T-GM to provide frictional resistance against the T-GM surface and thus prevent slippage of the T-GM relative to the lower shear box below it. The adhesive emery cloth was manufactured by 3M and was moisture resistant.

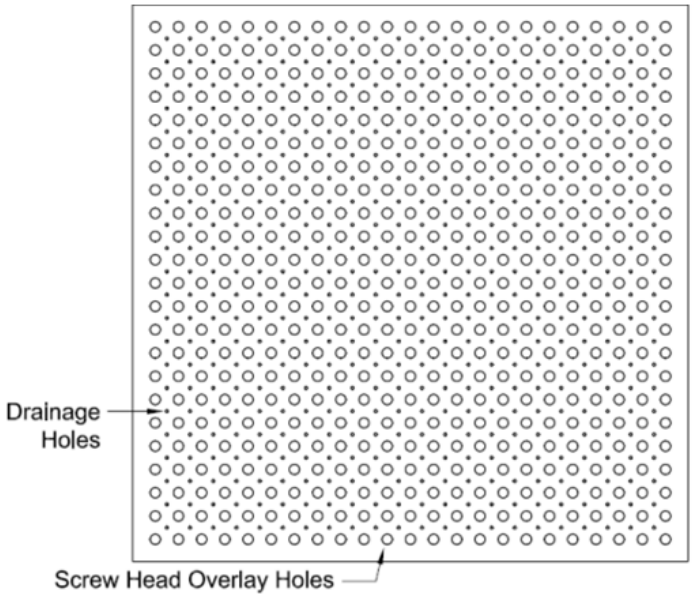

Figure 3.4. Schematic of Upper GCL Gripping Plate

The other T-GM gripping system was a clamping gripping system built into the large scale direct shear device consisting of 7 bolts (with washers and nuts) passing through the shearing direction of the T-GM. The nuts were tightened over the washers, clamping the T-GM to provide a “pulling” mechanism. The clamping T-GM gripping system provided additional mechanical resistance to slipping of the T-GM relative to the lower shear box.

3.2.2.3 Temperature Control

A thermally controlled chamber (Figure 3.5) was constructed to contain the shear device to maintain constant temperature during testing. The chamber was assembled using 12-mm-thick particle board to provide rigidity, with polyurethane expanding spray foam sealant and fiberglass providing insulation. The roof of the box was hinged to allow quick access to the direct shear device between tests.

The temperature of the GCL and T-GM specimens was controlled by heating or cooling the air and shear device inside the insulation box using copper tubing. Temperature controlled water was circulated through 8.5 mm and 6.4 mm diameter copper refrigeration tubing (Type L) inside the insulation box and wrapped around the shear box. The 6.4 mm diameter copper tubing was formed in coils approximately 400 mm in diameter and tightly wrapped on top and around the shear box, while the 8.5 mm tubing was wrapped loosely around the shear box.

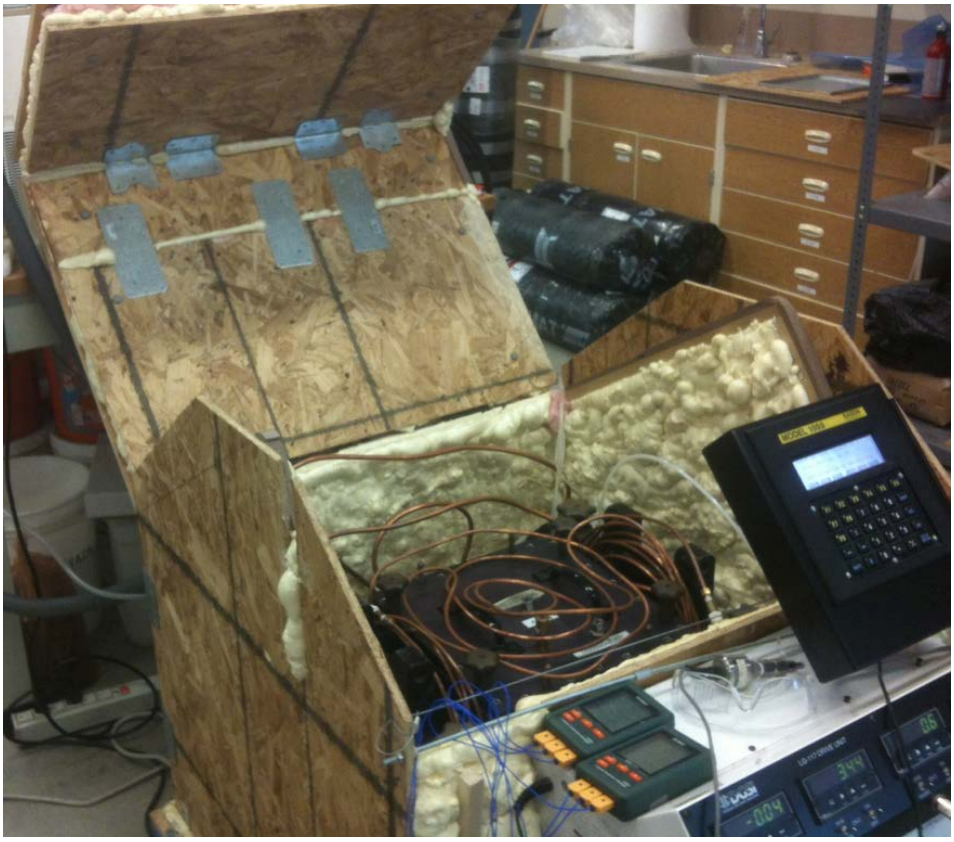

Figure 3.5. Photograph of Thermally Controlled Chamber Containing Large-Scale Direct Shear Device

A NESLAB RTE 10 Digital Plus refrigerated bath was used to control the temperature and to pump water through the copper tubing. The 9.8 L (2.6 gallon) capacity refrigerated bath was capable of controlling the temperature from -25 to 150 °C and accurate to 0.1 °C. The built-in pump (15 L/min) supplied the temperature controlled water to the 6.4 mm tubing, and a submersible pond pump (16 L/min) placed in the temperature controlled tank supplied water to the 9.5 mm tubing. PVC flexible tubing transported the water from the refrigerated bath to the insulation box, where the copper tubing was connected to ensure greater heat transfer to materials in the thermally controlled chamber.

Depending on the ambient laboratory temperature, the pump temperatures were set from 48 to 52 °C, 19 to 21 °C, and -11 to -9 °C to result in geosynthetic temperatures of 40, 20, and 2 °C, respectively due to heat loss. A mixture of 50% propylene glycol and water was used to prevent freezing in the tubing and tank when the circulation fluid temperature was set below 0 °C.

3.2.3 Specimen Preparation

3.2.3.1 Interface Direct Shear Testing

The GCL samples were delivered in four 4.4 x 0.86 m sections. The GCL rolls were stored according to ASTM D5888-06, and after opening, were double sealed in two plastic bags to prevent moisture change. The specimens were trimmed using a 300 x 300 mm steel template and a sharp utility knife. The template was placed over a section of the GCL roll no less than 75 mm from the edge of the sample. The potential for granular bentonite falling out of the exposed (i.e., newly cut) GCL edges was eliminated by adding a measured amount of water using a squeeze wash bottle with a fine stream nozzle at a constant rate along the perimeter of the template immediately before trimming the specimen. This added moisture hydrated the bentonite into a paste-like consistency, preventing loss of bentonite from the specimen edges during trimming and handling. Half of the applied water was assumed to remain in the final cut specimen and was accounted for in future moisture content calculations. The specimens were trimmed and then taped with a 25 mm wide strip of duct tape along all four exposed edges to prevent future bentonite loss. Approximately one-third of the width of the tape was placed along the white

(shearing) side and two-thirds of the width was placed along the gray (non-shearing) side to minimize interaction of the tape with the tested interface. The specimens were weighed, labeled with an identification number and orientation of the machine direction, and sealed in a labeled zip top bag. Throughout the specimen preparation and testing, any transport of the GCLs was conducted by sliding the GCL along its non-shearing side to prevent alteration/breakage of GT fibers and by supporting the specimen with an acrylic plate to prevent flexural deformations of the specimen.

The T-GM specimens were obtained from two 1.1 x 5 m samples. The T-GM specimens were trimmed using a sharp utility knife and a template with the desired T-GM dimensions. The trimmed T-GM specimens were immediately labeled with an identification number and an orientation of the machine direction. The template, containing holes at the clamping locations, was placed over the trimmed T-GM specimen and holes were drilled at the bolt locations (Figure 3.6), where washers and nuts were tightened to apply the clamping gripping system (Figure 3.7).

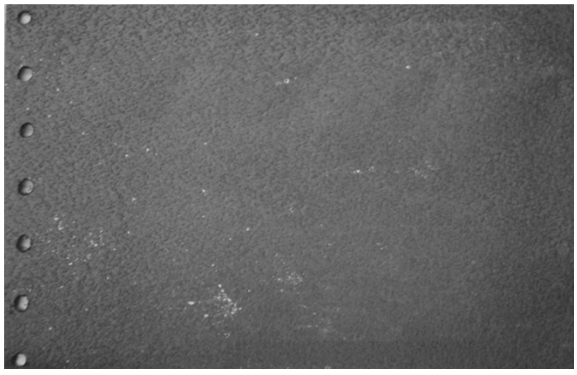

Figure 3.6. Photograph of T-GM Specimen with Holes for Clamping

Figure 3.7. Photograph of T-GM Gripping Clamping System

3.2.4 Testing Program

The variables of the testing programs were selected to investigate the effects of temperature and moisture on interface shear strengths of T-GM/GCL and bentonite extrusion under representative landfill conditions.

3.2.4.1 Interface Shear Testing

A total of 45 interface direct shear tests was conducted. Tests were conducted at temperatures of: 2, 20, and 40 °C. Specimens were prepared at three different bentonite moisture contents: as-received (AR), 50%, and 100%. Interface shear tests were conducted at normal stresses of 10, 20, 30 kPa (to represent cover liner conditions) and 100, 200, and 300 kPa (to represent bottom liner conditions). Specimens sheared at cover liner normal stresses are referred to as “cover liner specimens” and specimens sheared at bottom liner normal stresses are referred to as “bottom liner specimens”. A summary of the interface shear testing program is presented in Table 3.2.

Moisture contents of the GCLs for the testing program indicate the targeted bentonite moisture content immediately after hydration. Some deviation from target moisture contents was expected during consolidation and shearing,

due to both expulsion of water by consolidation and limited exposure to air inside the temperature control chamber. The GCLs were minimally exposed to the environment during the consolidation and testing stages. Even during this exposed period, access to air was limited due to the specimen being confined between the GCL gripping plate, T-GM, and the sides of the large scale direct shear box. After shearing, moisture contents were recorded to determine moisture changes between hydration and after shearing.

Table 3.2 Summary of Testing Program

Confining Stress Condition	Normal Stress (kPa)	Moisture Content for 2 °C Test	Moisture Content for 20 °C Test	Moisture Content for 40 °C Test
Low Normal Stress (Cover Liner)	10	AR	AR	AR
		50	50	50
		100	100	100
	20	AR	AR	AR
		50	50	50
		100	100	100
	30	AR	AR	AR
		50	50	50
		100	100	100
High Normal Stress (Bottom Liner)	100	N/A	AR	AR
		N/A	50	50
		N/A	100	100
	200	N/A	AR	AR
		N/A	50	50
		N/A	100	100
	300	N/A	AR	AR
		N/A	50	50
		N/A	100	100

N/A = Not Applicable

3.2.5 GCL Conditioning

Due to changes in behavior of the bentonite component in GCLs when exposed to moisture, proper conditioning of each GCL specimen was important. Test specimen conditioning included a hydration stage and consolidation stage. The hydration stage consisted of attaining the target GCL moisture content, and the consolidation stage consisted of applying the shearing normal stress while relieving any excess pore pressures. A modified accelerated hydration and consolidation procedure was used based on Fox et al. (1998), including a hydration and consolidation stage.

The hydration stage was labeled as stage 1, the consolidation stage was labeled as stage 2, and the shearing stage was labeled as stage 3. Stage 2 was comprised of two parts: Stage 2a and Stage 2b. Stage 2a consisted of increasing the normal stress from hydration normal stress (1 kPa) to shearing normal stress. Stage 2b consisted of bringing specimens to thermal equilibrium at the target shearing temperature. The timing of stages is presented in Table 3.3.

Table 3.3. Timing of GCL Conditioning and Shearing Stages

Stage	Description of Stage	Hours from Start of Stage 1
1	Hydration of GCL	0-48
2a	Increasing Normal Stress	48-72
2b	Equilibration of Temperature	72-96
3	Interface Shear Test	96-97

3.2.5.1 Stage 1

Stage 1 involved hydration of the GCL specimens. The GCL specimens were prepared at a total of three target bentonite gravimetric moisture contents: AR, 50%, and 100%. The AR moisture contents varied between 18 and 19%. The GT mass per unit area was assumed to remain constant throughout each specimen, at 200 g/m^2 for each carrier and cover GT, thus the remainder of the GCL mass was assumed to be bentonite and moisture.

The GCL specimens were placed in a shallow stainless steel pan and tap water was applied evenly over both sides using a mist sprayer until the required predetermined mass of water was applied. The required amount of water to be added to reach the desired moisture content was calculated using Equation 2 (ASTM D5993-99).

$$W_{\text{clay}} = \lfloor (M_{\text{i}}/A) - m_{\text{GCL}} \rfloor / m_{\text{clay}} \times 100 \quad (2)$$

where:

W_{clay} = initial moisture content of clay component (%)

M_{i} = mass of GCL specimen (g)

A = specimen area (m^2)

m_{GCL} = mass per unit area of dried GCL product (g/m^2)

m_{clay} = mass per unit area of dry clay (g/m^2)

The GCL specimens were placed white side up in a shallow stainless steel pan with two 600 x 510 mm zip top bags to prevent moisture loss. The shallow

pan was custom-formed from sheet metal of adequate thickness (1 mm) and stiffness to prevent deformation from lateral pressure of the GCL edges. A plate just smaller than the inner dimensions of the pan was placed over the GCLs to provide even distribution of normal stress. A bucket of sand equivalent to 1 kPa of normal stress on the GCLs was placed over the plate to provide the hydration normal stress recommended by Fox et al. (1998).

Each of the four GCL rolls was assumed to be at a specific moisture content that was constant throughout each roll, which was determined prior to GCL hydration.

3.2.5.2 Stage 2

After 48 hours of hydration in the shallow pan, the GCL specimens were then subjected to consolidation. The T-GM specimens were oriented with the machine direction in the shearing direction of the shear device and gripped using the previously described T-GM frictional and clamping methods. The GCL specimens were then weighed to confirm that no or little change in moisture occurred. The white sides of the GCLs were placed facing downward toward the T-GM, and the machine direction was oriented facing the direction of shearing. The GCL gripping system was placed over the GCL, and two thermocouples were placed in two holes in the gripping system, protruding into the upper carrier NW GT of the GCL. The thermocouples were used to monitor the temperature of the GCL throughout Stages 2b and 3. The two square tubes and aluminum plate were placed over the GCL gripping system as described in section 3.2.2.3. A

rigid steel cap (which is connected to the air bladder) was anchored to the frame of the shear box to provide a reaction force against the air bladder.

Stage 2a

Two different procedures were used to apply consolidation normal stress to a specimen for stage 2a: a procedure for the cover liner specimen tests and a five step procedure for the bottom liner specimen tests. The spacers contribute approximately 1 kPa of normal stress to the specimen; thus, when referring to a value of applied normal stress, 1 kPa results from the spacers and the remainder results from application through the air bladder.

The stage 2a consolidation procedure for cover liner specimen tests consisted of applying normal stress in 10 kPa increments every 10 minutes until the desired testing normal stress was reached. An alternate loading apparatus (load frame) was used to consolidate some specimens during stage 2a to expedite the testing program per ASTM D6243-09. The load frame (Figure 3.8) consisted of a lever arm (5:1 ratio) where weights were hung to apply sufficient load to result in the desired consolidation normal stress. The load was applied as a point load to the center of the 305 x 305 mm steel plate to provide distributed stress to the GCL. The GCL was double sealed in two 600 mm x 510 mm zip top bags to maintain constant moisture. A load cell was used to calibrate and verify correct normal stress application. In accordance with ASTM D6243-09, the GCL specimens were not damaged by the transfer from the alternate loading device to the direct shear device and transfer time was kept to a minimum. After 24 hours of consolidation during stage 2a, the GCL specimens

that were consolidated in the alternate load frame were carefully and quickly transferred to the direct shear device over a period of less than 2 minutes to minimize change in moisture content and swelling of the bentonite.

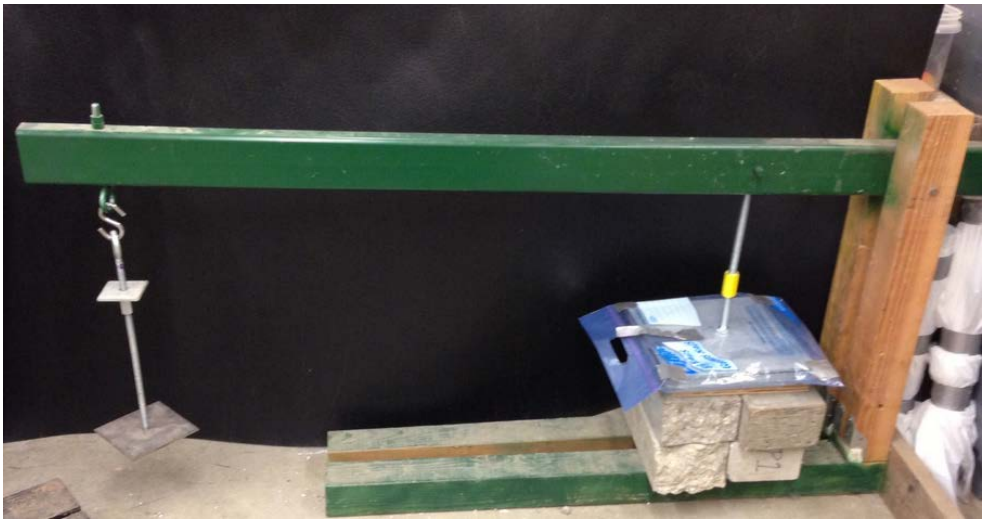

Figure 3.8. Photograph of Load Frame

The stage 2a procedure for the bottom liner specimens consisted of five steps:

1. Increase stress from 0 kPa to 10 kPa
2. Increase stress to 20 kPa after 10 minutes
3. Increase stress to one quarter of testing normal stress after 10 minutes
4. Increase stress to one half of testing normal stress after 8 hours +/- 2 hours
5. Increase stress to full testing normal stress after 8 hours +/- 2 hours

A load increment ratio (LIR) of approximately 1.0 was maintained throughout the testing program to minimize excess pore pressures and excess bentonite extrusion beyond typical landfill conditions, where relatively continuous loading associated with gradual waste placement allows for dissipation of excess pore pressures.

Stage 2b

Stage 2b (temperature equilibrium) began 24 hours after the start of stage 2a. Temperatures were maintained within 0.5 °C of the target temperature for the entire duration of shearing. Prior trial testing of the system was conducted to determine the fluid temperature needed to result in the desired test temperature. Approximately 12 hours were required to reach thermal equilibrium at the test temperatures. Shorter duration was required for 20 °C tests, where less temperature change was introduced. Upon calibration of the system, the pump was set to a specific temperature which would result in the specimens reaching within 0.5 °C of the desired shearing temperature.

Complete consolidation of the bentonite due to increased normal stresses (stage 2a) was assumed to occur within 24 hours. Changes were expected to occur in behavior of the bentonite and geosynthetics due to increased or decreased temperatures. The bentonite and geosynthetics were subjected to change in temperature during stage 2b to allow for behavioral changes to occur separately from changes due to normal stress. In the field, MSW liners are subjected to increased temperatures after placement of waste. In the testing

program, increase in normal stress and increase in temperature occur in the same order as in the field.

3.2.5.3 Stage 3

Stage 3 (shearing) occurred at a minimum of 6 hours after the final temperature had been reached and 48 hours after the start of Stage 2. A shear displacement rate (SDR) of 1 mm/min was used, as recommended by Triplett and Fox (2001), Fox and Stark (2004), and McCartney et al. (2009a). Normal stress within 2% of the target normal stress was maintained, in accordance with ASTM D6243-09. Every test reached a shear displacement of at least 50 mm as recommended by Fox and Stark (2004). After shearing, each GCL specimen was weighed and photographed. Thickness measurements of GCL test specimens were recorded at a minimum of six points along each edge with digital calipers. In addition, notable observations of the shearing surfaces were recorded. The GCL specimens were then sealed in a zip top bag, labeled, and stored for inventory of tested specimens. In addition, each T-GM specimen was labeled and stored.

3.3 Bentonite Extrusion Testing Program

Testing was performed to determine the effects of moisture content, temperature, and normal stress on bentonite extrusion. Liquid limit and bentonite extrusion tests were conducted to determine the effects of moisture and normal stress on behavior of bentonite extrusion. A total of 6 bentonite extrusion tests were performed for DN GCL specimens. Tests were performed at moisture contents of 50% and 150% at 300 kPa and at a moisture content of 100% at 100,

200, 300, and 400 kPa. Liquid limit tests were performed in accordance with ASTM D4318-10 at temperatures of 2, 20, and 40 °C. Both bentonite extrusion tests and liquid limit tests were performed as index tests to determine effects of moisture content, temperature, and normal stress on bentonite extrusion.

3.3.1 Bentonite Extrusion Tests

Bentonite extrusion tests were conducted by applying normal stress to the GCL specimen using a 1-D consolidometer. The GCL specimens were trimmed using a 63.5 mm diameter 5.8 mm thick brass cutting template and a sharp utility knife. The same trimming method was used for bentonite extrusion testing GCL specimens as the interface shear testing GCL specimens. The GCL edges were sealed with duct tape that had been pre-trimmed to a specific shape. The duct tape provided a sealed edge to minimize bentonite squeezing out the edge and the duct tape was cut to a shape resulting in a constant 51 mm diameter GCL surface exposed to allow bentonite extrusion (Figure 3.9). A 51 mm diameter circle was trimmed on a 70 mm x 70 mm square piece of duct tape. The GCL specimen was placed with the white side oriented toward the open circle of the duct tape and the rest of duct tape was wrapped around non-extruding side of the GCL. The duct tape provided a constant geotextile area for the bentonite to extrude through and prevented bentonite from squeezing out of the trimmed edges.

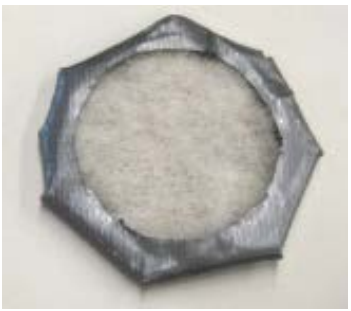

Figure 3.9. GCL Specimen with Sealed Edge

Window screen was placed against the surface of the GCL and to generate space for movement of extruded bentonite. The window screen was weighed prior to and after testing to determine mass of bentonite extrusion. If the window screen was not placed against the GCL, the extruded bentonite would be confined within the GT. Window screen was trimmed using the 63.5-mm diameter template used for GCL trimming. Eight layers of window screen were used during each test. The GCLs and window screen assemblies were wrapped in plastic film to minimize moisture loss. The GCLs were placed in the consolidometer and loaded for one hour. Subsequent to load application, the GCL-screen assemblies were taken apart. Then, the screens with extruded bentonite were oven dried and weighed to determine mass of extruded bentonite. The screens exhibited loss in mass while in the oven, so it was assumed some coating on the fiberglass screen volatilized in the oven. Extensive testing was conducted to quantify the loss of mass for the polymer window screen over the duration of the 21 hour drying period. The loss was established to be 0.71% of the original screen mass.

3.3.2 Liquid Limit Tests

Liquid limit tests were conducted to determine the effects of temperature on bentonite shear strength. Liquid limits of bentonite at temperatures of 2, 20, and 40 °C were determined. Bentonite for the liquid limit tests was obtained by disassembling the GCLs by cutting the needle-punching. The bentonite was allowed to drop into a clean underlying bin where it was collected for testing.

A temperature control chamber (TCC) was constructed to perform liquid limit tests in a temperature controlled environment. The temperature control chamber was 559 mm x 405 mm x 305 mm constructed of 9 mm thick fiberboard. A layer of 18.5 mm thick expanded polystyrene insulation lined the inside of the TCC. A clear 229 mm x 191 mm polycarbonate sheet was installed in place of fiberboard on top of the TCC to provide an observation window during liquid limit testing. Two 89 mm diameter holes were cut into a side of the TCC and covered with 100 m square sheets of rubber with 50 mm diameter holes in the rubber. The two access holes allowed the operator to place their hands inside the TCC and perform liquid limits tests without exposing the interior to ambient temperature. For bentonite tested at 40 °C, a heat lamp (150 watts) connected to a dimmer switch set to a specific magnitude provided constant temperature inside the TCC. For bentonite tested at 2 °C, ice was placed inside the TCC until thermal equilibrium at 2 °C was reached. Thermal equilibrium was confirmed by monitoring bentonite temperatures with thermocouples.

Figure 3.10. Photograph of TCC Including Observation Window and Access Holes.

Water was added and mixed thoroughly to prepare the sample for the liquid limits test. The sample was placed in two zip top bags for at least 16 hours in accordance with ASTM D4318-10. The multi-point method from ASTM D4318-10 was used to determine the liquid limit of the bentonite. The double sealed bentonite was placed in the TCC and allowed to reach thermal equilibrium to the target temperature overnight. The bentonite was thoroughly mixed in a mixing bowl prior to testing, and then liquid limit tests were performed following ASTM D4318-10. Bentonite was collected to determine moisture content immediately following completion of each test to minimize moisture content change.

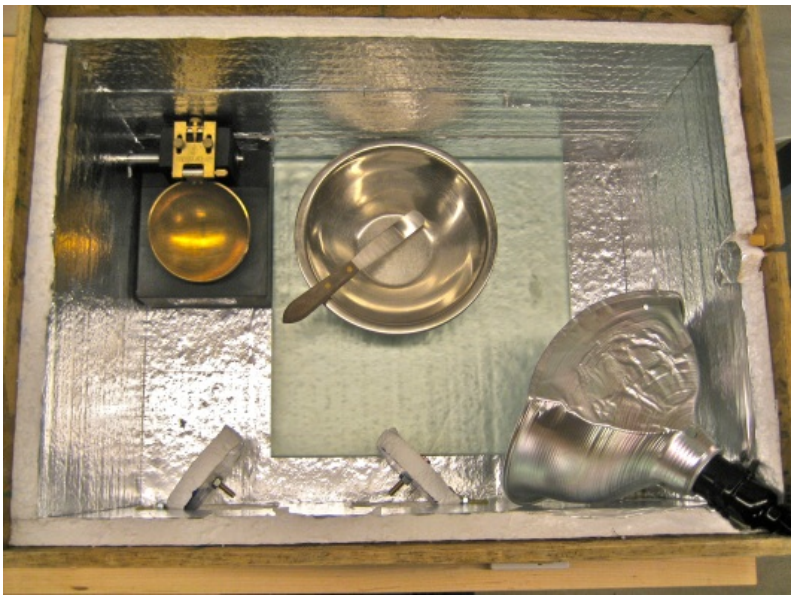

Figure 3.11. Photograph of TCC Including Heat Lamp and Mixing Bowl.

Chapter 4: Results and Analysis

4.1 Introduction

Results of the interface direct shear test program are presented in this chapter in two sections: specimens sheared at cover liner normal stresses and at bottom liner normal stresses. Peak and large displacement shear strengths were determined for each shear test. Specimens sheared at cover liner normal stresses (10, 20, and 30 kPa) and bottom liner normal stresses (100, 200, and 300 kPa) were plotted to establish Mohr-Coulomb failure envelopes. Linear regression was used to determine interface friction angle (δ) and adhesion (*a*) from the failure envelopes. Specimens sheared at cover liner normal stresses are termed “cover liner specimens”, and specimens sheared at bottom liner normal stresses are termed “bottom liner specimens”. In addition, results of the bentonite extrusion testing program are presented in this chapter including two types of tests: bentonite extrusion testing at multiple moisture contents and bentonite liquid limit tests at multiple temperatures.

4.2 Interface Shear Strength Parameters

For convenience, interface shear strength is typically divided into friction-based and adhesion-based shear strength for MSW landfill slope design. However, only analyzing interface friction angle (δ) and adhesion (*a*) may result in misleading interpretation of interface behavior mechanisms. Analyzing the recorded interface shear strengths (τ) can provide additional interpretation of interface behavior mechanisms. Thus, the recorded interface shear strengths (τ) and calculated interface shear strength parameters (δ and *a*) are used in this

chapter to investigate the effects of temperature and moisture on interface shear strength mechanism behavior. Peak (τ_p, δ_p, and a_p) and large-displacement (τ_{ld}, δ_{ld}, and a_{ld}) values are used for analyses.

Adhesion-based strength can be divided into two sources: true adhesion and apparent adhesion. True adhesion with T-GM/GCL interfaces (interface shear strength at zero normal stress) is caused by mechanical interaction between surfaces. Apparent adhesion can occur due to data interpretation rather than strength measurement. A decreased interface friction angle at elevated normal stresses results in increased apparent adhesion. The graphic in Figure 4.1 displays a hypothetical curvilinear failure envelope fitted with two linear segments (envelope 1 and envelope 2). Envelope 1 has some true adhesion. Envelope 2 represents a decreased friction angle, resulting in an increased adhesion. The decreased friction angle resulted in the appearance of an increased y-intercept (adhesion) in τ–σ space resulting in apparent adhesion. However, determining the magnitude of apparent adhesion requires extensive experimental testing. Thus, increased adhesion as a function of temperature and moisture may be explained as increased apparent adhesion. Decreased interface friction angle may occur due to damage of geosynthetic material or bentonite extrusion, which is discussed in later sections.

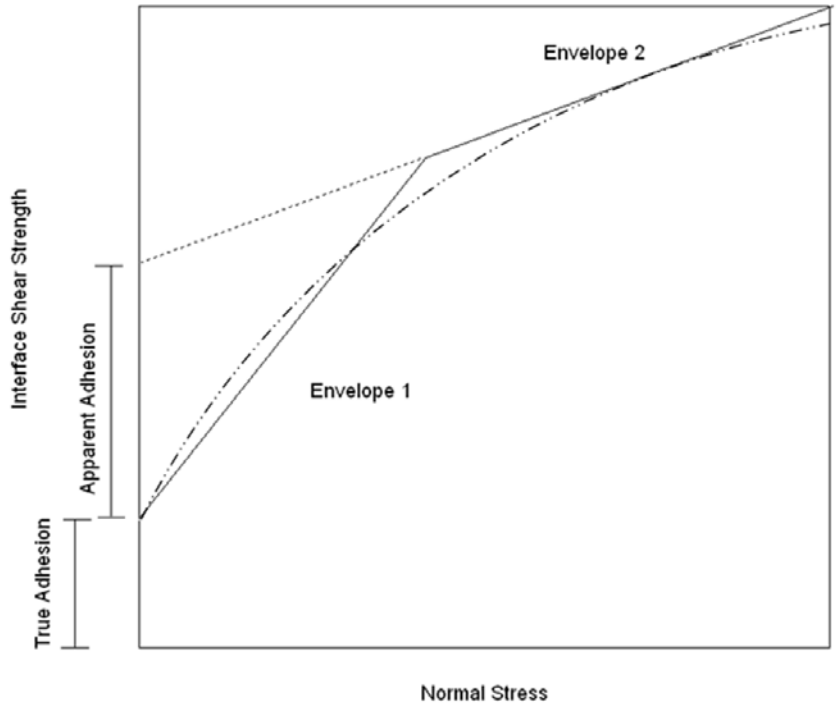

Figure 4.1 Apparent Adhesion and True Adhesion of Hypothetical Non-Linear Failure Envelope

4.3 Cover Liner Normal Stress

Cover liner specimen results and analyses are presented in terms of temperature effects and moisture effects on interface shear strength. Analyses of temperature and moisture effects on interface shear strength at a typical cover liner normal stress are also presented. Within each section (temperature effects and moisture effects) data and analyses are presented in the order of τ, δ, and *a*. In addition, interpolation factors are provided for interpolation of δ as a function of temperature. Multiple tests were duplicated to confirm repeatability. Interface shear strengths of cover liner specimens are presented in Tables 4.1 and 4.2.

Table 4.1 Peak Interface Shear Strengths (kPa) of Cover Liner Specimens

	AR Moisture			50% Moisture			100% Moisture		
σ_n (kPa)	2 °C	20 °C	40 °C	2 °C	20 °C	40 °C	2 °C	20 °C	40 °C
10	7.00	6.13	4.94	9.35	5.70	5.37	9.67	7.09	6.45
20	13.01	11.82	9.67	14.4	10.43	9.14	11.18	11.61	9.78
30	14.94	17.20	13.11	19.24	15.05	12.79	16.32	15.91	13.97

Table 4.2 Large-Displacement Interface Shear Strengths (kPa) of Cover Liner Specimens

	AR Moisture			50% Moisture			100% Moisture		
σ_n (kPa)	2 °C	20 °C	40 °C	2 °C	20 °C	40 °C	2 °C	20 °C	40 °C
10	5.05	5.37	4.51	6.66	4.73	4.73	7.09	5.80	5.70
20	9.46	9.57	8.17	9.46	8.71	7.20	8.17	9.46	7.85
30	11.39	11.93	10.53	13.22	12.25	10.64	11.61	12.36	11.39

4.3.1 Temperature Effects

Temperature was determined to have a significant effect on interface shear strength and interface shear strength parameters for cover liner specimens. Specimens sheared at 2 °C experienced consistently larger peak interface shear strength (τ_p) than those sheared at either 20 °C or 40 °C. Results of failure envelopes separated by temperature are presented in Figure 4.2. The trend of higher τ_p with lower temperature may be due to increased modulus of polypropylene and polyethylene at lower temperatures. Large-displacement interface shear strength (τ_{ld}) was higher for specimens sheared at 20 °C than 2 °C of normal stresses at 20 and 30 kPa (Figure 4.3). The relationship of τ_{ld} between 2 and 20 °C in Figure 4.3 may be due to brittle behavior of polypropylene at 2 °C resulting in a large post peak strength reduction.

Polypropylene at a temperature of 2 °C is nearing its glass transition temperature of -10 ˚C (Ebewele 1996), resulting in an increased modulus and relatively brittle behavior. Comparing peak versus large-displacement results displayed in Table 4.3 concur with polypropylene behaving in a more brittle manner at 2 °C. Two trends were observed from results in Table 4.3 The percent difference of τ from 2 to 20 °C was larger for peak than for large-displacement. Percent difference of τ was calculated as the quotient of difference of τ and τ_p. A brittle material (polymers at 2 °C) would likely exhibit more decrease from peak to large-displacement than a ductile one (polymers at 20 °C). In addition, the percent difference of τ from 2 to 20 °C was greatest at 10 kPa for both peak and large-displacement. Relatively brittle materials could exhibit more breakage while relatively ductile materials could exhibit less breakage at higher stresses. Lower normal stresses may not induce sufficient shear stress to break as many polypropylene filaments as increased normal stresses do, where greater tensile stresses are imparted on the filaments. Greater tensile stresses imparted on the filaments would likely result in increased amount of broken fibers and lower τ. In addition, relatively brittle behavior could result in lower τ_{ld} because at large-displacements, more filaments would tend to break at 2 °C compared to 20 °C, while more filaments would tend to stretch at 20 °C compared to 2 °C.

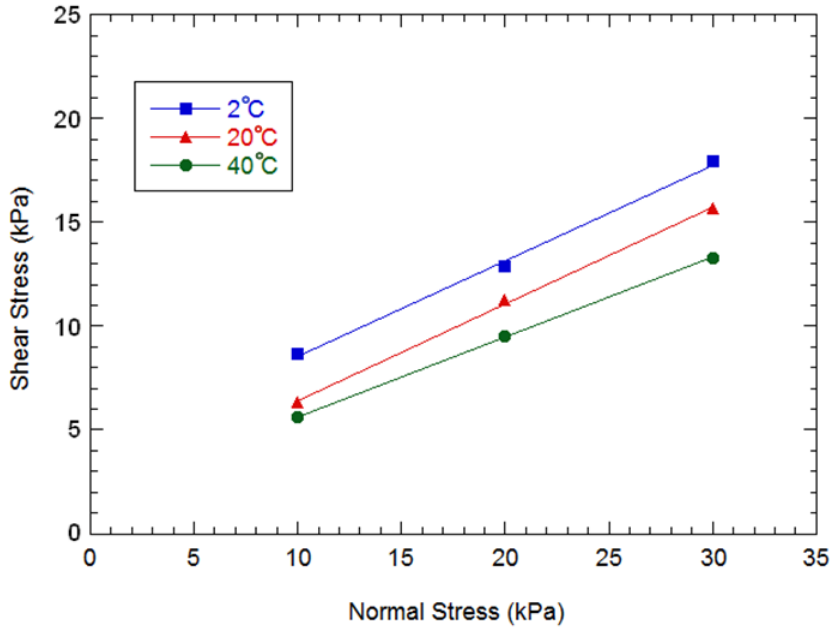

Figure 4.2. Average Peak Failure Envelope for Cover Liner Specimens

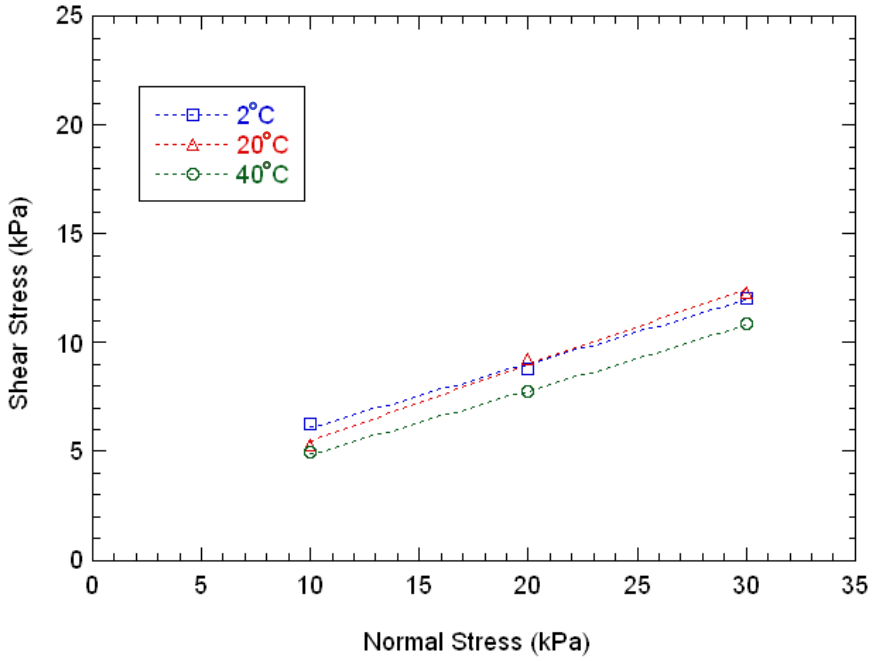

Figure 4.3. Average Large-Displacement Failure Envelope for Cover Liner Specimens

Table 4.3. Percent Difference of τ from 2 to 20 °C

Normal Stress (kPa)	Peak	Large-displacement
10	27%	15%
20	12%	-5%
30	13%	-2%

Conversely, polypropylene at a temperature of 40 °C behaves further in the rubbery phase (See Figure 2.19), resulting in a decreased modulus and more ductile behavior. Every specimen sheared at 40 °C experienced less τ_p and τ_{ld} than respective specimens sheared at 2 and 20 °C. The specimens sheared at 40 °C experienced up to 16% decrease in τ_p and τ_{ld} from control specimens at 20 °C (Table 4.4.). The decrease in interface shear strength is significant considering landfill slopes are designed using shear strength values obtained from shear testing at room temperature.

Table 4.4. Percent Difference in τ from 20 to 40 °C

Normal Stress (kPa)	Peak	Large-displacement
10	-11%	-6%
20	-16%	-16%
30	-15%	-12%

Specimens sheared at 20 °C generally resulted in greater peak interface friction angle (δ_p) and large-displacement interface friction angle (δ_{ld}) than those sheared at 2 °C, and in every case resulted in greater δ_p and δ_{ld} than those sheared at 40 °C (Figure 4.4). Increased geosynthetic damage at 2 °C and 40 °C are possible mechanisms of interface friction angle behavior with temperature.

Increased geotextile damage at 2 °C may be a result of breakage of filaments at large-displacement, while geotextile damage at 40 °C may be a result of lower tensile strength of GT filaments and lower shear strength of GM asperities.

In Figure 4.4, specimens sheared at 2 °C and 50% moisture content exhibited a significantly larger δ_p than those sheared at 2 °C at AR and 100% moisture contents. It is possible at 2 °C and at 50% moisture content that the bentonite may have behaved differently due to coupled effects of strength from temperature and moisture content.

Adhesion data generally resulted in a consistent trend: specimens sheared at 2 °C exhibited larger peak and large-displacement adhesion values than those sheared at 20 and 40 °C (Figure 4.5, Figure 4.6). The trend of increased adhesion at 2 °C may be attributed to more geotextile damage (due to brittle behavior of polypropylene at 2 °C) at higher normal stresses resulting in lower interface friction angle and larger apparent adhesion.

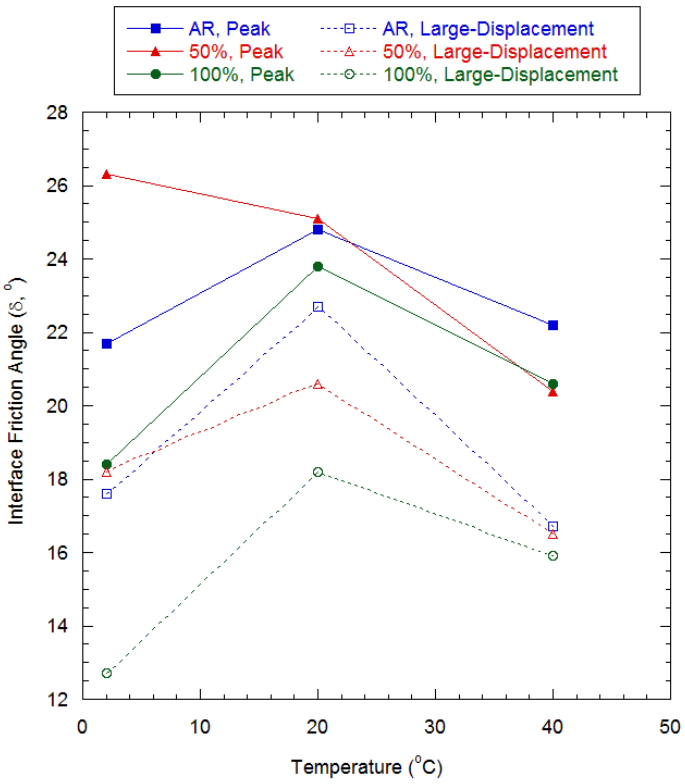

Figure 4.4. Interface Friction Angle versus Temperature for Cover Liner Specimens

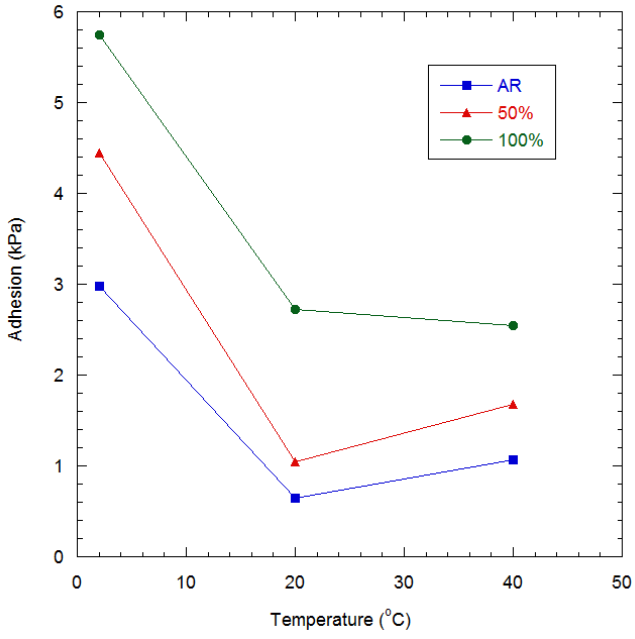

Figure 4.5. Peak Adhesion versus Temperature for Cover Liner Specimens

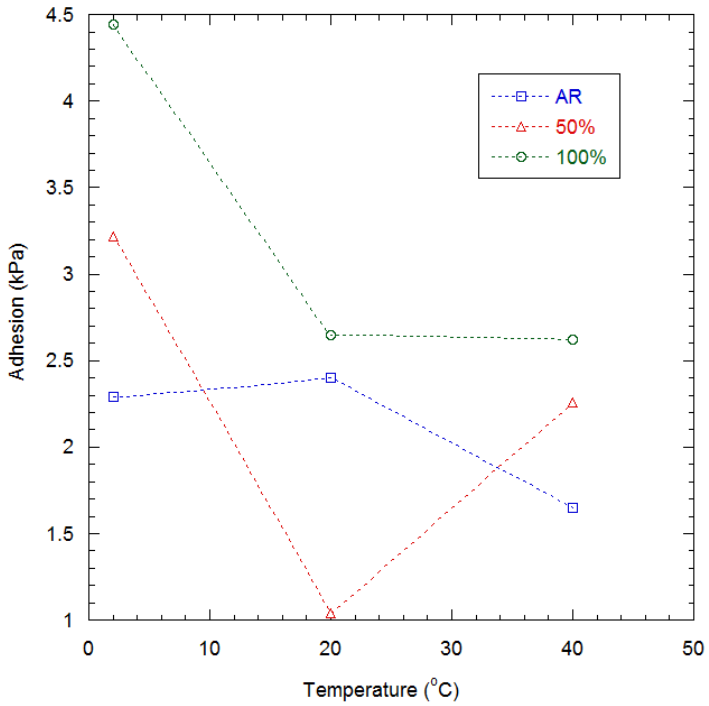

Figure 4.6. Large-Displacement Adhesion versus Temperature for Cover Liner Specimens

Analyses were performed to determine the change of interface friction angle per °C (interpolation factor) for cover liner specimens between temperatures of 2, 20, and 40 °C (Table 4.5). These interpolation factors may be used as framework to interpolate δ_p and δ_{ld} at temperatures between 2 and 40 °C after δ_p and δ_{ld} are determined at one temperature between 2 and 40 °C. From 20 to 2 °C, values of 0.41 degrees/ °C and 0.31 degrees/ °C can be used for δ_p and δ_{ld}, respectively. From 20 to 40 °C, values of 0.34 degrees/ °C and 0.21 degrees/ °C can be used for δ_p and δ_{ld}, respectively.

Table 4.5. Interpolation Factors for δ_p and δ_{ld} for Cover Liners at 20 °C to 2 and 40 °C

Interpolation Factor	AR	50%	100%
δ_p 20 °C to 2 °C (degrees/ °C)	0.406	-0.067	0.300
δ_p 20 °C to 40 °C (degrees/ °C)	0.340	0.235	0.160
δ_{ld} 20 °C to 2 °C (degrees/ °C)	0.033	0.133	0.306
δ_{ld} 20 °C to 40 °C (degrees/ °C)	0.075	0.205	0.115

Due to cover liner specimens generally exhibiting lowest adhesions at 20 °C, applying adhesion interpolation factors would result in a less conservative shear strength value. Adhesion values at 2 or 40 °C do not exhibit a significant decrease from adhesion values at 20 °C. The author recommends using the adhesion value determined from testing at 20 °C if the bentonite was hydrated between AR and 100% moisture content. These interpolation factors are recommended to be applied only to interfaces of products similar to those tested under similar conditions.

4.3.2 Moisture Content Effects

A trend of slightly increasing τ_p with increasing moisture content for cover liner specimens was observed (Figure 4.7). Specimens sheared at 10 kPa exhibited 22% increase in τ_p from AR to 100% moisture content. The increase in τ_p between AR and 100% moisture content specimens was similar at all three cover liner normal stress (approximately an increase of 1 kPa); however, the percent increase was greatest for 10 kPa.

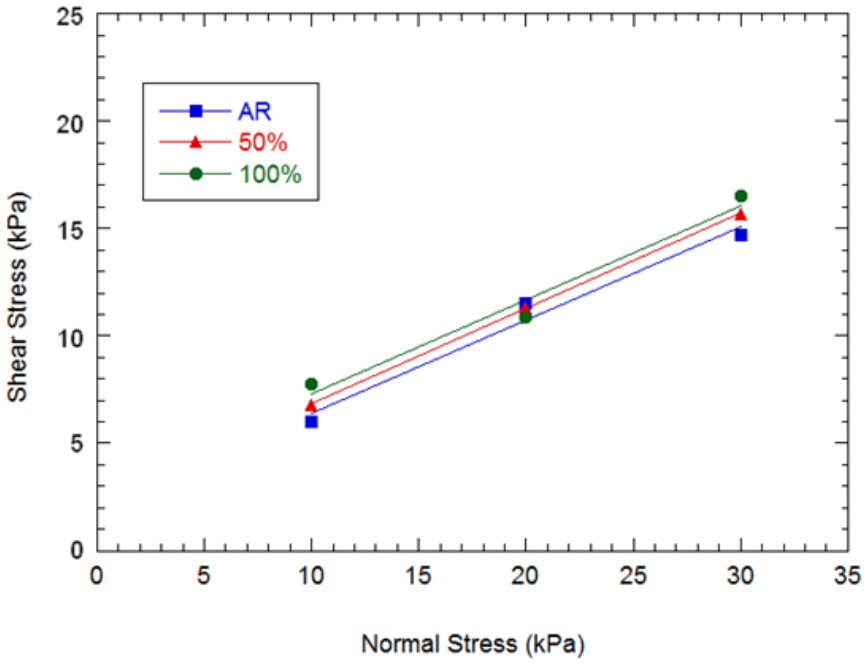

Figure 4.7. Average Peak Failure Envelopes of Cover Liner Specimens

The trend of increased moisture content resulting in increased τ is significant because the majority of previous interface shear testing has been performed under a "worst case scenario", in which the GCL was sheared in saturated condition. It is possible the "worst case scenario" for T-GM/GCL shear testing for low normal stresses is not when the GCL is fully saturated. Possible explanations of increased interface shear strength as a function of increased moisture content at cover normal stresses include the following:

1. Softening of bentonite at higher moisture contents may have resulted in a softer GCL product. GM asperities may have been able to extend further into the nonwoven filaments because the hydrated bentonite was able to be deformed at asperity locations. Asperities extending

into the GT would result in increased interface shear strength due to greater interaction between T-GM and NW GT.

2. Needle-punching of GCLs at AR moisture content may not hold the filaments together as well as needle-punching at 100% moisture content. At 100% moisture content, bentonite experiencing swelling may tighten the needle-punching and filaments, minimizing the ease of pullout of filaments.
3. While SI Geosolutions (1997) indicated polypropylene nonwoven geotextile filaments are moisture resistant, it is possible when wetted, the filaments become more flexible than when dry and more able to grip the geomembrane textures, as reported by Seo et. al (2007).

Specimens sheared at 50% moisture content generally demonstrated higher δ_p and δ_{ld} than those sheared at 100% moisture content. No consistent trend was exhibited between AR and 50% moisture content (Figure 4.8). The trend of decreasing moisture content with increasing δ agrees with previous work (McCartney et al. 2004, Seo et al. 2007, Vukelic et al. 2008, Chen et al. 2010) and is likely due to increased bentonite extrusion. Under cover liner normal stresses, the extruded bentonite may clog the spaces between the geotextile filaments and lubricate the geotextile filaments, decreasing the amount of hook and loop interaction and in turn, decreasing the interface friction angle.

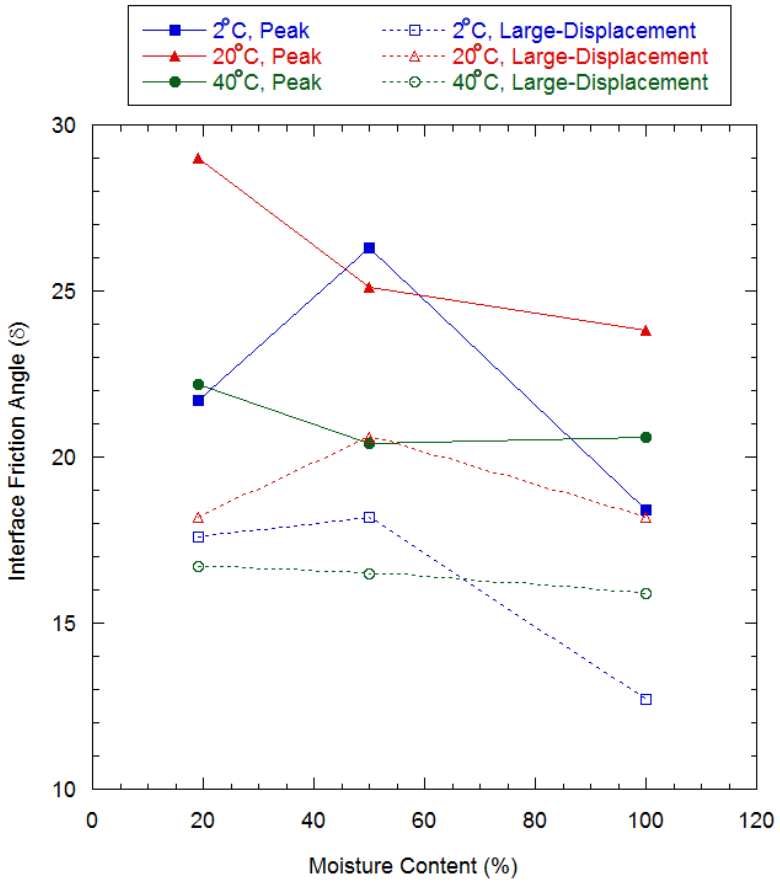

Figure 4.8. Interface Friction Angle versus Moisture Content of Cover Liner Specimens

Specimens sheared at 100% moisture content consistently exhibited the greatest peak adhesion (a_p) and greatest large-displacement adhesion (a_{ld}) at all three temperatures (Figures 4.9 and 4.10). The increased adhesions at 100% moisture content are possibly due to increased bentonite extrusion, resulting in lower interface friction angle and higher apparent adhesion. Visual observation of bentonite extrusion at 100% moisture content was confirmed.

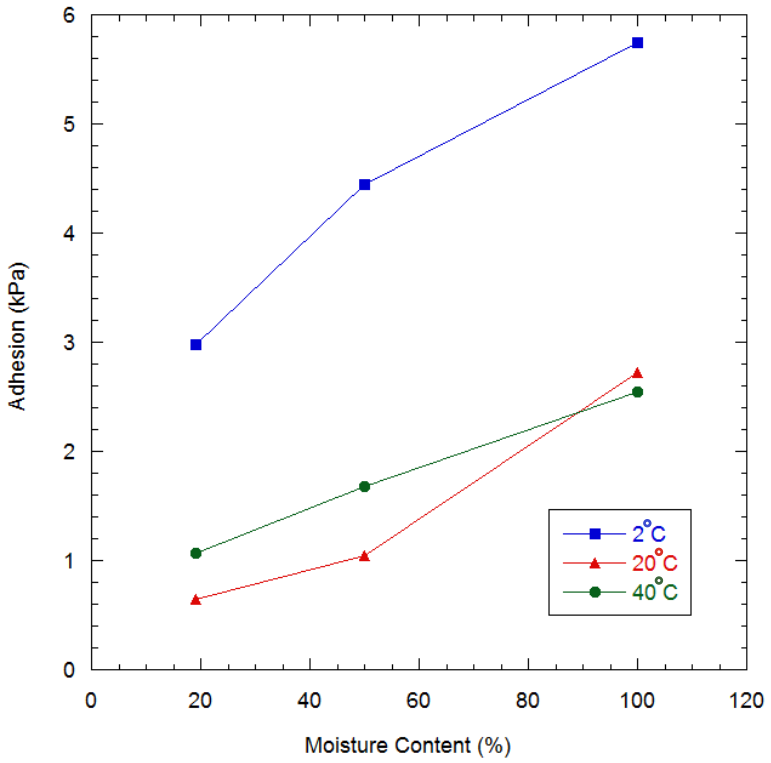

Figure 4.9. Peak Adhesion versus Moisture Content for Cover Liner Specimens

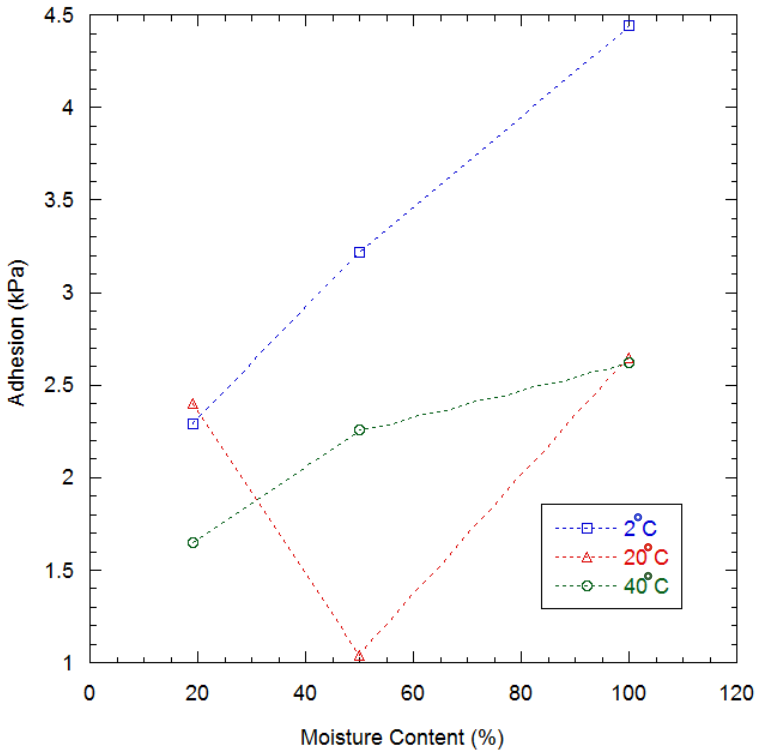

Figure 4.10. Large-Displacement Adhesion versus Moisture Content for Cover Liner Specimens

Interface friction angle and adhesion values of the failure envelopes at cover liner normal stresses are summarized in Tables 4.6 and 4.7. The coefficient of determination (R^2 values) of failure envelopes determined by linear regression was provided as well. The R^2 values for cover liner specimen failure envelopes varied between 0.91 and 1.0, with 15 of 18 failure envelopes above 0.95 and 10 of 18 failure envelopes above 0.99.

Table 4.6. Interface Friction Angle Results of Cover Liner Specimens

Interface Shear Strength Parameter	Moisture Content %	2 °C Specimens [δ (°), R^2]		20 °C Specimens [δ (°), R^2]		40 °C Specimens [δ (°), R^2]	
Peak	19%[1]	21.7	0.919	29.0	0.999	22.2	0.992
	50%	26.3	0.998	25.1	1.0	20.4	1.0
	100%	18.4	0.910	23.8	0.999	20.6	0.996
Large-Displacement	19%[1]	17.6	0.952	18.2	0.975	16.7	0.985
	50%	18.2	0.955	20.6	0.999	16.5	0.991
	100%	12.7	0.917	18.2	0.996	15.9	0.980

[1] AR moisture content

Table 4.7. Adhesion Results of Cover Liner Specimens

Interface Shear Strength Parameter	Moisture Content %	2 °C Specimens	20 °C Specimens	40 °C Specimens
Peak Adhesion (kPa)	19%[1]	3.0	0.7	1.1
	50%	4.4	1.0	1.7
	100%	5.7	2.7	2.6
Large-displacement Adhesion (kPa)	19%[1]	2.3	2.4	1.7
	50%	3.2	1.0	2.3
	100%	4.4	2.7	2.6

[1] AR moisture content

Temperature was determined to have a greater influence on interface shear strength than moisture content for cover liner specimens. Interface shear strengths varied by up to 36% for the range of temperatures tested, and varied up to 22% for the range of moisture contents tested.

4.3.3 Typical Cover Liner Normal Stress Analysis

τ_p and τ_{ld} were plotted to determine the effects of temperature and moisture content at a typical cover liner normal stress of 15 kPa (approximately 1 m of overlying soil, vegetation, and geosynthetics). Increased temperatures resulted in decreased τ_p at 15 kPa normal stress (Figure 4.11). Up to 39% decrease in τ_p occurred between 2 and 40 °C and up to an 18% decrease in τ_p occurred between 20 and 40 °C at 15 kPa. A different relationship existed with τ_{ld} at 15 kPa, where specimens sheared at 20 °C resulted in highest τ_{ld}, followed by 2 and 40 °C. Up to 11% decrease in τ_{ld} occurred between 2 and 40 °C and up to a 16% decrease in τ_{ld} occurred between 20 and 40 °C at 15 kPa. The decrease from τ_p to τ_{ld} was greater for 2 °C than 20 or 40 °C (Figures 4.11, 4.12). This decrease from τ_p to τ_{ld} is likely due to brittle behavior of the geotextile filaments and geomembrane asperities at 2 °C. Increased modulus could result in breakage of GT filaments prior to large-displacements, decreasing the τ_{ld}.

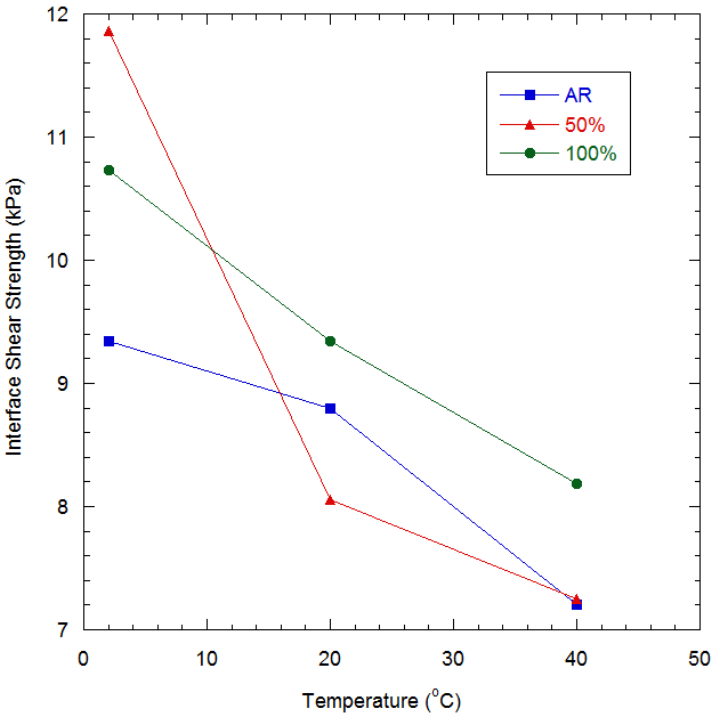

Figure 4.11. Peak Interface Shear Strengths at 15 kPa versus Temperature

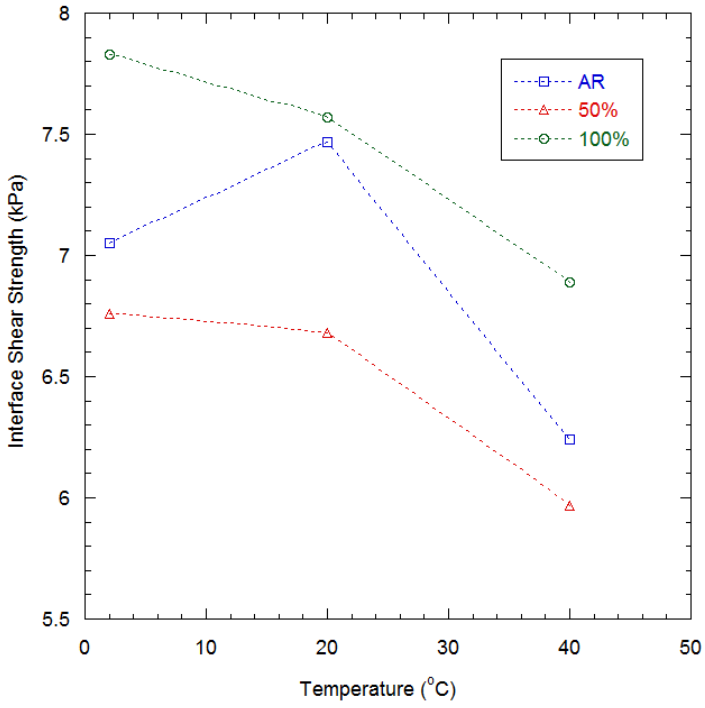

Figure 4.12. Large-Displacement Interface Shear Strengths at 15 kPa versus Temperature

4.4 Bottom Liner Normal Stress

Bottom liner specimen results and analyses are presented in terms of temperature effects and moisture effects on interface shear strength. Analyses of temperature and moisture effects on interface shear strength at a typical bottom liner normal stress are also presented. Within each section (temperature effects and moisture effects) data and analyses are presented in the order of τ, δ, and *a*. In addition, interpolation factors at the end of each section are provided for interpolation of δ as a function of temperature or moisture. Multiple tests were duplicated to confirm repeatability. Interface shear strengths of bottom liner specimens are presented in Tables 4.8 and 4.9.

Table 4.8. Peak Interface Shear Strengths (kPa) of Bottom Liner Specimens

	AR Moisture		50% Moisture		100% Moisture	
σ_n (kPa)	20 °C	40 °C	20 °C	40 °C	20 °C	40 °C
100	46.22	40.63	45.69	43.86	45.26	42.03
200	97.29	89.76	89.22	86.00	83.63	78.08
300	138.03	122.44	129.86	117.60	118.25	112.98

Table 4.9. Large-Displacement Interface Shear Strengths (kPa) of Bottom Liner Specimens

	AR Moisture		50% Moisture		100% Moisture	
σ_n (kPa)	20 °C	40 °C	20 °C	40 °C	20 °C	40 °C
100	34.18	30.85	33.75	34.29	27.52	24.62
200	64.07	53.75	53.10	54.82	41.28	43.00
300	90.08	78.80	70.30	66.43	64.50	55.90

4.4.1 Temperature Effects

Temperature was determined to have a significant impact on interface shear strength and interface shear strength parameters of T-GM/GCL interface at bottom liner normal stresses. Specimens sheared at 40 °C exhibited lower τ_p and τ_{ld} than those sheared at 20 °C (Figure 4.13). The decrease in τ_p and τ_{ld} from 20 to 40 °C was as much as 12% and 16%, respectively. The decrease was not solely due to the presence of bentonite extrusion, as AR specimens did not exhibit bentonite extrusion, yet experienced decreased interface shear strengths from 20 to 40 °C (Figures 4.14). Thus, a mechanism between geosynthetic components was likely the cause of decreased interface shear strength with increasing temperature. A reasonable explanation is softening (decrease in strength) of the carrier geotextile filaments and asperities of the geomembrane that resulted in decreased magnitude of hook and loop interaction.

Interface shear testing has been performed for T-GM/GT as a function of temperature. Both studies that investigated the effects of temperature on T-GM/GT reported increasing interface shear strength with increasing temperature. The results of this testing program of decreasing interface shear strength with increasing temperature do not agree with results provided by Akpinar and Benson (2005) and Karademir and Frost (2011). Even so, T-GM/GT may behave significantly differently than T-GM/GCL as a function of temperature even at AR moisture content due to presence of bentonite below the GT.

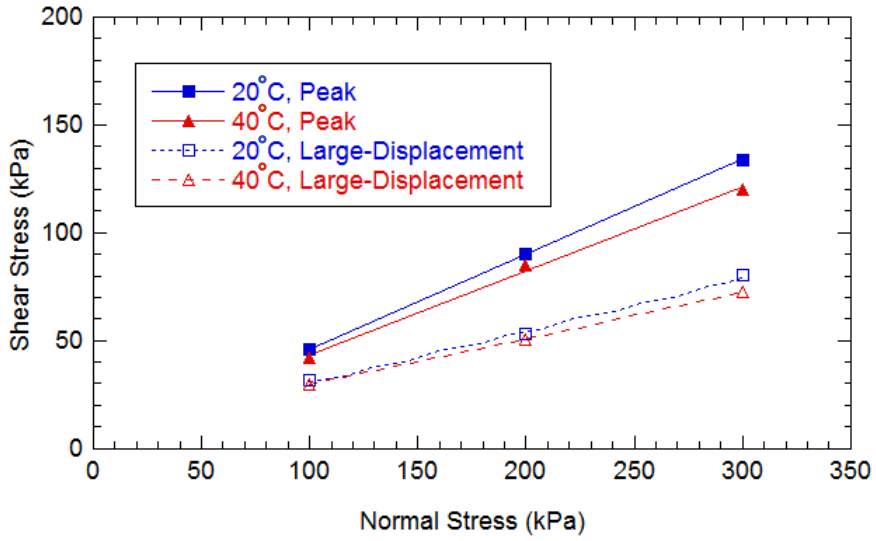

Figure 4.13. Average Peak and Large-Displacement Failure Envelopes for Bottom Liner Specimens

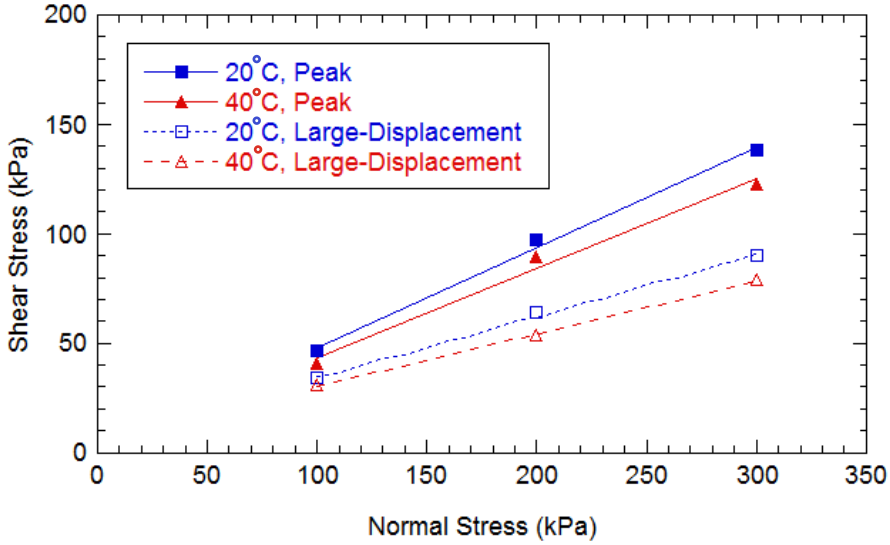

Figure 4.14. Peak and Large-Displacement Failure Envelopes at AR Moisture Content for Bottom Liner Specimens

Bentonite extrusion is believed to have contributed to decreased interface shear strength with increasing temperatures for specimens sheared at 50% and 100% moisture content (discussed in detail in the next section).

δ_p and δ_{ld} decreased by approximately 2° and 1.5° from 20 to 40 °C, respectively. A likely cause of the decrease in interface friction angle with increasing temperature is softening of geotextile filaments and geomembrane asperities and increased bentonite extrusion.

Adhesion (both a_p and a_{ld}) increased with increasing temperatures from 20 °C to 40 °C at moisture contents of 50% and 100%. Increased bentonite extrusion with increasing temperature may have resulted in decreased interface friction angle at elevated normal stress. It is believed the increased adhesion is partly due to increased apparent adhesion caused by decreased δ.

Analyses were performed to determine the change of interface friction angle per °C for bottom liner specimens between temperatures of 20 and 40 °C (Table 4.10). This analysis may be used as framework to interpolate δ_p and δ_{ld} at temperatures between 20 and 40 °C after δ_p and δ_{ld} are determined at one temperature between 20 and 40 °C. Values of 0.13 degrees/ °C and 0.105 degrees/ °C should be used for δ_p and δ_{ld}, respectively, from 20 to 40 °C.

Table 4.10. Interpolation Factors for δ_p and δ_{ld} for 20 °C to 40 °C

Interpolation Factor	AR	50%	100%
δ_p 20 °C to 40 °C (degrees/ °C)	0.13	0.13	0.03
δ_{ld} 20 °C to 40 °C (degrees/ °C)	0.11	0.07	0.08

Due to cover liner specimens generally exhibiting lowest adhesions at 20 °C, applying adhesion interpolation factors would result in a less conservative shear strength value. Adhesion values at 40 °C do not exhibit a significant

decrease from adhesion values at 20 °C. The author recommends using the adhesion values determined from testing at 20 °C if the bentonite was hydrated between AR and 100% moisture content to be conservative. These interpolation factors are recommended to be applied to interfaces of products similar to those tested under similar conditions.

4.4.2 Moisture Content Effects

Moisture content was determined to have a large influence on interface shear strength for bottom liner specimens. Increased moisture contents resulted in decreased interface shear strengths for almost all specimens. The decreased interface shear strengths at higher moisture contents (Figures 4.15) agree with previous work (McCartney et al. 2004, Seo et al. 2007, Vukelic et al. 2008, Chen et al. 2010) and provide more refined trend (i.e., more increments of moisture content) than what was provided by other investigators.

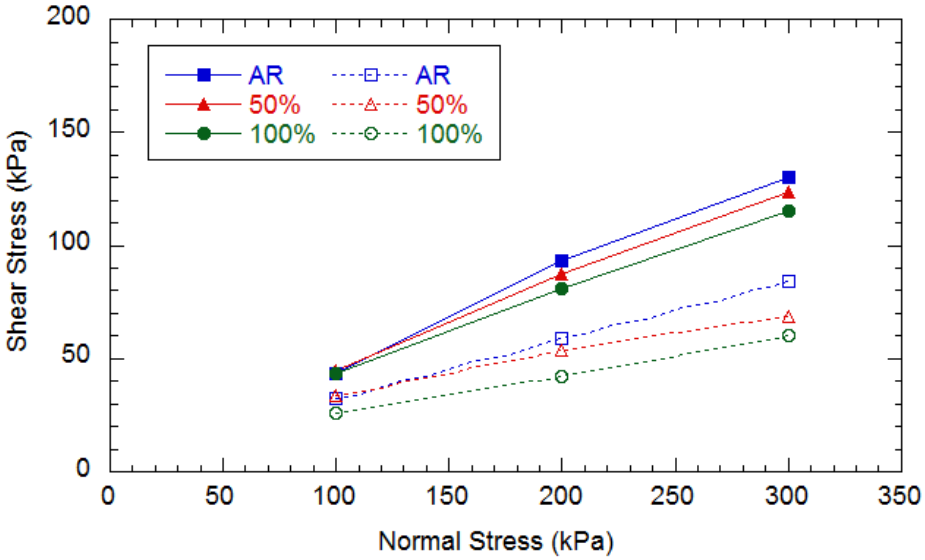

Figure 4.15. Average Peak and Large-Displacement Failure Envelopes for Bottom Liner Specimens

The trend of decreasing interface shear strength with increasing moisture content is likely attributed to bentonite extrusion, based on the following observations:

1. Specimens sheared at higher moisture contents resulted in lower interface shear strengths. This relationship agrees with higher moisture content bentonite having lower shear strength, thus extruding more and lubricating the surfaces more. In addition, increased extruded bentonite at higher moisture content was visually observed.
2. Chen et al. (2010) reported that the majority of bentonite extrudes during shearing rather than during consolidation, which would explain the large decrease from τ_p to τ_{ld}. Since the majority of bentonite extrudes during shearing, more bentonite would be extruded at large-displacements than at peak displacements. Increased bentonite extrusion at increased shear displacements may be due to larger GT openings after removal of filaments and plowing of GM asperities into the GT (and bentonite).

Other mechanisms caused by moisture may affect interface shear strength besides bentonite extrusion. One or more of the following mechanisms may have occurred, resulting in coupled effects along with bentonite extrusion to affect interface shear strength.

1. Softening of bentonite at higher moisture contents may have resulted in a softer GCL product. GM asperities may have been able to embed further into the nonwoven filaments because the hydrated bentonite could allow

more deformations at asperity locations. This mechanism may result in increased interface shear strength.

2. Swelling of bentonite at higher moisture contents (specifically 100%) increased the GCL thickness. The bentonite produced increased thickness. Tightening of geotextile filaments due to swelling may have changed the stress concentrations of GT filaments, resulting in more GT breakage.

Investigation of the effects of moisture on the interface shear strength parameters of bottom liner specimens was conducted. A relationship of interface friction angle and moisture content was established, as displayed in Figure 4.16. Test results exhibited a trend of decreasing δ_p with increasing moisture content, which agrees with results of T-GM/GCL provided by Seo et al. (2007). δ_p at both 20 and 40 °C exhibited a relatively linear downward trend with increasing moisture content. δ_{ld} exhibited a decrease from AR to 50% moisture content and relatively no decrease from 50% to 100% moisture content. A possible explanation for the behavior of δ_{ld} maintaining its value from 50% to 100% moisture content relates to reaching an upper threshold of bentonite extrusion. Since the majority of bentonite extrusion may have occurred during shearing, the amount of bentonite extrusion at 100% would have been greater than 50% at peak displacement, but similar at large-displacement. It is possible that little increase of bentonite extrusion occurred beyond a certain moisture content. A possible cause of little change of bentonite extrusion with increasing moisture content may be the lack of additional volume on the interface for the bentonite

extrusion to occur. Polishing of the geomembrane asperities and tearing of the geotextile filaments could lead to bentonite already having filled all available space. The difference between δ_p and δ_{ld} may be attributed to geosynthetic damage and bentonite extrusion. As the moisture content was increased from AR to 50%, increased bentonite extrusion occurred for all cases. Further increase in moisture content from 50% to 100% resulted in additional decrease in δ_p and almost no decrease in δ_{ld}.

Adhesion (both a_p and a_{ld}) increased as the moisture content increased from AR to 100% moisture. Increased bentonite extrusion would result in decreased interface friction angle at elevated normal stress. It is believed the increased adhesion is partly due to increased apparent adhesion caused by decreased δ.

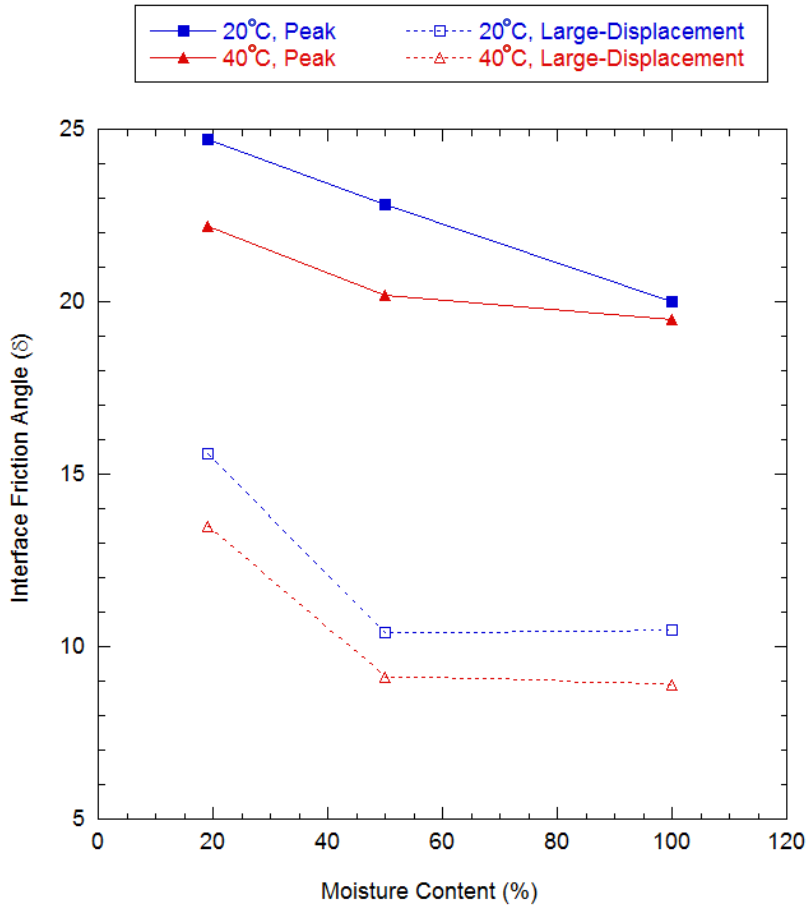

Figure 4.16. Average Failure Envelopes at Bottom Liner Specimens by Moisture Content

Analyses were performed to determine the change of interface friction angle per percentage point moisture content. In these analyses, percentage point of moisture content is termed w%. The analyses were performed for bottom liner specimens between moisture contents of AR, 50%, and 100% (Table 4.11). Positive interpolation factors represent decreasing δ. This analysis may be used as framework to interpolate δ_p and δ_{ld} at moisture contents between AR and 100% after δ_p and δ_{ld} are determined at one moisture content between AR and 100%. An interpolation factor of 0.065 degrees/ w% can be used for δ_p

from AR to 100% moisture content. An interpolation factor of 0.17 degrees/w% can be used for δ_{ld} from AR to 100% moisture content.

Table 4.11. Interpolation Factors for δ_p and δ_{ld} for AR, 50%, and 100% Moisture Content

Interpolation Factor	20 °C	40 °C
δ_p AR to 50% (degrees/w%)	0.061	0.065
δ_{ld} AR to 50% (degrees/w%)	0.056	0.014
δ_p 50% to 100% (degrees/w%)	0.168	0.142
δ_{ld} 50% to 100% (degrees/w%)	-0.002	0.004

Interpolation factors for adhesion values would not be conservative from AR to 100% moisture content. Adhesion values at AR do not exhibit a decrease from adhesion values at 50% or 100% moisture content. The author recommends using the adhesion value determined from testing at AR moisture content if the bentonite was hydrated between AR and 100% moisture content. These interpolation factors are recommended to be applied only to interfaces of products similar to those tested under similar conditions.

Interface friction angle and adhesion values of the failure envelopes at bottom liner normal stresses are summarized in Tables 4.12 and 4.13. The coefficient of determination (R^2 values) of failure envelopes determined by linear regression was provided as well. The R^2 values for cover liner specimen failure envelopes varied from 0.91 to 1.0, with 16 of 18 failure envelopes above 0.95 and 12 to 18 failure envelopes above 0.99.

Table 4.12. Interface Friction Angle Results of Bottom Liner Specimens

Interface Shear Strength Parameter	Moisture Content %	20 °C Specimens [δ (°), R^2]		40 °C Specimens [δ (°), R^2]	
Peak	19%[1]	24.7	0.996	22.2	0.987
	50%	22.8	1.0	20.2	0.993
	100%	20.0	0.999	19.5	1.0
Large-Displacement	19%[1]	15.6	0.998	13.5	0.999
	50%	10.4	0.999	9.1	0.975
	100%	10.5	0.979	8.9	0.990

[1] AR moisture content

Table 4.13. Adhesion Results of Bottom Liner Specimens

Interface Shear Strength Parameter	Moisture Content %	20 °C Specimens	40 °C Specimens
Peak Adhesion (kPa)	19%[1]	2.04	2.47
	50%	4.09	8.75
	100%	9.39	6.75
Large-displacement Adhesion (kPa)	19%[1]	6.88	6.52
	50%	15.8	19.7
	100%	7.45	9.89

[1] AR moisture content

4.4.3 Bottom Liner Normal Stress Analysis

Analysis was conducted on the test data related to interface shear strength of T-GM/GCL interface to determine the effects of moisture and temperature under a typical bottom liner normal stress of 150 kPa. A normal stress of 150 kPa is equivalent to approximately 15 m of overlying waste. Linear regression was used to determine the equation for each failure envelope. The interface shear strength of the failure envelope at 150 kPa was determined and the results were plotted against moisture content and temperature (Figure 4.17).

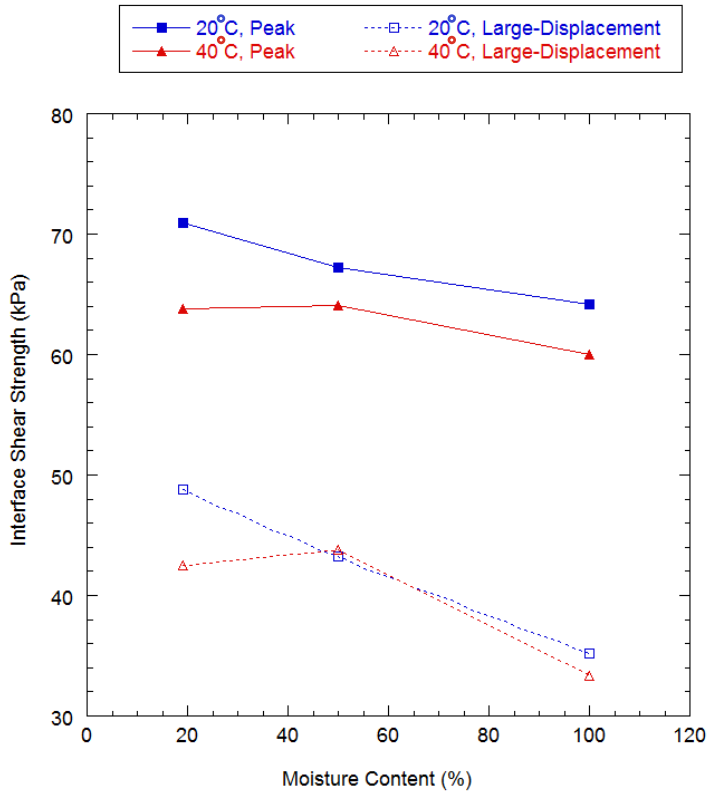

Figure 4.17. Peak and Large-Displacement Interface Shear Strengths at 150 kPa

Trends for both τ_p and τ_{ld} with moisture content at 20 °C were relatively linear. This linear trend could indicate that an increasing linear trend of bentonite extrusion occurred with increasing moisture content. τ was greater at 20 °C than at 40 °C at almost all tested moisture contents, which agrees with increased geosynthetic damage and increased bentonite extrusion occurring at higher temperatures.

4.5 Post-Shearing Observations

Subsequent to shearing, all geomembrane and GCL specimens were evaluated for physical condition, photographed, weighed to determine final bentonite moisture content, and characterized visually.

4.5.1 Bentonite Extrusion

For cover liner specimens, increased bentonite extrusion and deposition of bentonite on the geomembrane surfaces were observed on the nonwoven geotextiles at elevated temperatures and increased moisture contents. Specimens hydrated to 100% moisture content and sheared at 20 and 30 kPa exhibited an observable amount of bentonite extrusion, whereas specimens hydrated to AR and 50% moisture content did not exhibit bentonite extrusion to a level that was observed visually.

Significant bentonite extrusion was observed on bottom liner specimens with moisture contents of 50% and 100%. Bentonite was observed to be deposited on the geotextile surface and geomembrane surface between GM asperities. Increased bentonite extrusion was observed with increasing temperature (Figure 4.18), increasing moisture content (Figure 4.19), and increasing normal stress (Figures 4.20). In Figures 4.18 to 4.20, dark shading on GCLs and lighter shading on GMs represent bentonite extrusion.

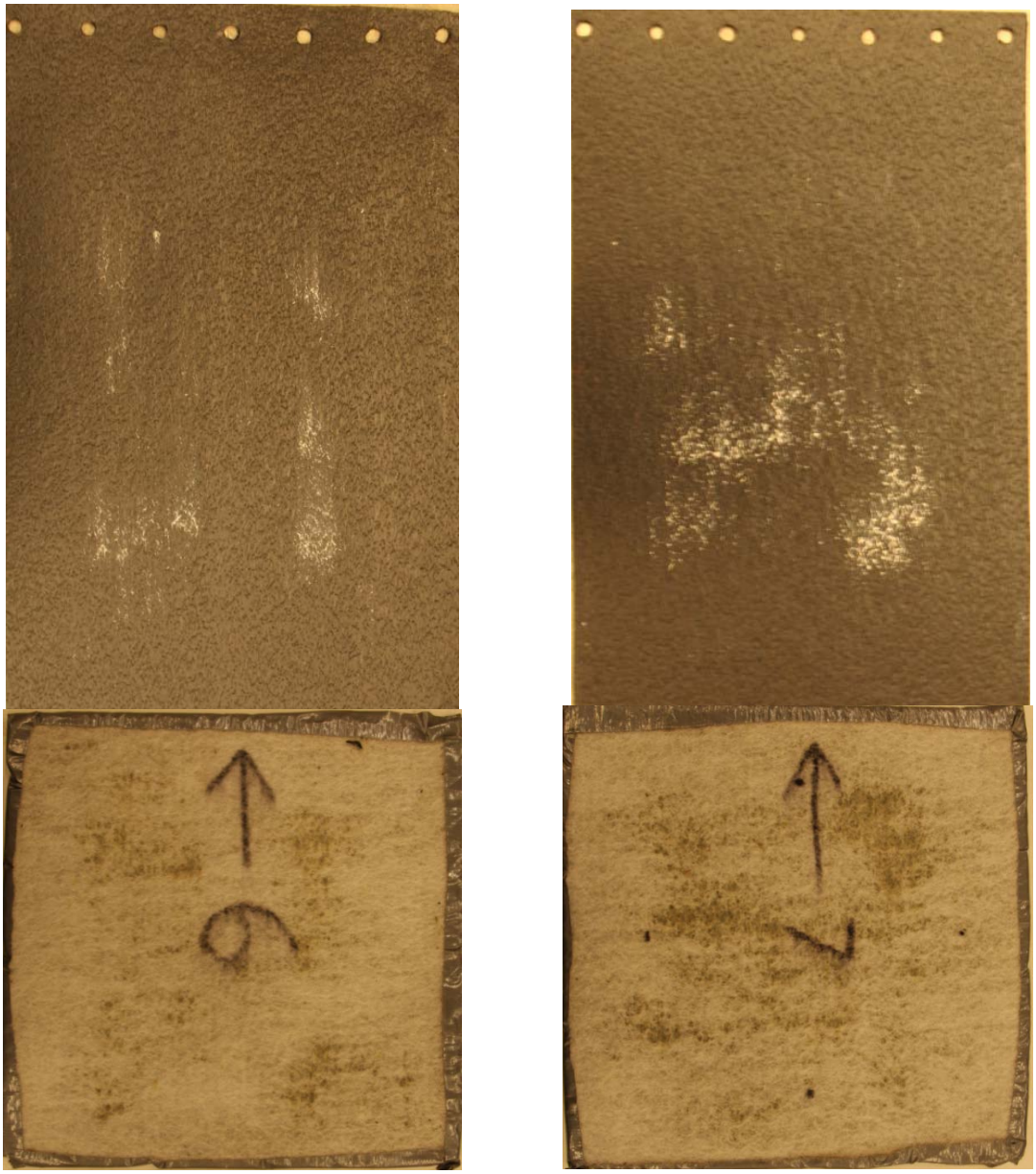

Figure 4.18. Photographs of 50% Moisture Content Specimens Sheared at 100 kPa at 20 °C (left) and 40 °C (right)

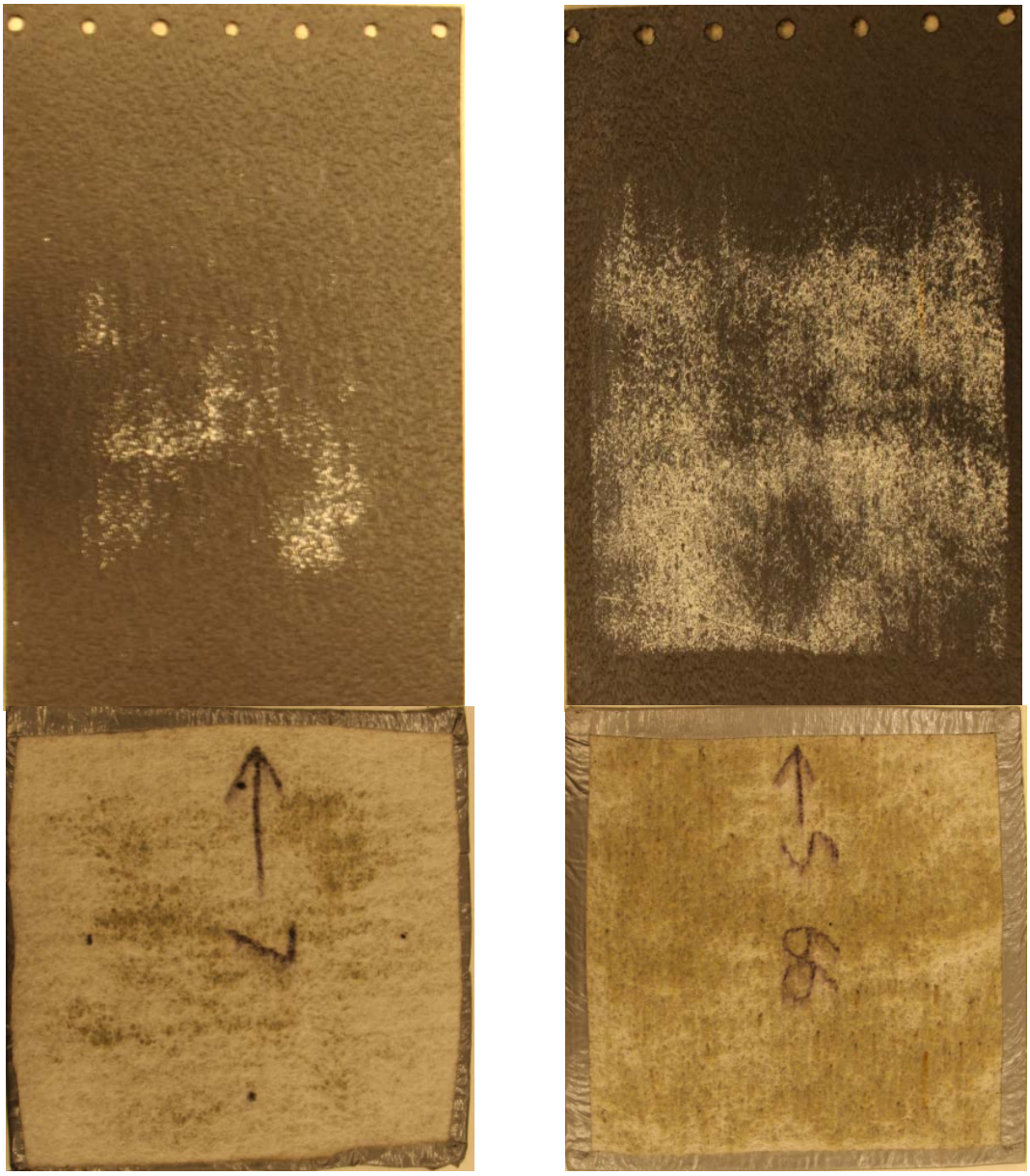

Figure 4.19. Photographs of 20 °C Specimens Sheared at 100 kPa at Moisture Contents of 50% (left) and 100% (right)

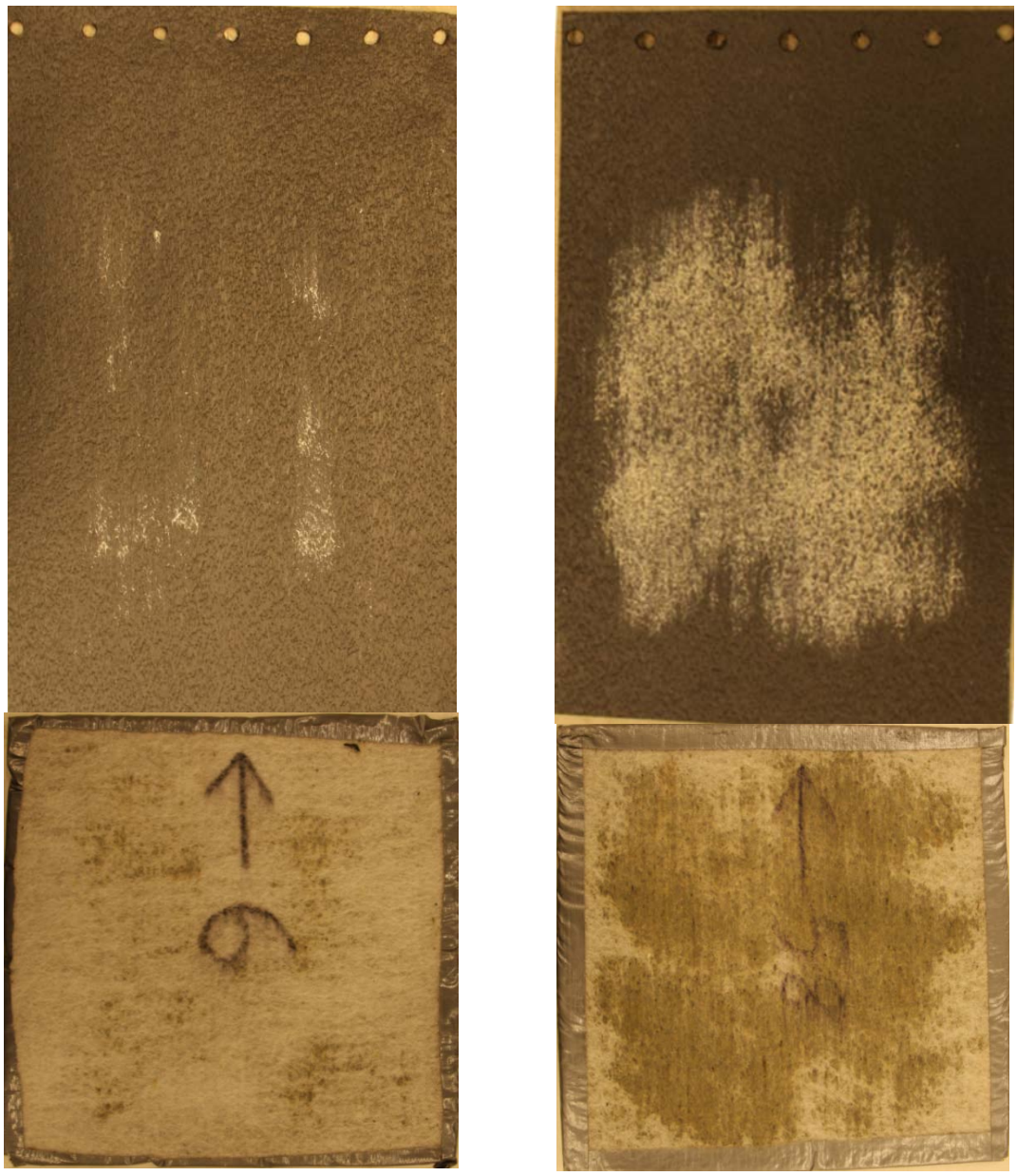

Figure 4.20. Photographs of 50% Moisture Content Specimens Sheared at 20 °C at 100 kPa (left) and 200 kPa (right)

4.5.2 Geosynthetics Damage

Damage to the geosynthetic materials was determined to be the primary cause of post-peak strength loss for cover liner specimens. Polishing of the geomembrane surface and pullout and tearing of the geotextile filaments was observed. Geotextile filaments were reoriented and “combed” in the shearing direction. Pullout of filaments was observed to occur over a slightly longer distance with specimens sheared at 40 °C than those sheared at 20 °C, possibly occurring due to lower polypropylene modulus at 40 °C causing the fibers to be stretched rather than torn. Observation through a 20 times magnification optical microscope of partially pulled out geotextile filaments after shearing. The GT filaments were aligned with the shearing direction, overlaying the duct tape on the GCL edge. Photographs of the microscope images indicated that filaments of specimens sheared at 2 °C (Figure 4.21) resulted in a more angular configuration. Filaments of specimens sheared at 20 °C (Figure 4.22) were observed to be less angular, agreeing with the behavior of a more ductile material at higher temperatures. Specimens sheared at 40 °C were observed to have straighter filaments oriented opposite to the shearing direction (Figure 4.23).

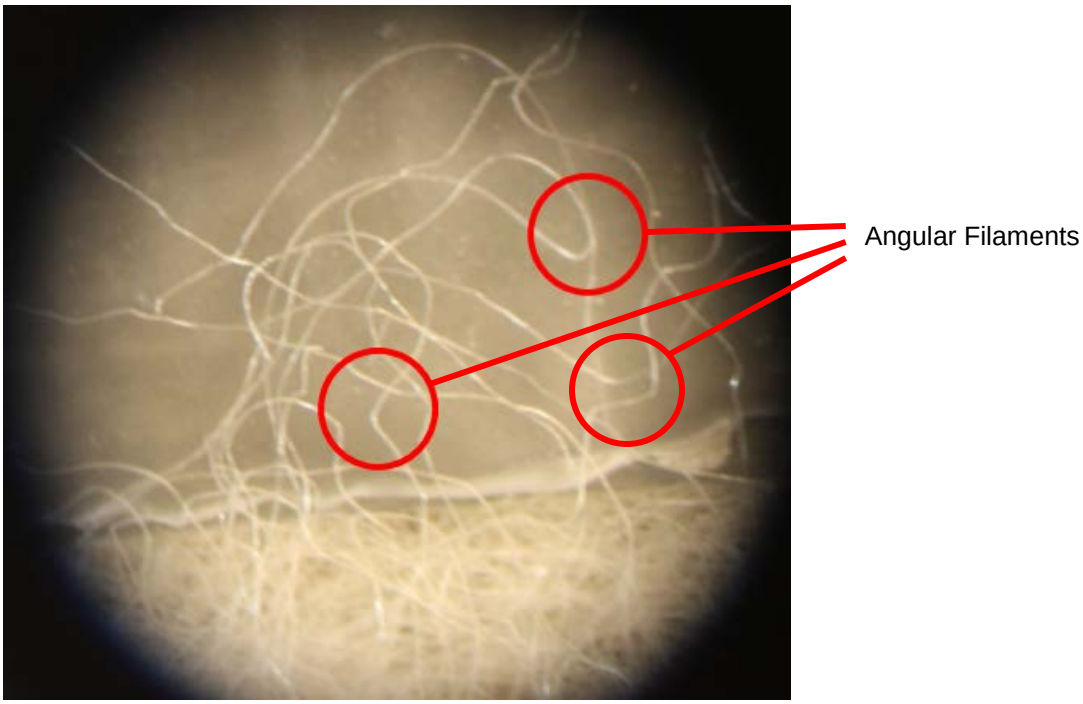

Figure 4.21. Photograph of GT Filaments of Specimen Sheared at 2 °C

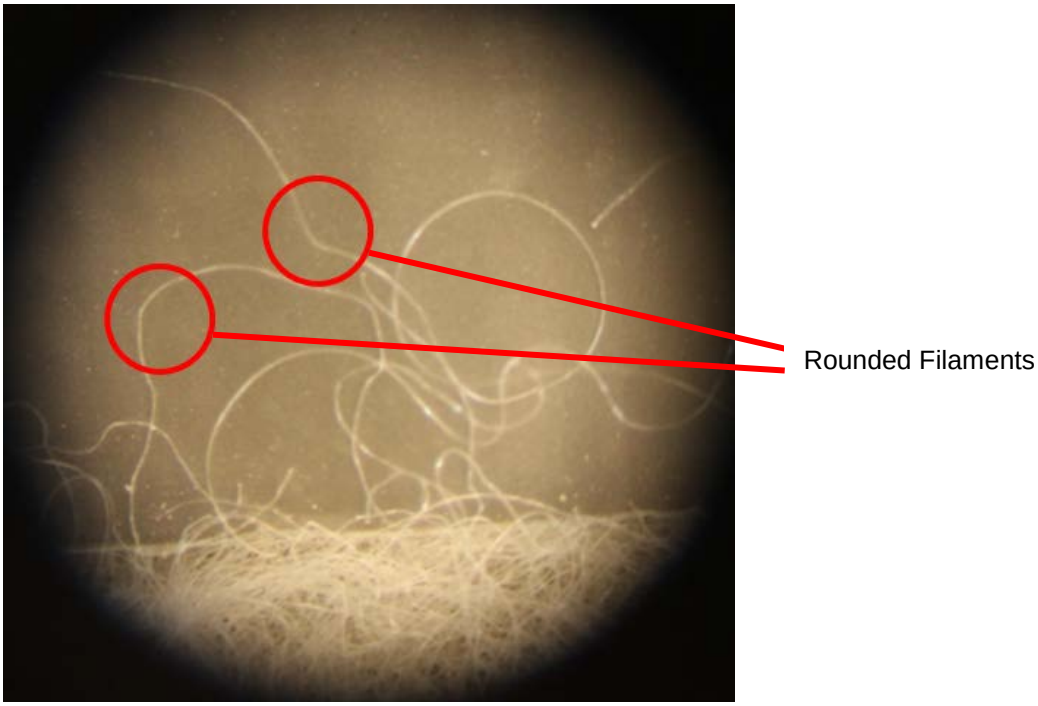

Figure 4.22. Photograph of GT Filaments of Specimen Sheared at 20 °C

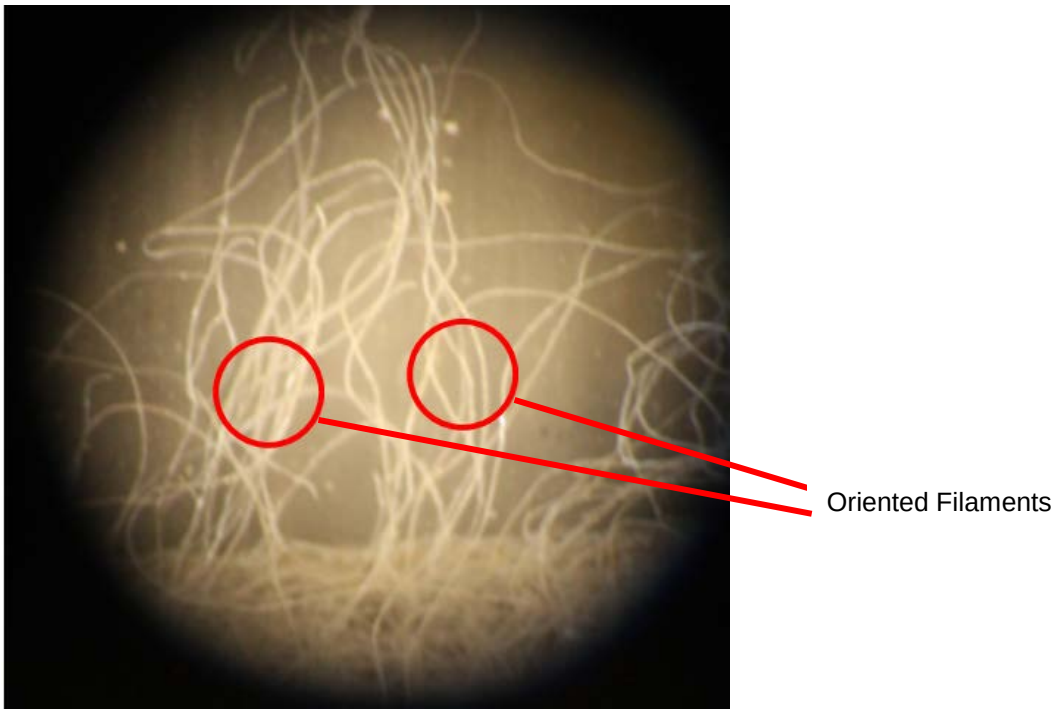

Figure 4.23. Photograph of GT Filaments of Specimen Sheared at 40 °C

Damage to the geosynthetic materials was determined to be a cause for post-peak strength loss for bottom liner specimens along with bentonite extrusion. Significant polishing of the geomembrane textures was observed with bottom liner specimens. Texture asperity heights were decreased and peaks were deformed oriented opposite of the shearing direction. A photograph of a virgin GCL specimen is presented in Figure 4.24. Unlike cover liner specimens, where geotextile filaments were partially pulled out (Figure 4.25), bottom liner specimens were entirely pulled out or torn, leaving a fewer number of filaments and shorter free ends at the sheared surface torn (Figure 4.26).

Figure 4.24. Photograph of Virgin GCL Specimen

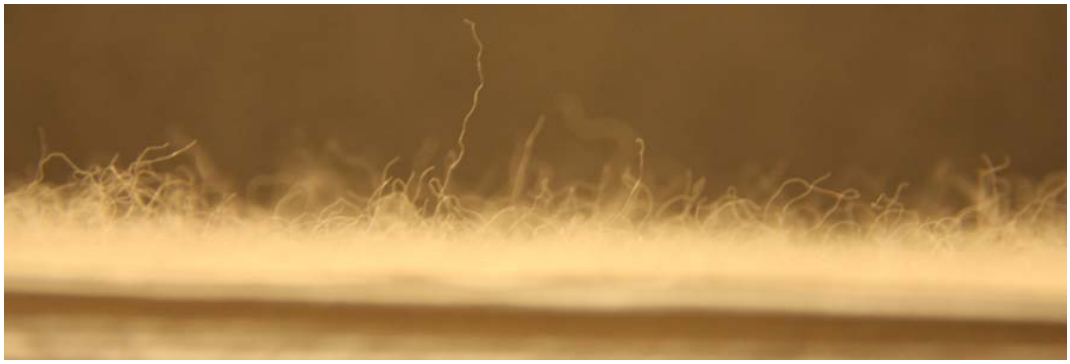

Figure 4.25. Photograph of Pulled and Torn Geotextile Filaments from Cover Liner Specimen Subsequent to Shearing

Figure 4.26. Photograph of Torn Geotextile Filaments from Bottom Liner Specimen Subsequent to Shearing

4.5.3 Consolidation

Consolidation of GCL specimens was evaluated using moisture content and thickness data. Deposited water was observed after shearing with the 100% moisture content specimens in 200-and 300-kPa normal stress tests, indicating that consolidation of the bentonite had occurred. No other specimens exhibited evidence of consolidation (i.e., free water) throughout the testing program.

Mass of GCL specimens was determined before and after shearing to determine moisture change (due to evaporation or consolidation) and final bentonite moisture content. The calculated final moisture contents of some specimens were overestimated because extruded bentonite on the textured geomembrane contributed to decrease in final GCL mass. Overestimation of final bentonite moisture content was determined to be insignificant at less than 1%. AR moisture content specimens exhibited between approximately 1 and 2% points decrease in moisture content from their original moisture content of 18% to 19%. The majority of 50% moisture content specimens resulted in post-shearing moisture contents from 44 to 46%. Cover liner specimens at 100% moisture content resulted in a final post-shearing bentonite moisture content of approximately 95%, while 100% moisture content specimens decreased due to consolidation and shearing to approximately 90% for 100 kPa, 85% for 200 kPa, and 78% for 300 kPa bottom liner specimens. Consolidation of 100% moisture content specimens at 200 and 300 kPa was confirmed when water was observed after shearing. No significant correlation between temperature and final moisture content was observed.

GCL thicknesses were measured before and after shearing. Unhydrated specimens directly from the GCL sample typically were 5 to 6 mm thick. Cover liner specimens hydrated to 100% moisture content typically experienced 1 to 2 mm of swelling, while specimens at AR and 50% moisture contents maintained their original thickness. Bottom liner specimens hydrated to 100% moisture content typically experienced approximately 2 mm of consolidation/settlement after their 1 to 2 mm of swelling during stage 1. Specimens at AR and 50% moisture content typically experienced 1 mm of settlement after no swelling during stage 1. The lack of GCL swelling of AR and 50% moisture content specimens indicates that there may have been air voids between bentonite granules. Needle-punching and GT filaments may have not been as taut as they would be in a 100% moisture content specimen.

4.6 Post-Peak Strength Reduction

Post-peak strength reduction is well documented with T-GM/GCL and T-GM/GT interfaces (e.g., Stark et al. 1996, Triplett and Fox 2001, McCartney et al. 2009a). Investigation of large-displacement interface shear strength is critical due to the large displacements experienced between geosynthetic surfaces during and after waste placement. In addition to determining strength reduction values, mechanisms resulting in post-peak strength reduction as a function of temperature and moisture were investigated. To determine the effects of temperature and moisture on post-peak strength reduction, normalized large-displacement shear strength (τ_{ld}/τ_p) was plotted against temperature and moisture for tested specimens.

Cover liner specimens exhibited decreased post-peak strength reduction (increased τ_{ld}/τ_p) with increasing temperature. Specimens sheared at 2 °C exhibited significantly more post-peak strength reduction than those sheared at 20 and 40 °C (Figure 4.27). Specimens sheared at 20 °C experienced slightly more post-peak strength reduction than those sheared at 40 °C. Little correlation between moisture and normalized large-displacement shear strength was observed for cover liner specimens. The bounds of highest and lowest normalized large-displacement shear strengths for all cover specimens are presented in Figure 4.28.

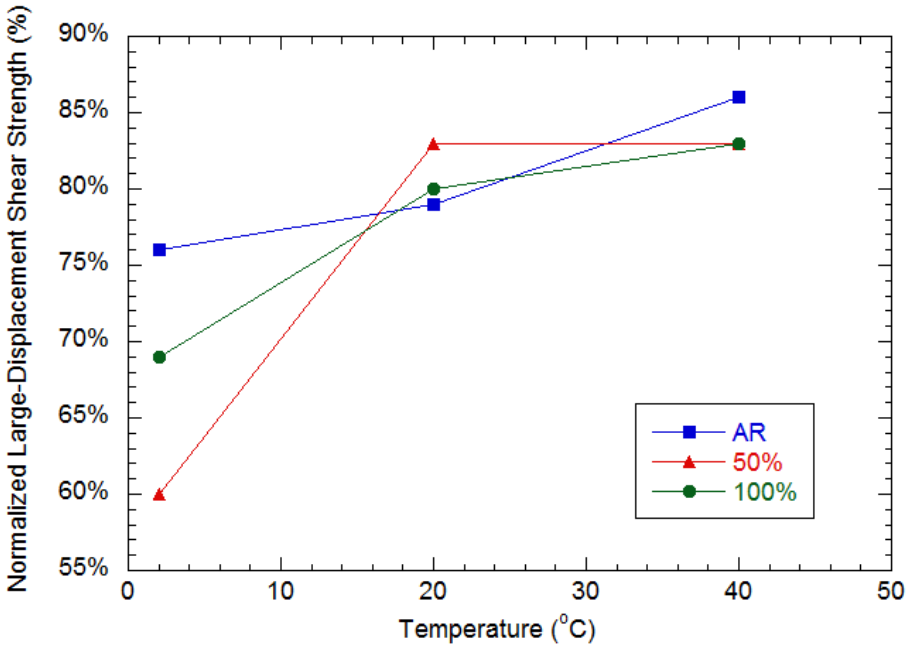

Figure 4.27. Average Percent Normalized Large-Displacement Shear Strength for Cover Liner Specimens versus Temperature

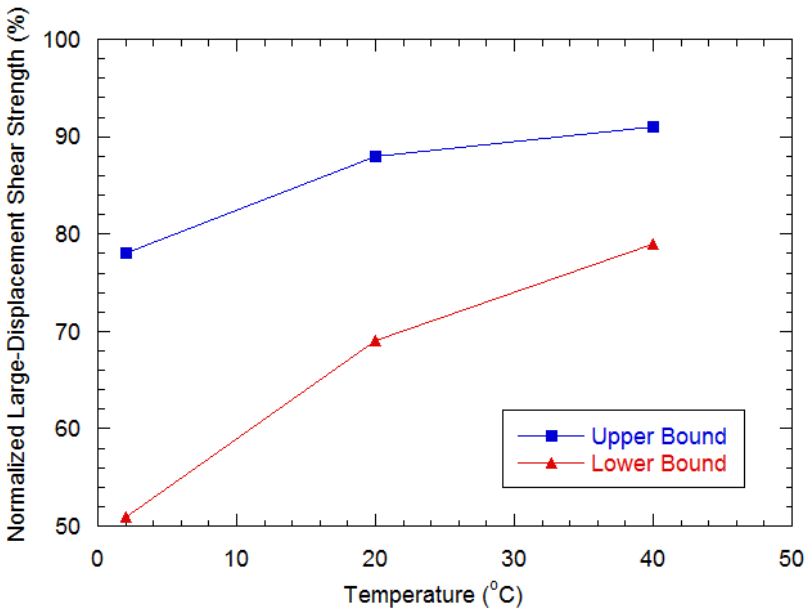

Figure 4.28. Upper and Lower Bound of Percent Normalized Large-Displacement Shear Strength for Cover Liner Specimens versus Temperature

The decrease in normalized large-displacement shear for bottom liner specimens was likely due to increased bentonite extrusion. τ_{ld}/τ_p decreased significantly in Figure 4.29. Increased bentonite moisture content resulting in increased bentonite extrusion post-peak has been documented by Chen et al. (2010). No bentonite extrusion was observed with AR specimens and progressively more was observed on 50% and 100% moisture content specimens, as presented in Figure 4.19.

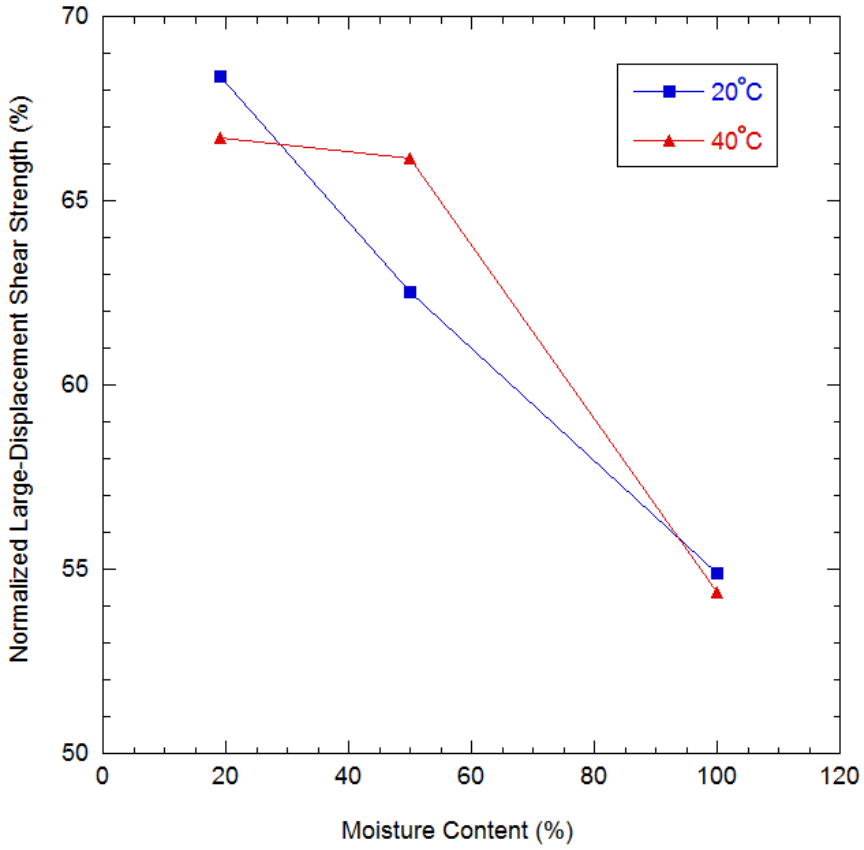

Figure 4.29. Percent Normalized Large-Displacement Shear Strength for Bottom Liner Specimens versus Moisture Content

For comparison between cover liner and bottom liner specimens, average normalized large-displacement shear strength for AR moisture content specimens was plotted against temperature (Figure 4.30). This plot isolates the mechanism causing post-peak strength loss due to normal stress by removing moisture effects (i.e., bentonite extrusion). A significant drop of (τ_{ld}/τ_p) was observed when comparing cover liner specimens to bottom liner specimens. It is possible the cause for decreased normalized large-displacement shear strength is increased geosynthetic damage. Higher normal stresses applied to the specimens would result in higher shear stresses imparted on the geomembrane

asperities and geotextile filaments. Increased geosynthetic damage occurring at large-displacements would result in lower normalized large-displacement shear strength for bottom liner specimens than for cover liner specimens.

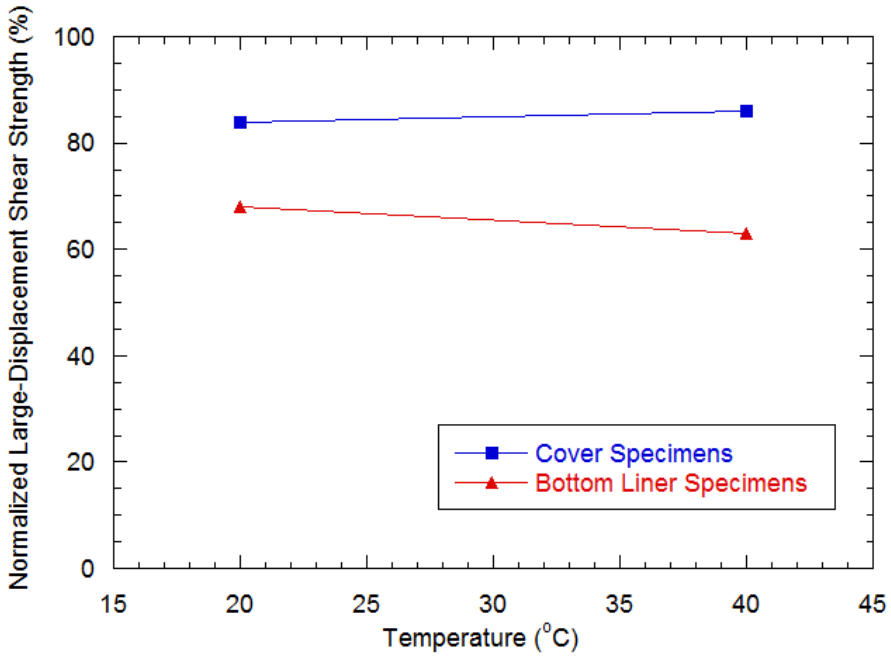

Figure 4.30. Average Percent Normalized Large-Displacement Shear Strength for AR Specimens

In addition to interpretation of results, visual observation of geosynthetic damage was observed. Geotextile filaments within cover liner specimens were observed to be partially pulled out. Geotextile filaments within bottom liner specimens were observed to be torn or completely pulled out and a small amount of fully intact filaments were observed. The ends of filaments were observed to be torn. Torn and pulled out filaments would likely result in decreased interface shear strength. Filaments of sheared specimens at 50% or 100% moisture

content were not as easily visible due to large amounts of bentonite smeared on and between them.

4.7 Shear Displacement

4.7.1 Peak and Large-Displacement Shear Displacements

The peak shear displacements were determined by identifying the shear displacement at which the peak shear strength occurred. The average peak shear displacement was determined to occur at approximately 10 mm. For cover liner specimens, peak shear displacements were determined to be not significantly affected by temperature or moisture content. For bottom liner specimens, peak shear displacements were determined to be slightly affected by temperature (Figure 4.31). Peak shear displacements of cover liner specimens occurred at between 8 and 11 mm in 24 of 27 tests. Peak shear displacements of bottom liner specimens occurred at between 9 and 12 mm in 18 of 24 tests. Large-displacement shear displacements were determined to occur at a shear displacement of 50 mm for cover liner specimens and 55 mm for bottom liner specimens. The shear stress corresponding to 50 mm and 55 mm shear displacement was used as the large-displacement shear strength for cover and bottom liner specimens, respectively. McCartney et al. (2005) reported that shear strengths have been observed to be effectively constant after approximately 50 mm for T-GM/GCL interface. A schematic of stress-displacement curve with peak and large-displacement shear stresses and peak and large-displacement shear displacements is presented for cover liner specimens in Figure 4.32.

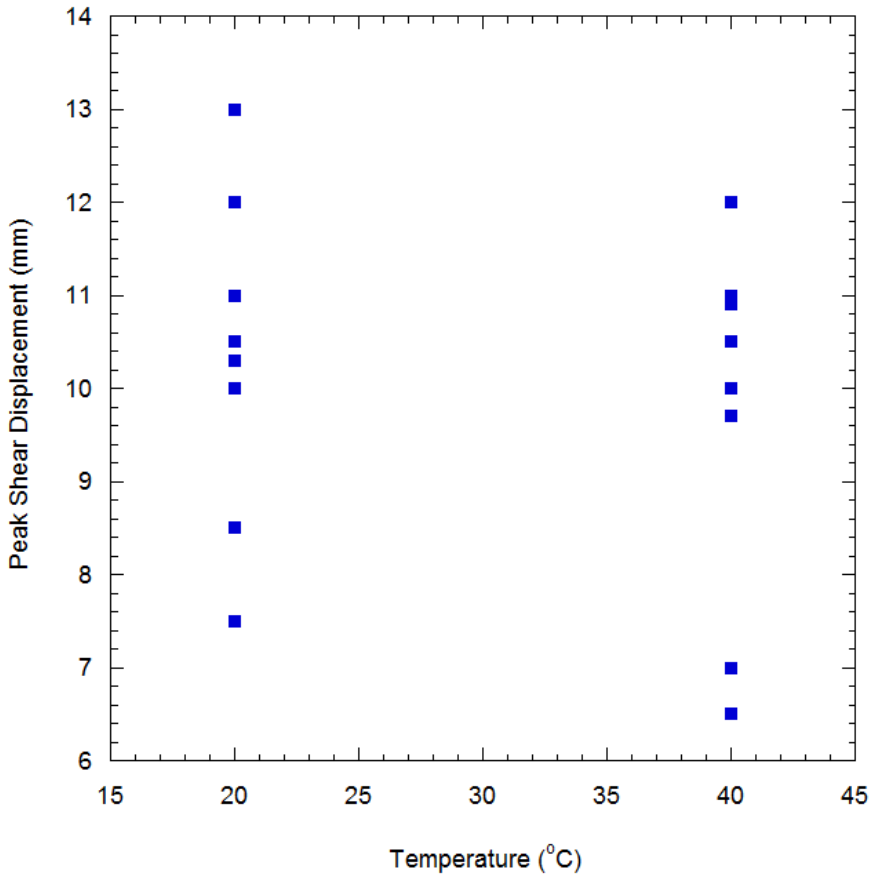

Figure 4.31. Peak Shear Displacements for Bottom Liner Specimens versus Temperature

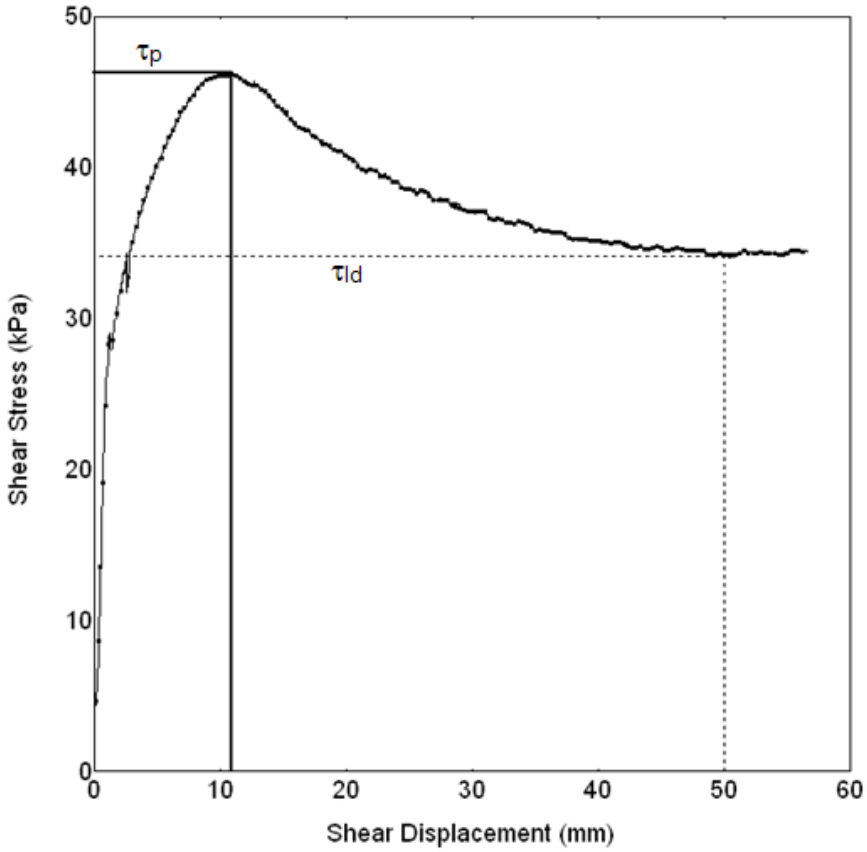

Figure 4.32. Peak and Large-Displacement Shear Displacements with Corresponding Shear Stresses

4.7.2 Shear Displacement at Near Peak Interface Shear Strength

Determining the magnitude of peak shear displacement is important to establish if peak or large-displacement shear strength values will be used in design. Determining the shear displacement assumed to occur in the field could establish whether to use τ_p or τ_{ld}. It is also important to determine over what displacement the interface will retain near its peak shear strength. Analysis was performed to investigate the effects of moisture and temperature on the displacement of at least 90% of τ_p (Figure 4.32). Analysis was performed using

shear stress-displacement data to determine the displacement 90% of τ_p would occur for each large-scale direct shear test.

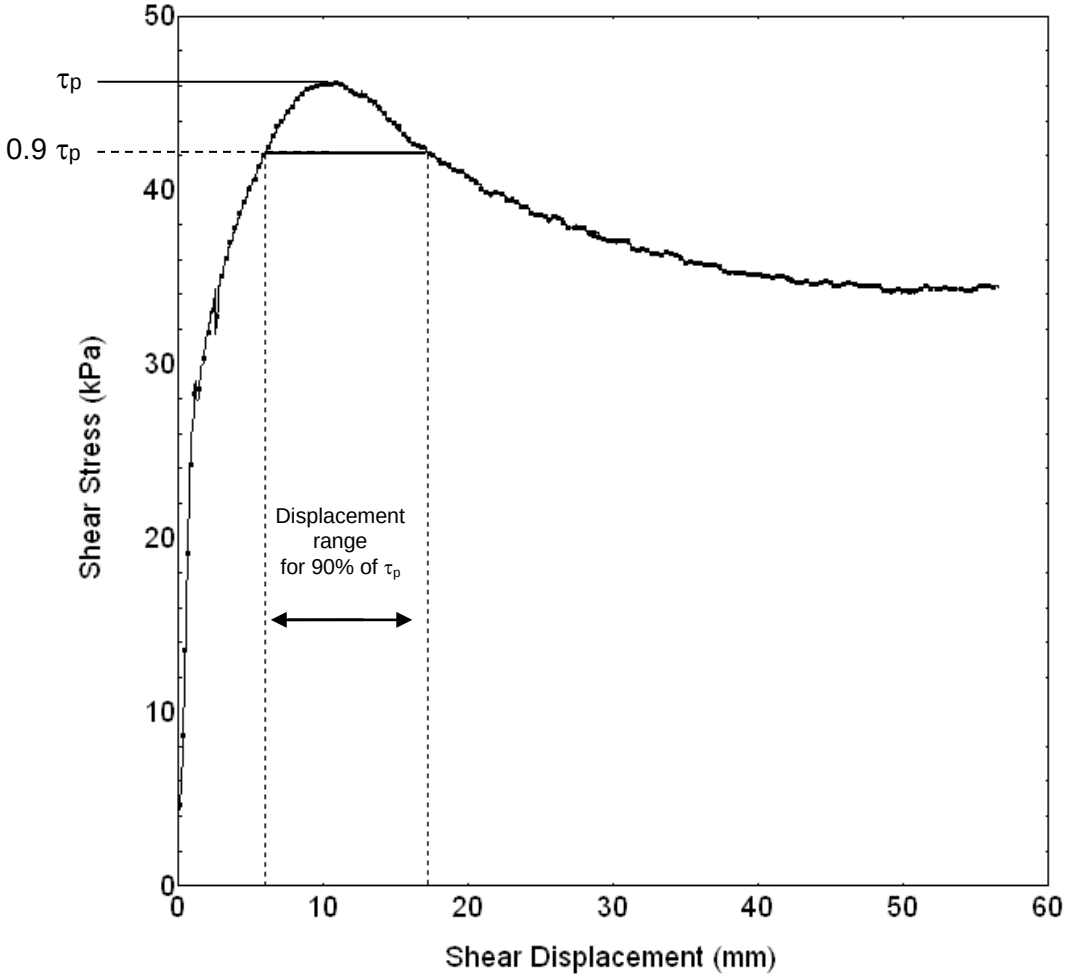

Figure 4.33. Displacement for 90% Peak Shear Strength

Normal stress was determined to have a large effect on displacement range achieved at 90% peak interface shear strength (Figure 4.34). Temperature was determined to have an effect on displacement range for 90% of τ_p for cover liner and bottom liner specimens. Cover liner specimens experienced increased displacement ranges of 90% of τ_p at higher temperatures (Figure 4.35). Increased ductility and decreased geosynthetic modulus may

have attributed to larger displacements for an equal shear stress. A similar mechanism was expected to occur for bottom liner specimens, as a similar relationship between temperature and displacement range for 90% of τ_p was observed (Figure 4.36).

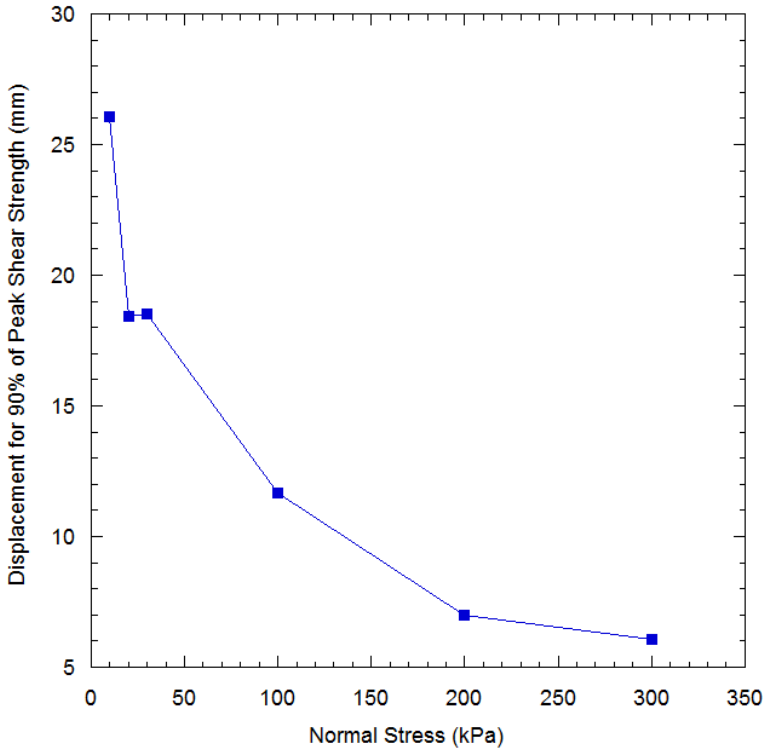

Figure 4.34. Average Displacement Ranges for 90% Peak Shear Strength

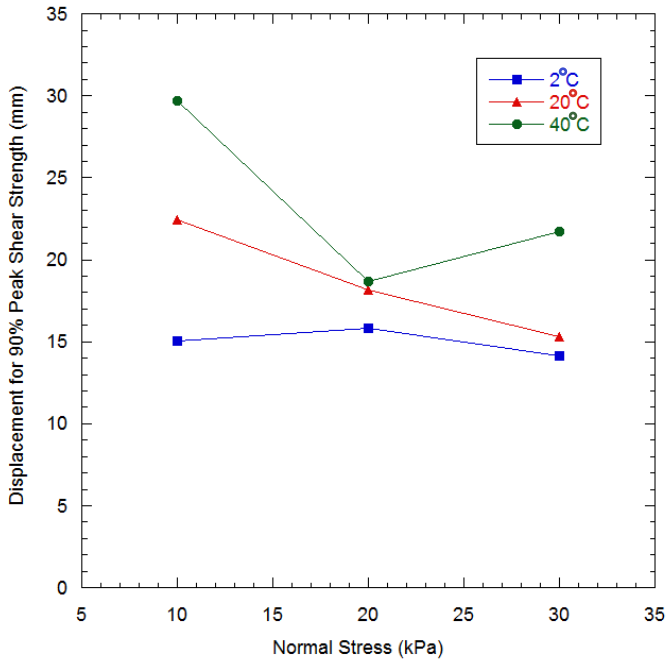

Figure 4.35. Average Displacement Ranges for 90% of τ_p with Temperature for Cover Liner Specimens

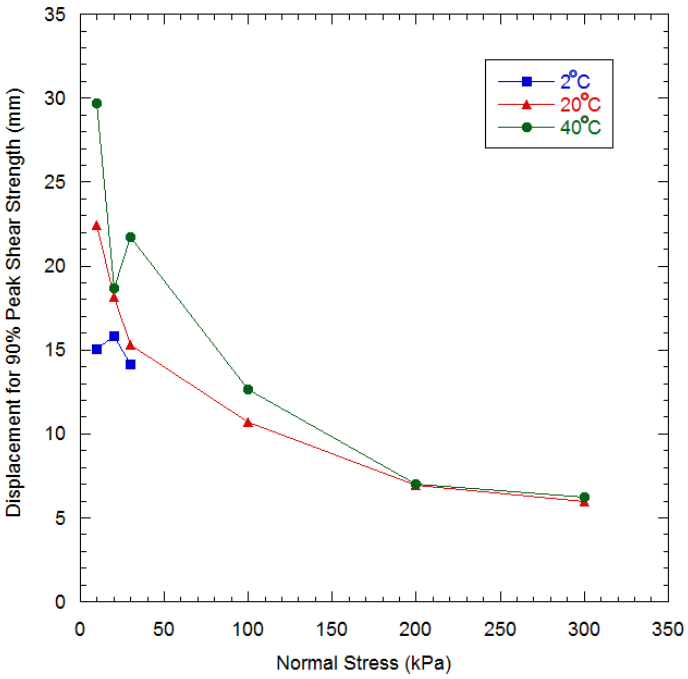

Figure 4.36. Average Displacement Ranges for 90% of τ_p with of Temperature for Cover Liner and Bottom Liner Specimens

Displacement ranges for 90% of τ_p for cover liner specimens were not observed to be affected by moisture content, whereas displacement range for 90% of τ_p for bottom liner specimens was determined to be affected by moisture content. Specimens sheared at 100% moisture content exhibited significantly less displacement range for 90% of τ_p than those sheared at AR and 50% moisture content (Figure 4.37). Specimens sheared at 100% moisture content may experience significant bentonite extrusion at a lower displacement than specimens sheared at 50% moisture content. High bentonite extrusion during peak displacement would result in an earlier drop of interface shear strength, decreasing the displacement range for 90% of τ_p.

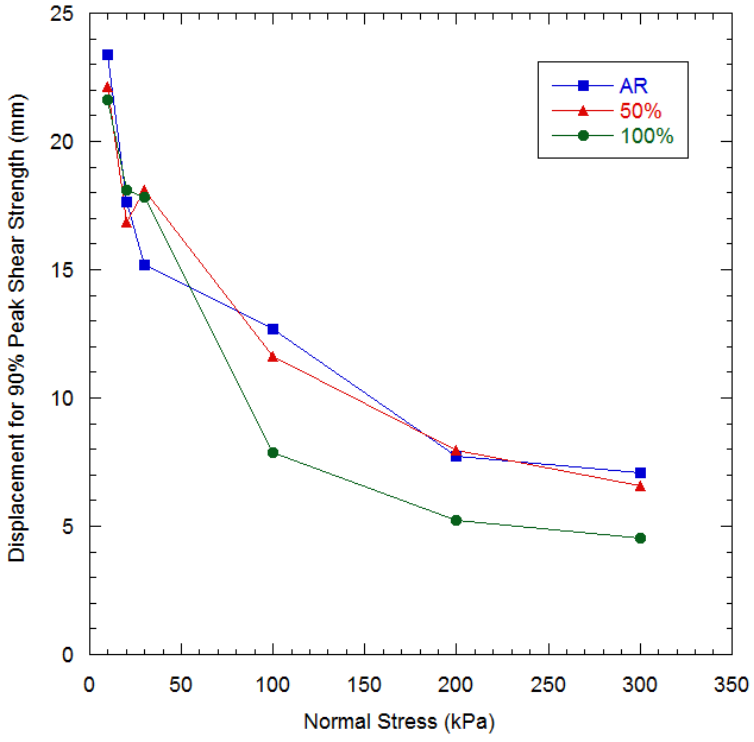

Figure 4.37. Average Displacement Ranges for 90% of τ_p with Moisture Content for All Specimens

Overall, higher temperatures and lower moisture contents resulted in increased displacement ranges for 90% of τ_p. Up to 15 mm of difference between 40 °C and 2 °C was determined for displacement ranges for 90% of τ_p. Moisture had less of an effect on 90% of τ_p displacement than temperature. Up to 3 mm of difference between AR and 100% moisture content was determined for displacement ranges for 90% of τ_p.

4.8 Bentonite Extrusion Testing

Bentonite extrusion testing and liquid limit testing were performed to evaluate the effects of moisture, temperature, and normal stress on bentonite extrusion.

4.8.1 Bentonite Extrusion

Increased bentonite extrusion was determined to occur with increasing normal stress and moisture content. Moisture content was determined to have a significant effect on bentonite extrusion. Measurements from this testing program are used as indicators for trends in bentonite extrusion. Amounts of extrusion reported represent bentonite that resides on the screens. It was feasible not to quantify amount of extrusion that was still attached to the geotextile filaments. Specimens tested at 300 kPa were hydrated to moisture contents of 50%, 100%, and 150%, which extruded 0.001 g, 0.005 g, 0.123 g and of bentonite, respectively. Normal stress was determined to have a slightly less effect on bentonite extrusion. Specimens experienced an increase from 0.005 g to 0.0142 g of bentonite extrusion with an increase in normal stress from 100 kPa

to 400 kPa (Figure 4.38). Increased bentonite extrusion as a function of increased normal stress is in agreement with visual observations of tested specimens.

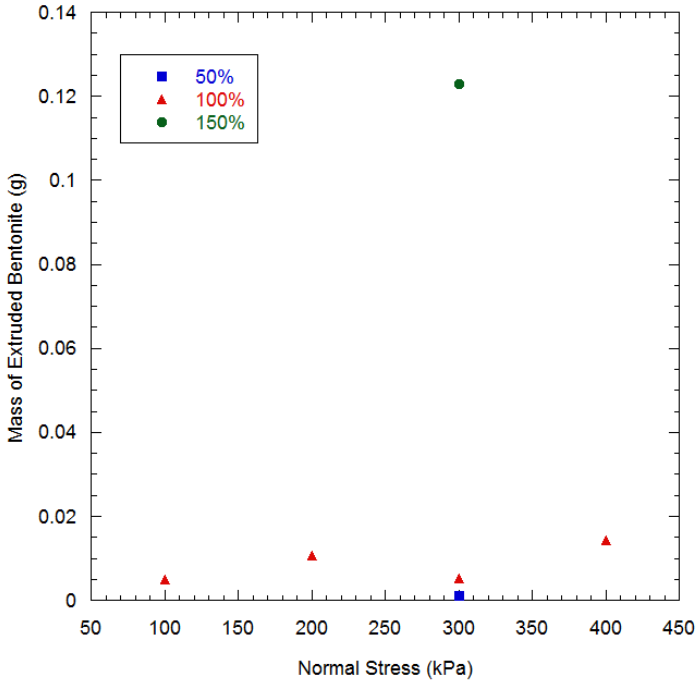

Figure 4.38. Mass of Extruded Bentonite

4.8.2 Liquid Limit

Liquid limit of bentonite was determined to decrease with increasing temperature. Liquid limit of bentonite at 2 °C of 580% was greater than the liquid limit at 20 °C and 40 °C. Liquid limits at 20 °C and 40 °C were 549% and 543%, respectively (Table 4.14). The liquid limit values can be used as an indicator of bentonite shear strength as a function of temperature. Decreased liquid limit values with increasing temperature indicates lower bentonite shear strength at higher moisture contents. Lower shear strength at higher moisture contents

would confirm the observation of increased bentonite extrusion and decreased interface shear strength.

Table 4.14. Bentonite Liquid Limits at 2, 20, and 40 °C

Temperature	Liquid Limit
2 °C	580%
20 °C	549%
40 °C	543%

Chapter 5: Engineering Significance and Future Research

5.1 Introduction

Slope stability analyses were performed for two representative landfill slopes to determine the engineering significance of the interface shear strength results. Preliminary analyses were conducted to determine that cover liner slopes and filled bottom slopes were most critical. Separate analyses were performed for cover liner and bottom liner slopes. Interface friction angle and adhesion data from T-GM/GCL interface shear strength tests were used as input for WinStabl slope stability analysis software to conduct numerical simulations. WinStabl employs 2-D limit equilibrium methods to establish the factor of safety (FS) for each liner condition.

5.2 Cover Liner Analysis

Slope stability analyses for cover liner slopes were performed assuming a finite slope with uniform cover liner soil thickness. Slope geometry was selected to represent a typical cover liner system and is presented in Figure 5.1. The slope profile was input to WinStabl along with geosynthetic interface strength parameters from testing data. The failure surface was defined prior to analysis to occur through the T-GM/GCL interface. Slope stability analyses for cover liner system were performed by applying the following assumptions:

- The failure plane was consistent with the T-GM/GCL interface
- No contribution of geosynthetic tension to resisting forces occurred
- The slope was 60 m long
- The slope was placed at 4:1 inclination

- The liner was overlain by 1.5 m of cover soil
- The cover liner soil had a unit weight of 18 kN/m^3

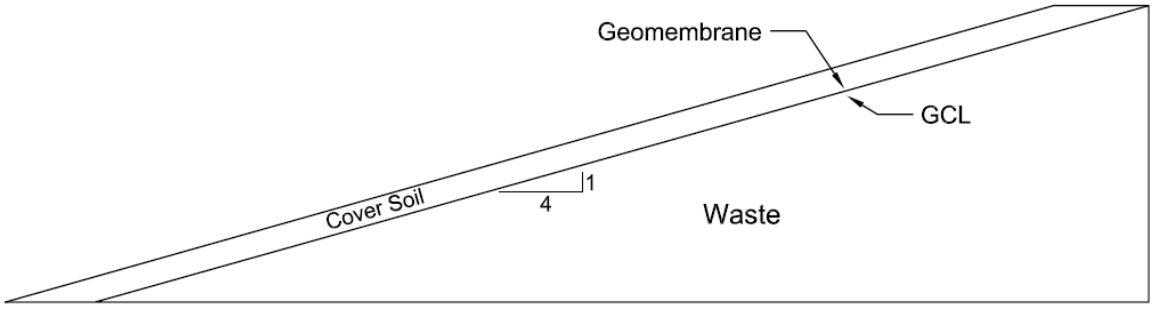

Figure 5.1. Schematic of Cover Liner and Waste Geometry

Slope stability analyses were performed for T-GM/GCL interface for a cover liner slope with a bentonite moisture content of 100% at temperatures of 2 °C, 20 °C, and 40 °C. Large-displacement interface shear strength parameters were used because large settlement deformations can be experienced by waste and overlying cover liner systems. As determined from testing results, peak interface shear strength parameters occur at approximately 10 mm, and any displacement other than the peak shear displacement would result in interface shear strengths less than those at peak. Contribution of resisting forces from geosynthetic tension was not considered, due to possible slack of liners caused by settlement or geosynthetic expansion (i.e., presence of wrinkles before placement of overlying soil). The interface shear strength parameters used for the analysis are presented in Table 5.1.

Table 5.1. Interface Shear Strength Parameters for Cover Liner Analysis

Temperature	δ (deg)	*a* (kPa)
2 °C	12.7	4.4
20 °C	18.2	2.7
40 °C	15.9	2.6

Cover liner temperatures of 20 °C were determined to provide the highest factor of safety at 1.88. Temperatures of 2 °C resulted in a factor of safety of 1.76, followed by the lowest FS of 1.68 at 40 °C. Cover liners at temperatures of 2 °C and 40 °C exhibited a decrease in factor of safety of 6.4% and 10.6%, respectively, relative to cover liners at 20 °C.

An analysis was performed to determine a reduction factor that can apply to interface shear strength parameters for a range of temperatures expected in field conditions. In all cases, δ was greatest at 20 °C, while *a* was generally greatest at temperatures other than 20 °C. Increasing *a* would provide additional strength, which is not a conservative method. An average δ for 2 and 40 °C was determined and was divided by δ for 20 °C to produce the reduction factor. The average δ_p for 2 °C and 40 °C was determined to be 21.6° while δ_p for 20 °C was determined to be 26.0°. The average of δ_{ld} for 2 °C and 40 °C was determined to be 16.3° while δ_p for 20 °C was determined to be 19.0°. Therefore, based on this analysis, reduction factors of 0.8 and 0.85 are recommended to be applied to δ_p and δ_{ld}, respectively for cover liner FS calculations to account for temperature effects on interface shear strength.

5.3 Bottom Liner Analysis

Slope stability analyses for bottom liner slopes were performed assuming a finite bottom liner side slope with waste placed on the base and side slope of the bottom liner. The bottom liner and waste geometry is presented in Figure 5.2. The slope stability analyses for bottom liner conditions were performed using the following assumptions:

- The waste was placed to a height of 30 m and at a 2:1 inclination
- The waste extended 60 m onto the base liner from the slope edge
- The waste was placed 90 m along the side slope
- The liner was sloped at 3:1 inclination
- The waste had a unit weight of 10 kN/m^3
- The failure plane occurred at the T-GM/GCL interface
- No contribution of geosynthetic tension to resisting forces occurred
- Textured GMs were used for base and side slopes

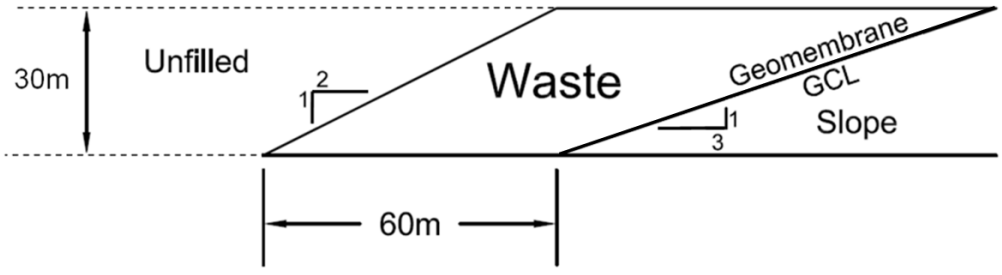

Figure 5.2. Schematic of Bottom Liner and Waste Geometry

Slope stability analyses were performed for T-GM/GCL interface for bottom liner slopes with a bentonite moisture content of 100% at temperatures of 20 and 40 °C. Peak values were used as interface shear strength parameters for the base liner, while large-displacement values were used as interface shear strength parameters for side slopes. A hybrid approach of using peak strength values for the base liner and large-displacement values for the side slopes was recommended by Thiel (2001) and Stark and Choi (2004). Contribution of resisting forces from geosynthetic tension was not considered due to possible slack of liners caused by settlement or geosynthetic expansion. The interface shear strength parameters used for the analysis are presented Table 5.2.

Table 5.2. Interface Shear Strength Parameters for Bottom Liner Analysis

Temperature	Interface Shear Strength Parameter	Base Liner [1]	Side Slope [2]
20 °C	δ (degrees)	20	10.5
	a (kPa)	9.4	7.5
40 °C	δ (degrees)	19.5	8.9
	a (kPa)	6.8	9.9

[1] Peak Parameters
[2] Large-Displacement Parameters

Bottom liner temperatures of 20 °C were determined to provide the highest factor of safety at 1.61. Bottom liner temperatures of 40 °C resulted in a factor of safety of 1.52. Bottom liner temperatures of 40 °C experienced a decrease in factor of safety of 5.6% relative to bottom liners at 20 °C.

An analysis was performed to determine a reduction factor that can apply to interface shear strength parameters for a range of temperatures expected in field conditions. In all cases, δ was greatest at 20 °C, while *a* was generally greatest at 40 C. Increasing *a* would provide additional strength, which is not a conservative method. The δ for 40 °C was divided by the δ for 20 °C to produce the reduction factor. δ_p for 40 °C and 20 °C were determined to be 20.6° and 22.5°, respectively. The average of δ_{ld} for 40 °C and 20 °C were determined to be 10.5° and 12.2°, respectively. Therefore, based on this analysis, reduction factors of 0.9 and 0.85 are recommended to be applied to δ_p and δ_{ld}, respectively for bottom liner FS calculations to account for temperature effects on interface shear strength.

This extensive testing program revealed that T-GM/GCL interface shear strength may be influenced by temperature and moisture content. Laboratory testing of interface shear strength may not be consistent with conditions representative of field applications. In the majority of conditions, interface shear testing at laboratory temperatures may provide an overestimation of T-GM/GCL interface shear strength. Reduction factors of 0.8 and 0.85 are recommended to be applied to δ_p and δ_{ld}, respectively, for cover liners. Reduction factors of 0.9 and 0.85 are recommended to be applied to δ_p and δ_{ld}, respectively, for bottom liners.

5.4 Future Research

Additional future research is recommended based on the results of this testing program. Results of the testing indicated that GMs subjected to low temperatures may result in brittle behavior. Long term oxidative degradation of GMs has been reported to result in increased brittleness of GMs. Investigation of the relationship of interface shear strength between GMs subjected to oxidative degradation and GMs exposed to low temperatures is recommended. In addition, investigation of the long term changes at elevated temperatures on interface shear strength is recommended. Exposure to long term elevated temperatures may result in decreased GT tensile strength and decreased GM shear strength.

Research of geosynthetic damage and bentonite extrusion at intermediate shear displacements is recommended to determine the quantity of bentonite extrusion and geosynthetic damage at various shear displacements. Investigation of bentonite extrusion over the long term is recommended. Bentonite extrusion over the long term may be greater or less than bentonite extrusion during laboratory testing. Increased bentonite extrusion may occur due to more time for the bentonite to extrude through the GT. Decreased bentonite extrusion may occur due to changes of bentonite over time (i.e., thixotropic hardening) or due to longer duration of normal stress application (i.e., decreased excess pore pressures). In addition, more extensive research is recommended to be conducted on quantifying the effects of moisture and temperature on bentonite extrusion.

Additional investigation is recommended on effects of intermediate moisture contents between AR and saturated on the interface shear strengths at cover liner normal stresses. The majority of previous research on T-GM/GCL interface shear strength has not focused on intermediate moisture contents between AR and saturated moisture contents. Experimental test results indicated increased moisture may result in increased interface shear strengths at cover liner normal stresses.

Additional experimental investigation on the effects of extremely elevated temperatures is recommended. Heat sources other than decomposition of MSW (e.g., mining tailings) may result in elevated temperatures beyond 40 °C.

Chapter 6: Summary and Conclusions

A systematic testing program was conducted to investigate the effects of temperature and moisture content on the interface shear strength of T-GM/GCL. Specimens were sheared using a large-scale interface direct shear device under cover liner and bottom liner normal stresses. Specimens were brought to thermal equilibrium for target temperatures and were hydrated to distinct target moisture contents.

Cover liner specimens were tested at temperatures of 2, 20, and 40 °C; at moisture contents of AR, 50%, and 100%; and at normal stresses of 10, 20, and 30 kPa. Interface shear strength for peak and large-displacement shear displacements are referred to as τ_p and τ_{ld}, and interface friction angle for peak and large-displacement shear displacements are referred to as δ_p, and δ_{ld} for analyses. Based on the data collected, the following conclusions regarding cover liner specimens were drawn:

1. Cover liner specimens exhibited a decreasing trend of τ_p with increasing temperature. τ_p at 2 °C was greater than τ_p at 20 °C by up to 27% and greater than τ_p at 40 °C by up to 36%. Increased τ_p at 2 °C may be attributed to increased geosynthetic stiffness. Tests conducted at cold conditions (2 °C) were near the glass transition temperature (-10 °C) for polypropylene, resulting in increased modulus (i.e., higher stress at a displacement prior to breakage). Decreased τ_p exhibited from 20 to 40 °C was potentially due to decreased geosynthetic strength.

2. Cover liner specimens generally exhibited bell shaped relationship of τ_{ld} with increasing temperature. τ_{ld} at 20 °C was generally larger than τ_{ld} at 2 °C for cover specimens by up to 5%. τ_{ld} at 10 kPa normal stress was generally greatest at 2 °C, while τ_{ld} at 20 and 30 kPa normal stress was generally greatest at 20 °C. τ_{ld} for specimens sheared at 40 °C was lowest for all normal stresses by up to 16%. Lower τ_{ld} at 2 °C than 20 °C may have been a result of brittle behavior of GT filaments and breakage of filaments at lower shear displacements (i.e., prior to large-displacements). Specimens sheared at 40 °C exhibited lower τ_{ld} than those sheared at 2 °C and 20 °C by as much as 21% and 16%, respectively.
3. Post-peak strength reduction for cover liner specimens was primarily attributed to geosynthetic damage. Polishing of GM asperities and pullout and tearing of geotextile filaments were observed after shearing. Greater post-peak strength reduction occurred at lower temperatures. Specimens sheared at 2 °C exhibited normalized large-displacement shear strength between 51 and 78%; 69 and 88%; and between 79 and 91% for 2, 20, and 40 °C, respectively. The greater post-peak strength reduction at 2 °C could possibly be attributed to brittle behavior of geosynthetics. Brittle behavior would result in greater strength at low displacements and lower strength at large-displacements. Increased breakage of geotextile filaments and increased asperity polishing at large-displacements would result in

increased post-peak strength reduction. Increased temperatures of thermoplastic polymers result in decreased modulus, causing the geosynthetics to behave in a ductile manner, possibly resulting in smaller post-peak strength reductions.

4. A bell shaped relationship was observed between δ_p and temperature. With the exception of 50% moisture content, specimens sheared at 2 °C exhibited lower δ_p than specimens sheared at 20 °C. δ_p ranged from 17.4 to 26.3°, 23.8 to 29°, and 20.4 to 22.2° for 2, 20, and 40 °C, respectively. δ_p decreased as much as 0.41 degrees/ °C from 20 °C to 2 °C and as much as 0.34 degrees/ °C from 20 to 40 °C.
5. A bell shaped relationship was observed between δ_{ld} and temperature, where specimens sheared at 20 °C exhibited greatest δ_{ld}. δ_{ld} ranged from 12.7 to 18.2°, 18.2 to 20.6°, and 15.9 to 16.7° for 2, 20, and 40 °C, respectively. Specimens sheared at 2 °C exhibited a lower δ_{ld} than 20 °C ranging from 2.4 to 5.5 degrees. Specimens sheared at 40 °C exhibited a lower δ_{ld} than 20 °C ranging from 2.3 to 6.0 degrees. δ_{ld} decreased as much as 0.31 degrees / °C from 20 °C to 2 °C and as much as 0.21 degrees / °C from 20 to 40 °C.
6. Peak and large-displacement adhesion was generally greatest at 2 °C and similar at 20 and 40 °C. The majority of calculated adhesion is believed to be attributed to decreased δ resulting in apparent adhesion.
7. Temperature was determined to have a greater influence on interface shear strength than moisture content for the range of conditions tested

for cover liner specimens. Interface shear strengths varied by up to 36% for the range of temperatures tested, and up to 22% for the range of moisture contents tested. Geosynthetic strength as a function of temperature may have influenced the interface shear strengths to a greater extent than hydration level of bentonite.

Bottom liner specimens were tested at temperatures of 20 and 40 °C; moisture contents of AR, 50%, and 100%; and at normal stresses of 100, 200, and 300 kPa. Based on the bottom liner experimental investigation, the following conclusions regarding bottom liner specimens were drawn:

1. Bottom liner specimens sheared at 40 °C exhibited lower τ_p than those sheared at 20 °C. Decrease of τ_p from 20 to 40 °C as high as 12% was documented. Decreased τ_p exhibited from 20 to 40 °C was attributed to increased bentonite extrusion and decreased geosynthetic strength. Bentonite liquid limit results (lower bentonite shear strength at higher temperature) and visual observation indicated that more bentonite extrusion occurred at increased temperatures, which would result in decreased τ_p. Geosynthetic damage was believed to contribute to decreasing τ_p due to possibly decreased geosynthetic strength at increased temperatures.
2. Bottom liner specimens sheared at 40 °C exhibited lower τ_{ld} than those sheared at 20 °C. Decrease of τ_{ld} from 20 to 40 °C ranging from 2% to 16% was documented. Similar mechanisms influencing the

relationship between τ_p and temperature were expected to influence the relationship between τ_{ld} and temperature.

3. Bottom liner specimens generally exhibited a decreased τ_p with increasing moisture content. The variation of τ_p ranged up to 17% between AR and 100% moisture content. τ_p was greater for AR than 100% moisture content specimens by up to 14%. Decreased τ_p with increased moisture content was largely attributed to increased bentonite extrusion. Bentonite extrusion testing performed at multiple moisture contents indicated that moisture content had a significant influence on level of bentonite extrusion. In addition, visual evidence of increased bentonite extrusion at increased moisture content was present. Increased bentonite extrusion caused by lowered bentonite shear strength would result in a lubricated surface, decreasing the τ_p. Findings regarding decreased interface shear strength with increasing moisture content agree with previous T-GM/GCL interface shear strength research.
4. Bottom liner specimens generally exhibited a decrease in τ_{ld} with increasing moisture content. In progressing from AR to 100% moisture content, the decrease of τ_{ld} ranged from 19% to 36%. The mechanisms causing decreased τ_{ld} with increasing moisture content were similar to the mechanisms causing decreased τ_p with increasing moisture content.

5. Post-peak strength reduction for bottom liner specimens was primarily attributed to increased bentonite extrusion and geosynthetic damage. τ_{ld} exhibited significantly more decrease than τ_p over the range of moisture contents tested. This was attributed to a combination of increased bentonite extrusion occurring after peak shear displacement (which has been documented by previous research) along with increased geosynthetic damage at large-displacements. Geosynthetic damage consisting of polishing of GM asperities and pullout and tearing of geotextile filaments was observed.
6. A trend of decreased δ_p with increased temperatures was exhibited. The δ_p ranged from 20° to 24.7° and 19.5° to 22.2° for 20 °C and 40 °C, respectively. The δ_p decreased by as much as 0.13 degrees/ °C from 20 to 40 °C and δ_{ld} decreased by as much as 0.11 degrees/ °C from 20 to 40 °C.
7. A trend of decreased δ_p with increased moisture contents was exhibited. The δ_p ranged from 19.5° to 24.7° from AR to 100% moisture content, respectively. The δ_p exhibited a relatively linear decreasing trend from AR to 100% moisture content at a slope of approximately 0.06 degrees/w% at 20 °C. The δ_{ld} decreased approximately 0.16 degrees/w% from AR to 100% moisture content at 20 °C. δ_p decreased approximately 0.065 degrees/w% from AR to 50% and decreased approximately 0.015 degrees/w% from 50% to 100% at 40 °C. The δ_{ld} did not significantly decrease at moisture

contents above 50%. This may have occurred because little additional volume between GM asperities may have been available for the extrusion of bentonite. At large-displacements, decreased asperity height (due to geosynthetic damage) and increased bentonite extrusion may have resulted in little additional volume available, minimizing further bentonite extrusion due to confinement.

8. For bottom liner specimens, moisture was determined to have a greater influence on interface shear strength than temperature for the range of tested conditions. Interface shear strengths varied by up to 11% for the range of temperatures tested and up to 28% for the range of moisture contents tested. A large amount of bentonite extrusion was observed, which has been documented to reduce interface shear strength. The large amount of observed geosynthetic damage (GT filament breakage and GM asperity polishing) indicates that hook and loop interaction may have contributed less to interface shear strength than frictional interaction between T-GM/GCL. Hook and loop interaction may be influenced more by geosynthetic strength than frictional interaction.

The following conclusions were drawn regarding both cover liner and bottom liner specimens:

1. Temperature was determined to have a greater effect on cover liner specimens than bottom liner specimens for the tested temperature

range. Cover liner specimens exhibited a decrease of τ_p up to 27% from 20 to 40 °C. Bottom liner specimens exhibited a decrease of τ_p up to 16% from 20 to 40 °C. GT filaments of cover liner specimens were observed to be more intact than those of bottom liner specimens post testing. It is possible temperature has a greater influence on hook and loop interaction (occurring with more intact GT filaments and larger GM asperities) than on frictional interaction (more torn GT filaments and more polished asperities). Hook and loop interaction largely relies on tensile strength of GT filaments, while frictional interaction largely relies on friction within the interface. Increased temperatures may decrease the tensile strength of GT filaments while increased temperatures may result in slightly less frictional resistance.

2. Moisture content was determined to have a greater effect on bottom liner specimens than cover liner specimens for the tested moisture content range. Cover liner specimens exhibited a decrease of τ_p up to 22% from AR to 100% moisture content. Bottom liner specimens exhibited a decrease of τ_p up to 36% from AR to 100% moisture content. Increased bentonite extrusion at increased normal stresses is believed to be the primary mechanism driving greater moisture effects on τ for bottom liner specimens.
3. Less post-peak strength reduction was exhibited for cover liner than bottom liner specimens, which was likely due to less geosynthetic damage and less bentonite extrusion. Normalized residual shear

strength at 20 and 40 °C for cover liner specimens ranged from 69% to 91%, respectively. Normalized residual shear strength at 20 and 40 °C for bottom liner specimens ranged from 49% to 78%, respectively. Normalized residual shear strength at 2 °C for cover liner specimens ranged from 51% to 78%.

4. Temperature and moisture content were both determined to influence interface shear strength response between T-GM and GCLs. Interface friction angles were greatest at 20 °C for both cover and bottom liners. To avoid overestimating interface shear strength, reduction factors can be utilized to account for decreased interface friction angles at temperatures other than 20 °C. For cover liners, reduction factors of 0.8 and 0.85 are recommended to be applied to δ_p and δ_{ld}, respectively. For bottom liners, reduction factors of 0.9 and 0.85 are recommended to be applied to δ_p and δ_{ld}, respectively.

References

ASTM D4318-10 (2012a). “Standard Test Methods for Liquid Limit, Plastic Limit, and Plasticity Index of Soils.” *Annual Book of ASTM Standards*, ASTM International.

ASTM D5888-06 (2012b). “Standard Test Method for Storage and Handling of Geosynthetic Clay Liners.” *Annual Book of ASTM Standards*, ASTM International.

ASTM D5993-99 (2012c). “Standard Test Method for Measuring Mass Per Unit of Geosynthetic Clay Liners.” *Annual Book of ASTM Standards*, ASTM International.

ASTM D6243-09 (2012d). “Standard Test Method for Determining the Internal and Interface Shear Resistance of Geosynthetic Clay Liner by the Direct Shear Method.” *Annual Book of ASTM Standards*, ASTM International.

Akpinar, M. V. and Benson, C. H. (2005). “Effect of Temperature on Shear Strength of Two Geomembrane-Geotextile Interfaces.” *Geotextiles and Geomembranes*. 23, 443-453.

Amaya, P., Queen, B., Stark, T. D., and Choi, H. (2005). “Case History of Liner Veneer Instability.” *Geosynthetics International*. 13(1), 36-46.

Bacas, B., Konietzky, H., Berini, J., and Sagaseta, C. (2011). “A New Constitutive Model for Textured Geomembrane/Geotextile Interfaces.” *Geotextiles and Geomembranes*. 29, 137-148.

Benson, C. H., Thorstad, P. A., Jo, H., and Rock, S. A. (2007). “Hydraulic Performance of Geosynthetic Clay Liners in a Landfill Final Cover Liner.”

Journal of Geotechnical and Geoenvironmental Engineering. 133(7), 814-827.

Boutwell, G. P. (2002). “Slides Happen.” North Carolina Section American Society Civil Engineers. Raleigh, NC. 3 Oct. 2002. Presentation. < http://geosynthetica.net/tech_docs/KoernerSympGordonBoutwell.pdf> (December 6, 2012).

CETCO (2011). “Bentomat CLT Geosynthetic Clay Liner Specification Guidelines TR 400.” *Technical Reference CETCO Lining Technologies*. (September 15, 2012).

Chen, Y., Lin, W., and Zhan, T. L. (2010). “Investigation of Mechanisms of Bentonite Extrusion from GCL and Related Effects on the Shear Strength of GCL/GM Interfaces.” *Geotextiles and Geomembranes*. 28, 63-71.

Daniel, D. E., Shan, H. Y., and Anderson, J. D. (1993). “Effects of Partial Wetting on the Performance of the Bentonite Component of a GCL.” Proceedings of the Geosynthetics 1993 Conference. Roseville, Minnesota. P 1483-1496.

Daniel, D. E., Koerner, R. M., Bonaparte, R., Landreth, R. E., Carson, D. A., and Scranton, H. B. (1998). “Slope Stability of Geosynthetic Clay Liner Test Plots.” *Journal of Geotechnical and Geoenvironmental Engineering*. 124(7), 628-637.

Ebewele, R. O. *Polymer Science and Technology*. CRC, 1996. Print.

EPA (United States Environmental Protection Agency) (2012a). *Municipal Solid Waste Generation, Recycling, and Disposal in the United States: Facts*

and Figures for 2010, <http://www.epa.gov/osw/nonhaz/municipal/pubs/msw2010-fs.pdf> (August 22, 2012).

EPA (United States Environmental Protection Agency) (2012b). *Summary of the Resource Conservation and Recovery Act*, <http://www.epa.gov/lawsregs/laws/rcra.html> (November 22, 2012).

EPA (United States Environmental Protection Agency) (2012c). *Geosynthetic Clay liners Used in Municipal Solid Waste Landfills*, <http://www.epa.gov/osw/nonhaz/municipal/landfill/geosyn.pdf> (November 25, 2012).

Fox, P. J., Rowland, M. G., and Scheithe, J.R. (1998). "Internal Shear Strength of Three Geosynthetic Clay Liners." *Journal of Geotechnical and Geoenvironmental Engineering*. 124(10), 933-944.

Fox, P. J., Stark, T. D., and Swan, R. H. (2004). "Laboratory Measurement of GCL Shear Strength." *Advances in Geosynthetic Clay Liner Technology: 2nd symposium*, ASTM STP 1456, R. E. Mackey, and K. von Maubeuge, Eds., ASTM International, West Conshohocken, PA, 2004.

Fox, P. J. and Stark, T. D. (2004). "State of the art Report: GCL Shear Strength and Measurement." *Geosynthetics International*, 11(3), 141-171.

Fox, P. J. and Kim, R. H. (2008). "Effect of Progressive Failure on Measured Shear Strength of Geomembrane/GCL Interface." *Journal of Geotechnical and Geoenvironmental Engineering*. 134(4), 459-469.

Frost, J. D., Zettler, T. E., DeJong, J. T., Lee, S. W., and Kagbo, S. (2002). "Strain Induced Changes in Geomembrane Surface Topography". *Geosynthetics International*. 9(1), 21-40.

GSE (2012). *GSE HD Textured Geomembrane Product Data Sheet.* <http://www.gseworld.com/content/documents/datasheets/membranes/U1 HD_Textured_Geomem_METRIC_DS.pdf (November 14, 2012).

Hanson, J. L., Yesiller, N., and Swarbrick, G. E. (2005) "Thermal Analysis of GCLs at a Municipal Solid Waste Landfill." *Waste Containment and Remediation*, ASCE GSP 142, A. Alshawabkeh et al., Eds, 1-15.

Hanson, J. L., Yesiller, N., and Oettle, N. K. (2010). "Spatial and Temporal Temperature Distributions in Municipal Solid Waste Landfills." *Journal of Environmental Engineering*. 136(8), 804-814.

Hebeler, G. L., Frost, J. D., and Myers, A. T. (2005). "Quantifying Hook and Loop Interaction in Textured Geomembrane-Geotextile Systems." *Geotextiles and Geomembranes*. 23, 77-105.

Hewitt, R. D., Soydemir, C., Stulgis, R. P., and Coombs, M. T. (1997). "Effect of Normal Stress During Hydration and Shear on the Shear Strength of GCL/Textured Geomembrane Interfaces." *Testing and Acceptance Criteria for Geosynthetics Clay Liners*, ASTM STP 1308, Larry W. Wells, Ed., American Society for Testing and Materials, 55-70.

Holtz, R. D., Kovacs, William D., and Sheahan, T. C. *An Introduction to Geotechnical Engineering*. Pearson: Upper Saddle River, NJ, 2011. Print.

Industrial Fabrics Association International – IFAI (2012). "Specifier's Guide 2012." *Geosynthetics*. 29(6), 110.

Jones, R. and Dixon, N. (1998) “Shear Strength Properties of Geomembrane/Geotextile Interfaces”. *Geotextiles and Geomembranes*. 16, 45-71.

Karademir, T. and Frost, H. D. (2011). “Elevated Temperature Effects on Geotextile-Geomembrane Interface Strength.” *Proceedings Geo-Frontiers 2011*, ASCE, Reston, VA, 1023-1033.

Koerner, R. M. and Soong, T. (2000). “Stability Assessment of Ten Large Landfill Failures.” *Proceedings Geo-Denver 2000*, 291, 1-38.

Koerner, R. M. (2005). *Designing with Geosynthetics*. Prentice Hall, Upper Saddle River, NJ, 2005.

Koerner, G. R. and Koerner, R. M. (2006). “Long Term Temperature Monitoring of Geomembranes at Dry and Wet Landfills.” *Geotextiles and Geomembranes*. 24, 72-77.

McCartney, J. S., Zornberg, J. G., and Swan, R. H. (2002). “Internal and Interface Shear Strength of Geosynthetic Clay Liners.” Geotechnical Research Report, Department of Civil, Environmental and Architectural Engineering, University of Colorado at Boulder.

McCartney, J. S., Zornberg, J. G., and Swan, R. H. (2004). “Effect of Specimen Conditioning on Geosynthetic Clay Liner Shear Strength.” *GeoAsia 2004: 3rd Asian Regional Conference on Geosynthetics*. Eds. Shim, J. G., Yoo, C., Jeon, H-Y. Seoul, Korea. 631-643.

McCartney, J. S., Zornberg, J. G., and Swan, R. H. (2005). “Effect of Geomembrane Texturing on GCL - Geomembrane Interface Shear Strength.” *ASCE GeoFrontiers 2005.* Austin, TX January 27-29, 2005.

McCartney, J. S., Zornberg, J. G., and Swan, R. H. (2009a). “Analysis of Large Database of GCL-Geomembrane Interface Shear Strength Results.” *Journal of Geotechnical and Geoenvironmental Engineering*, 135(2), 209-223.

McCartney, J. S., Zornberg, J. G., and Swan, R. H. (2009b). “Internal and Interface Shear Strength of Geosynthetic Clay Liners (GCLs).” Geotechnical Research Report, Department of Civil, Environmental and Architectural Engineering, University of Colorado at Boulder, 471 p.

Meer, S. R. and Benson, C. H. (2007). “Hydraulic Conductivity of Geosynthetic Clay Liners Exhumed from Landfill Final Cover liners.” *Journal of Geotechnical and Geoenvironmental Engineering*, 133(5), 550-563.

Mitchell, J. K. *Fundamentals of Soil Behavior*. John Wiley and Sons, 1993. Print.

Olsen, G. R. (2012). “Dimensional Stability of Geosynthetic Clay Liners in Landfill Applications.” M.S. Thesis, Department of Civil and Environmental Engineering, California Polytechnic University of San Luis Obispo.

Perkins, S. W. and Sjursen, M. (2009). “Effect of Cold Temperatures on Properties of Unfrozen Troll Clay.” *Canadian Geotechnical Journal*. 49, 1473-1481.

Plum, R. L. and Esrig, M. I. (1969). “Some Temperature Effects on Soil Compressibility and Pore Water Pressure.” US Highway Research Board Special Report 103, 231-242.

Qian, X., Koerner, R. M. and Gray, D. H. (2002). *Geotechnical Aspects of Landfill Design and Construction*, Prentice Hall, Upper Saddle River, NJ.

Rowe, R. K. (1998). “Geosynthetics and the Minimization of Containment Migration Through Barrier Systems Beneath Solid Waste.” Proc., 6th International Conf. on Geosynthetics, R. K. Rowe, ed., Vol. I, IFAI, Atlanta, 27-102.

Rowe, K. R. and Sangam, H. P. (2001). “Durability of HDPE Geomembranes.” *Geotextiles and Geomembranes*. 20, 77-95.

Rowe, R. K. and Brachman, R. W. I. (2004). “Assessment of Equivalence of Composite Liners.” *Geosynthetics International*. 11(4), 273-286.

Scalia, J. and Benson, C. H. (2011). “Hydraulic Conductivity of Geosynthetic Clay Liners Exhumed from Landfill Final Cover liners with Composite Barriers.” *Journal of Geotechnical and Geoenvironmental Engineering*, 137(1), 1-13.

Scott, Ronald F. *Principles of Soil Mechanics*. Reading, MA: Addison-Wesley Pub., 1963.

Seo, M. W., Park, J. B. and Park, I. J. (2007). “Evaluation of Interface Shear Strength Between Geosynthetics Under Wet Condition.” *Soils and Foundations*, Japanese Geotechnical Society. 47(5), 845-856.

Sherif, M. A. and Burrous, C. M. (1969). “Temperature Effects on the Unconfined Shear Strength of Saturated, Cohesive Soil.” US Highway Research Board Special Report 103, 267-272.

SI Geosolutions (1997). Smart Solutions Technical Note SM-404. “The Durability of Polypropylene Nonwoven Geotextiles for Waste Containment Applications.” < http://lining.cetco.com/DesktopModules/Bring2mind/DMX/Download.aspx?EntryId=1028&Command=Core_Download&PortalId=12&TabId=1476>

Sperling, L. H. *Introduction to Physical Polymer Science*. New York: Wiley, 2006.

Stark, T. D., Williamson, T. A. and Eid, H. T. (1996). “HDPE Geomembrane/Geotextile Interface Shear Strength.” *Journal of Geotechnical Engineering*. 122(3), 197-203.

Stark, T. D. and Choi, H. (2004). “Peak v. Residual Interface Strengths for Landfill Liner and Cover Design.” Geosynthetics International Journal, 11(6), 491-498.

Thiel, R. (2001). “Peak vs. Residual Shear Strength for Landfill Bottom Liner Stability Analyses.” *Proceedings of 15th Annual GRI Conference*, Thiel Engineering, Oregon House, CA.

Triplett, E., J. and Fox, P., J. (2001). “Shear Strength of HDPE Geomembranes/Geosynthetic Clay Liner Interfaces.” *Journal of Geotechnical and Geoenvironmental Engineering*. 127(6), 543-552.

Vukelic, A., Szavits-Nossan, A. and Kvasnicka, P. (2008). “The Influence of Bentonite Extrusion of Shear Strength of GCL/Geomembrane Interface.” *Geotextiles and Geomembranes*. 26, 82-90.

Yesiller, N., Hanson, J. L., and Liu, W. (2005). “Thermal Analysis of Cover liner Systems in Municipal Soil Waste Landfill.” *Journal of Geotechnical and Geoenvironmental Engineering*. 131(11), 1330-1334.

Yesiller, N., Hanson, J. L., Oettle, N. K., and Liu, W. (2008). “Thermal Analysis of Cover liner Systems in Municipal Soil Waste Landfill.” *Journal of Geotechnical and Geoenvironmental Engineering*. 134(11), 1655-1664.

Yesiller, N. and Shackelford, C. D. (2010). “Chapter 13: Geoenvironmental Engineering*.” Geotechnical Engineering Handbook,* B. M. Das Ed., J. Ross Publishing.

Zornberg, J. G. and McCartney, J. S. (2009). “Chapter 8: Internal and Interface Shear Strength of Geosynthetic Clay Liners.” *Geosynthetic Clay Liners for Waste Containment*, Bouazza, A., and Bowders, J.J. (Editors), CRC Press.

Appendix

Cover Liner Specimens

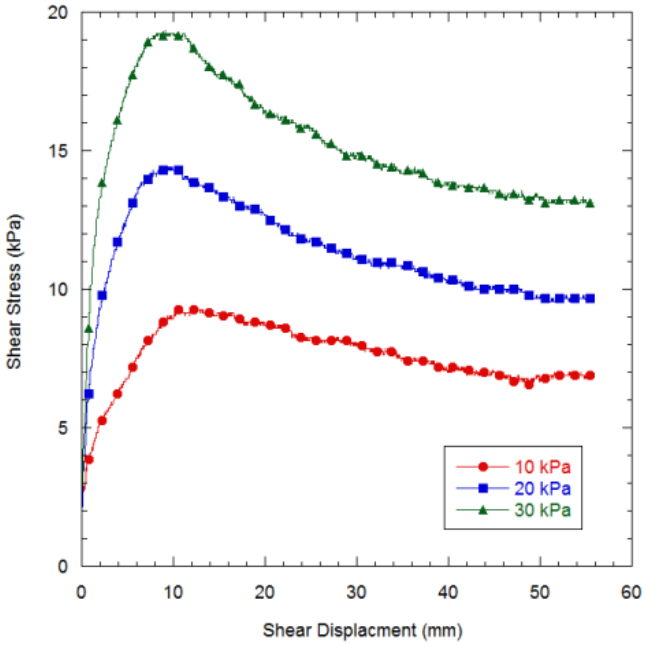

Figure A.1. Plot of Stress versus Displacment for Cover Liner Specimens (20 °C, AR)

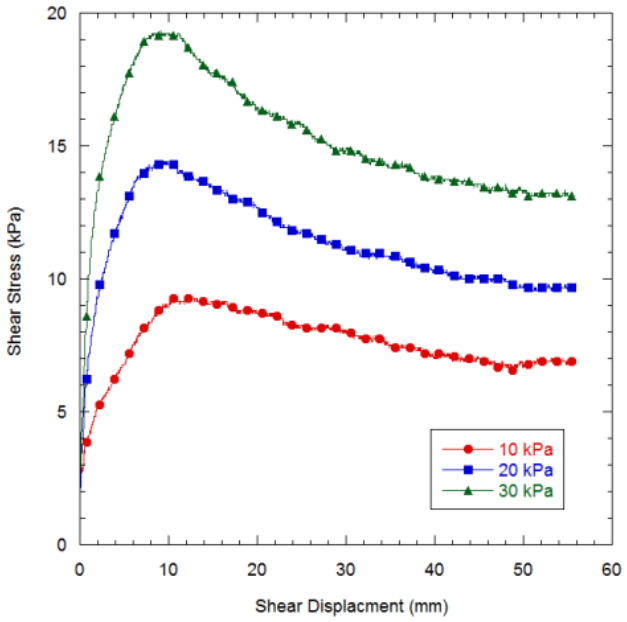

Figure A.2. Plot of Stress versus Displacment for Cover Liner Specimens (20 °C, 50%)

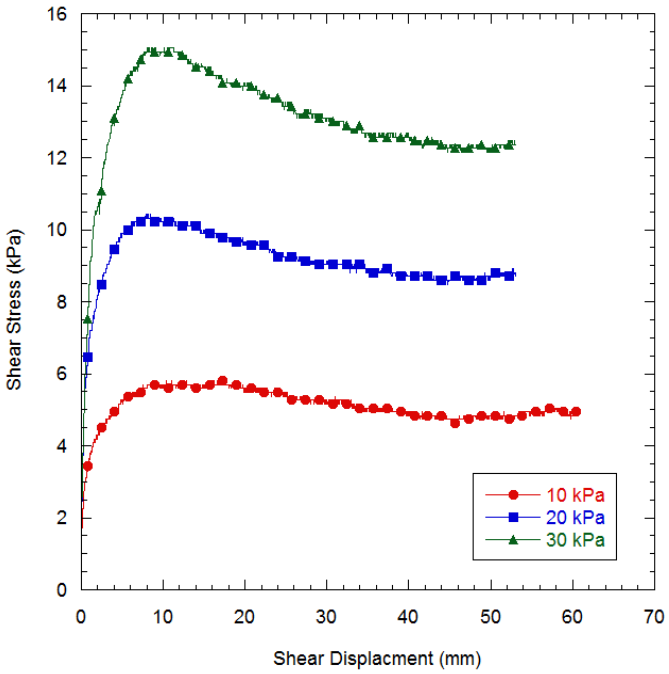

Figure A.3. Plot of Stress versus Displacment for Cover Liner Specimens (20 °C, 100%)

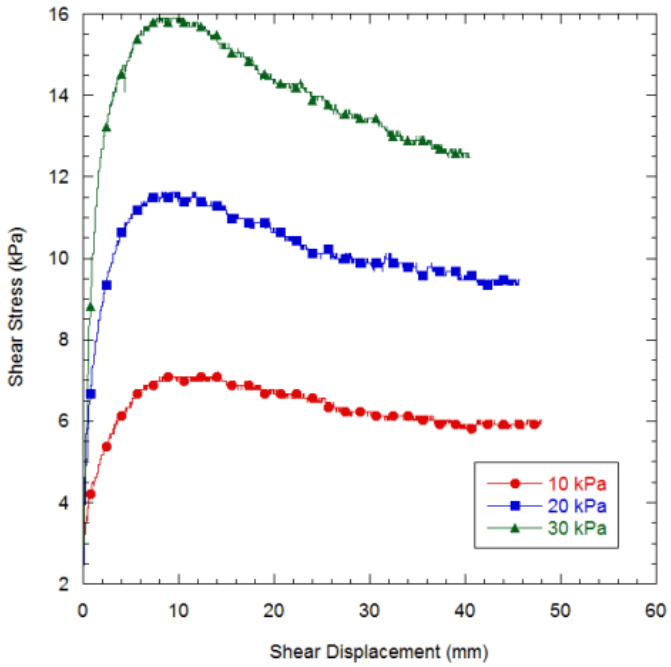

Figure A.4. Plot of Stress versus Displacment for Cover Liner Specimens (2 °C, AR)

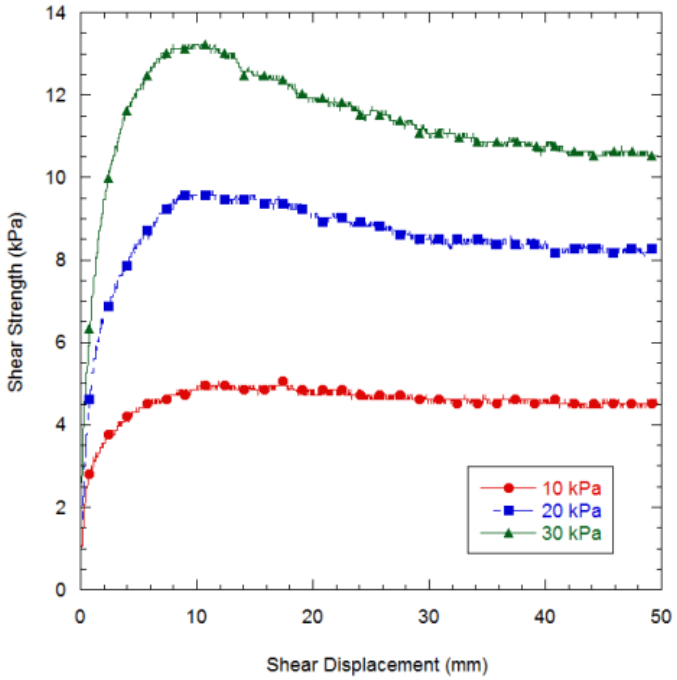

Figure A.5. Plot of Stress versus Displacment for Cover Liner Specimens (2 °C, 50%)

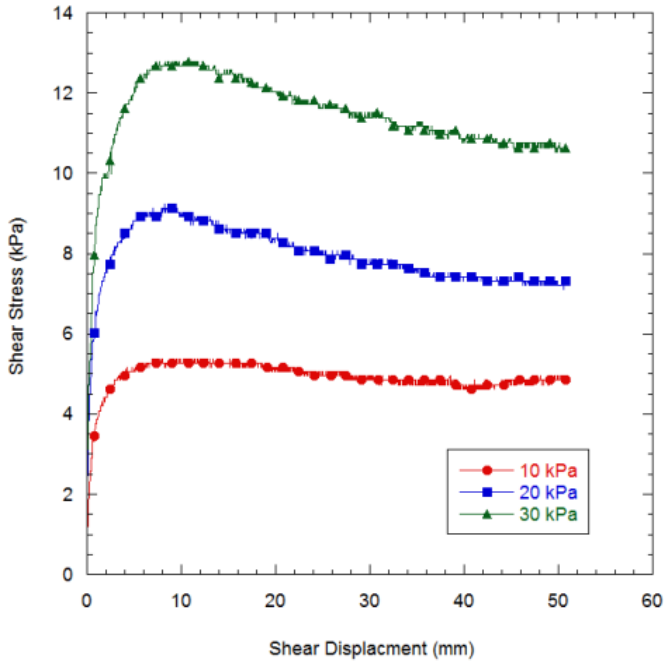

Figure A.6. Plot of Stress versus Displacment for Cover Liner Specimens (2 °C, 100%)

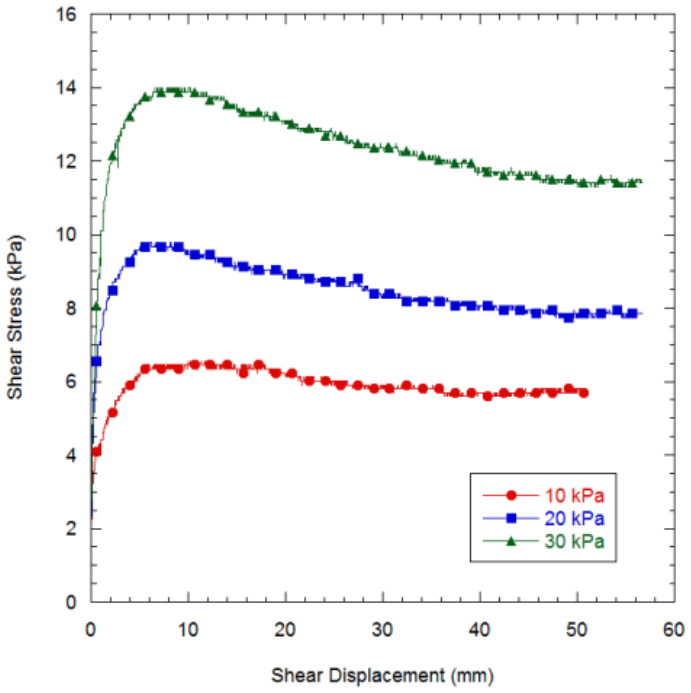

Figure A.7. Plot of Stress versus Displacment for Cover Liner Specimens (40 °C, AR)

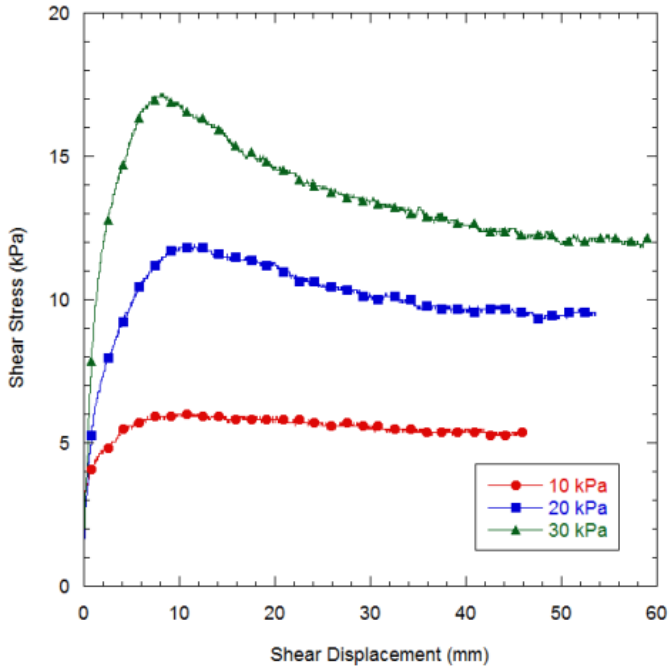

Figure A.8. Plot of Stress versus Displacment for Cover Liner Specimens (40 °C, 50%)

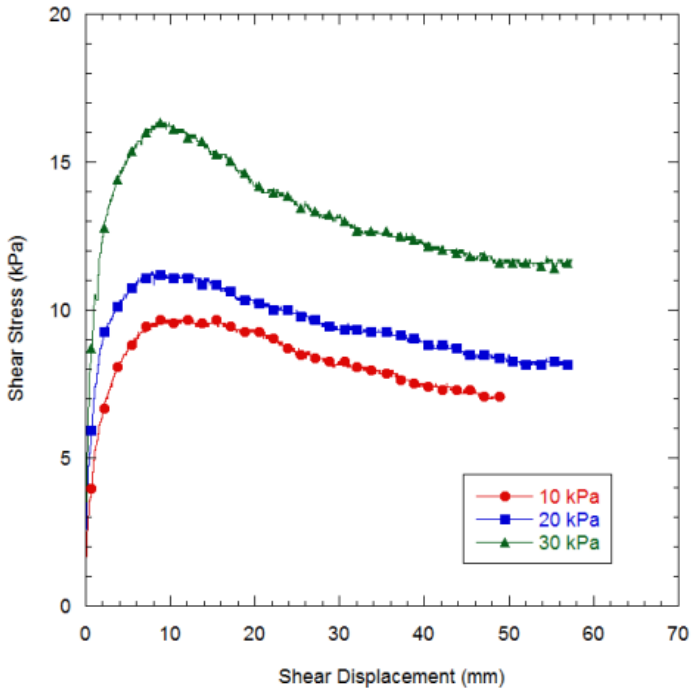

Figure A.9. Plot of Stress versus Displacment for Cover Liner Specimens (40 °C, 100%)

Bottom Liner Specimens

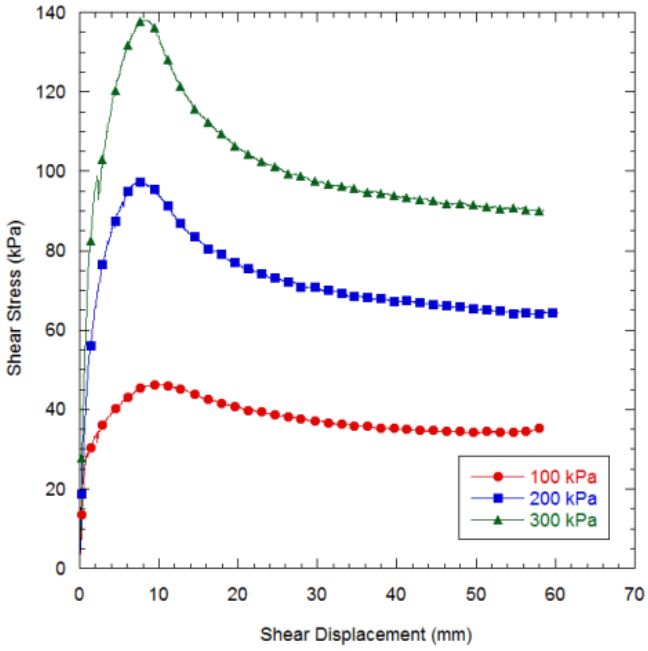

Figure A.10. Plot of Stress versus Displacment for Bottom Liner Specimens (20 °C, AR)

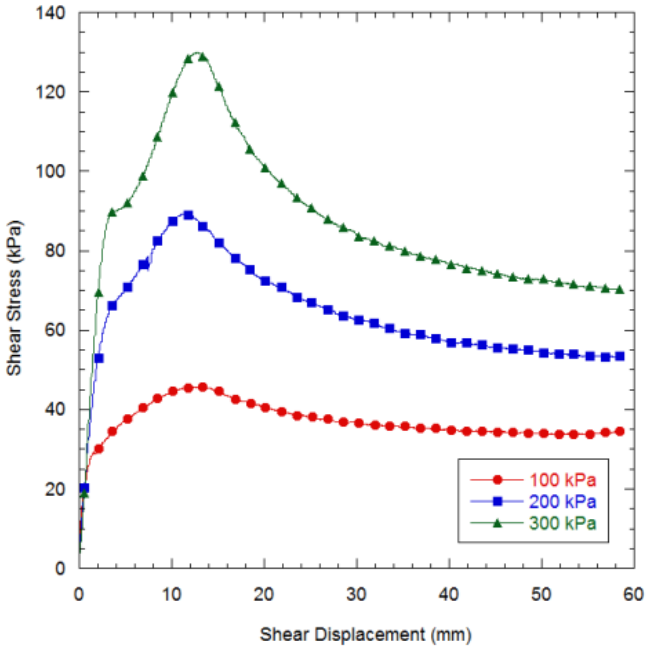

Figure A.11. Plot of Stress versus Displacment for Bottom Liner Specimens (20 °C, 50%)

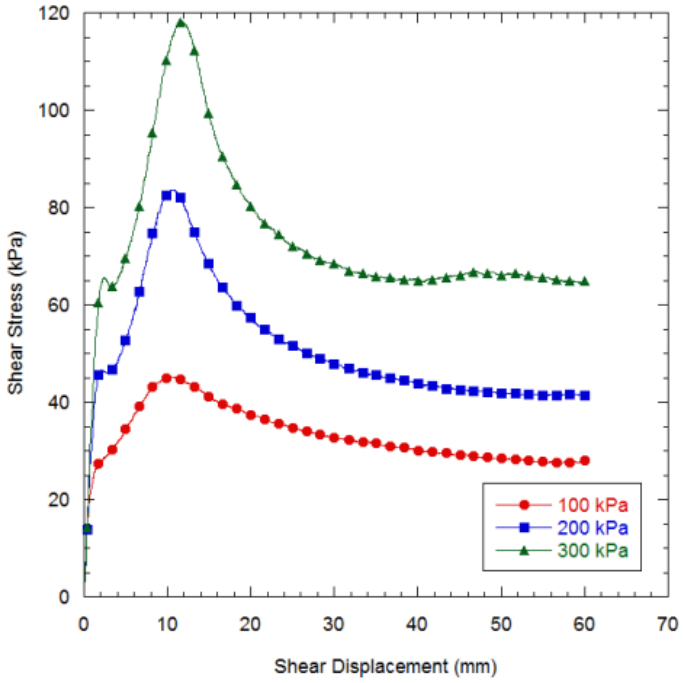

Figure A.12. Plot of Stress versus Displacment for Bottom Liner Specimens (20 °C, 100%)

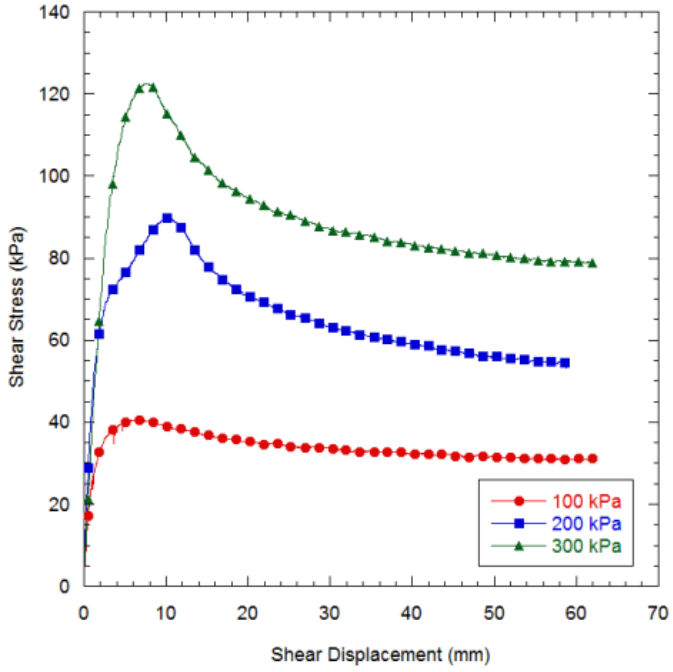

Figure A.13. Plot of Stress versus Displacment for Bottom Liner Specimens (40 °C, AR)

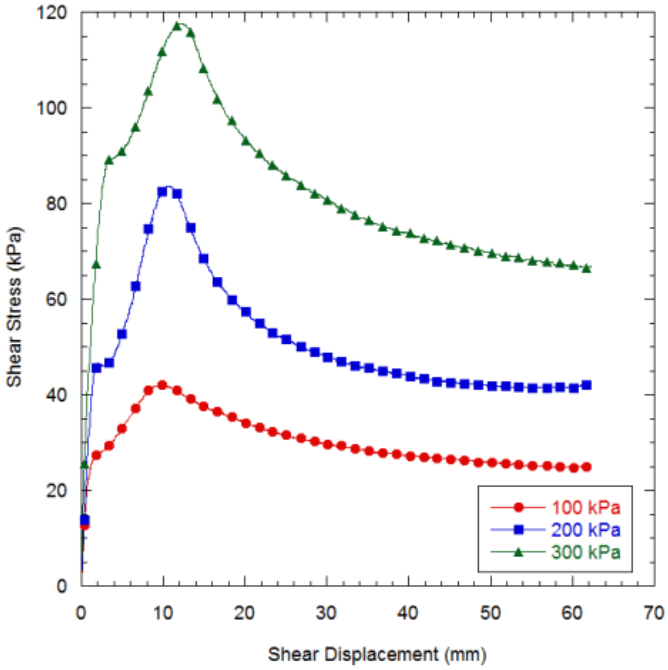

Figure A.14. Plot of Stress versus Displacment for Bottom Liner Specimens (40 °C, 50%)

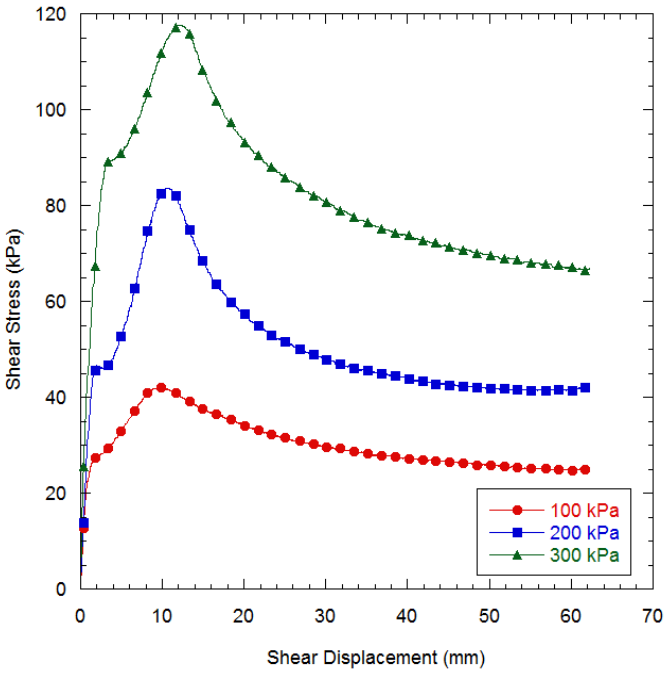

Figure A.15. Plot of Stress versus Displacment for Bottom Liner Specimens (40 °C, 100%)